STUDY ON SUBBAND ADAPTIVE ARRAY FOR SPACE-TIME CODES IN WIDEBAND CHANNEL

NORDIN BIN RAMLI

THE UNIVERSITY OF ELECTRO-COMMUNICATIONS
MARCH 2008

STUDY ON SUBBAND ADAPTIVE ARRAY FOR SPACE-TIME CODES IN WIDEBAND CHANNEL

by

NORDIN BIN RAMLI

A dissertation submitted in Partial Fulfillment
of the Requirements
for the Degree of

DOCTOR OF ENGINEERING

at

THE UNIVERSITY OF ELECTRO-COMMUNICATIONS
MARCH 2008

STUDY ON SUBBAND ADAPTIVE ARRAY FOR SPACE-TIME CODES IN WIDEBAND CHANNEL

APPROVED BY SUPERVISORY COMMITTEE

Chairperson Professor YOSHIO KARASAWA

Member Professor TAKESHI HASHIMOTO

Member Professor NOBUO NAKAJIMA

Member Professor YASUSHI YAMAO

Member Associate Professor TAKEO FUJII

広帯域無線通信における時空間符号化伝送のための サブバンドアダプティブアレーに関する研究

ノルディン・ビン・ラムリ

論文概要

近年、移動通信の利用が急激に増大し、マルチメディア情報通信への要求が高まるにつれ、より高速なデータ伝送が求められるようになっている。これを実現する手段の一つとして、アレーアンテナを送受信双方で用いることにより通信容量を飛躍的に増加させる MIMO(Multiple Input Multiple Output) システムについての研究が盛んになっている。MIMO システムでは、送信アンテナがチャンネル情報を持たない場合の伝送法として、送信ダイバーシチとブロック符号化変調を組み合わせた時空間ブロック符号化（STBC: Space-Time Block Coding）方式が注目されている。しかし STBC は、周波数選択性フェージング環境下においては、シンボル間干渉により特性が大幅に劣化してしまう。これに対して、タップ付遅延線型アダプティブアレー（TDLAA: Tapped Delay Line Adaptive Array）を用いた時空間符号化伝送法が提案されているが、最適ウエイトを算出する際の計算量が膨大になるという問題点があった。

そこで、本研究では周波数選択性フェージング環境下で、受信信号を周波数領域に変換し、サブバンドごとに適応等化処理を行うことにより計算量を大幅に軽減するサブバンドアダプティブアレー（SBAA: Subband Adaptive Array）アンテナを用いた時空間ブロック符号化伝送（STBC-SBAA）を提案する。また、適応等化処理の際、２種類の最適ウエイトベクトルが並列に算出される。適応処理では二つ連続ブロック時間を用いて、最適ウエイトを決定する。しかしながら、このようにして得られた STBC-SBAA の演算量は TDLAA に比べて大きく軽減できる反面、遅延波により信号干渉が起こることによる性能面では劣ってしまう。そこで、本研究では、遅延広がりを吸収できるサイクリックプレフィックス（CP: Cyclic Prefix）を用いた STBC-SBAA の提案も行っている。これにより受信側では、ガードインタバール（GI: Guard Interval）時間内の遅延を持つ全ての所望波を歪なく取り込んで、受信性能を向上することができる。さらに、マルチユーザ環境下において、MIMO を用いた符号分割多元接続方式（CDMA: Code Division Multiple Access）のための STBC-SBAA を提案し、STBC-TDLAA と比較する。この方式については高速通信を行うマルチコードマルチレート MIMO-CDMA における STBC-SBAA の構成法を提案し、その性能をシミュレーションによって評価した。

また、STBC-TDLAA の性能改善のため、マルチパス受信信号に各ユーザの信号成分を最適に合成し、最大の電力が得られる Modified STBC-TDLAA を提案する。提案方式には、同期及び非同期マルチユーザ STBC 伝送の場合を評価し、有効性を計算機シミュレーションによって明らかにした。

本論文は、8章から構成されている。主な内容は、第2章のMIMO及びSTBCの基礎、第3章のアダプティブアレーの基礎、第4章の時空間符号化伝送のためのサブバンドアダプティブアレー（STBC-SBAA）の構成・原理と評価、第5章のCDMAシステムにおけるSTBC-SBAAについての構成・評価、第6章の高速通信を行うマルチコードマルチレートCDMAシステムのSTBC-SBAAの構成と評価、第7章のModified STBC-TDLAAの構成・評価に大別される。

Study on Subband Adaptive Array for Space-Time Codes in Wideband Channel

Nordin Bin Ramli

Abstract

Recently, many works have been accomplished on transmit diversity for a high-speed data transmission through the wireless channel. A Multiple Input Multiple Output (MIMO) system which employs multiple antennas at transmitter and receiver has been shown to be able to improve transmission data rate and capacity of the system. When the channel state information (CSI) is unknown at the transmitter, an multiple input single output (MISO) system combined with the transmit diversity of space time coding modulation known as space-time block coding (STBC) has taken a great attention. However, the performance of STBC is deteriorated under frequency selective fading due to inter symbol interference (ISI). An STBC employing tapped delay line adaptive array (STBC-TDLAA) is known as a solution for this problem since it utilizes the delayed signals to enhance the desired signal instead of excluding them as interferences. However, this method requires a large computational load compared to the conventional adaptive array system.

In this dissertation, assuming the CSI is unknown at the transmitter, and at the receiver the CSI is exploited from pilot signal, we propose an MIMO transmission scheme using STBC with adoptive subband adaptive array (SBAA) processing, where the received signal is converted into the frequency-domain and adaptive processing is done in each subband. A novel construction of SBAA is introduced to process received signal based on STBC. In addition, to improve the performance of STBC-SBAA, single carrier cyclic prefix (CP) is also introduced. Simulation results demonstrate that the proposed scheme has a better performance compare to the conventional STBC, and has a better performance and less computational load compare to STBC-TDLAA.

Furthermore, we extend the proposed method to uplink multi-user space-time block coding (STBC) code division multiple access (CDMA) over a frequency selective fading channel. The proposed scheme utilizes CDMA with STBC and a receive array antenna with SBAA processing at the receiver. The received signal is converted into the frequency domain before de-spreading and adaptive processing is performed in each subband for each user. In order to reduce the effect of ISI and multiple access interference (MAI), a novel SBAA construction is introduced to process STBC CDMA signals. To improve the performance of the proposed scheme, we evaluate STBC-SBAA using spreading codes cyclic prefix (CP). Simulation results demonstrate an improved performance of the proposed system for single and multiuser environments compared to the conventional techniques.

Moreover, we also evaluate the STBC-SBAA for the multi-code multi-rate CDMA system.

Finally, we present a modified spatio-temporal adaptive array for multiuser STBC (Modified STBC-STAA) transmission in frequency selective fading channel with the presence of co-channel interferences (CCIs). This method based on the transversal filter adaptive array performing the joint interference suppression and equalization to overcome the problem of *one symbol delay*, namely codes synchronization error. The Modified STBC-STAA can maximize the transmission efficiency by incorporating the receive signal component for both non-conjugated and the complex conjugated version of desired signal in the receive signal, which is not only dispersed in space, but also in the time. Furthermore, Modified STBC-STAA overcomes the multiuser *timing errors* by re-aligning the asynchronous multiuser signal to undergo the synchronous joint interference suppression and equalization. Simulation results show that both our proposed scheme has a better performance than the conventional STBC-STAA for frequency selective fading channel.

Acknowledgments

In the name of Allah, the Most Gracious and the Most Merciful

All praise and glory to Almighty Allah (SWT) who gave me courage and patience to carry out this work.

First and foremost, I would like to express my heart-felt gratitude to my advisor, Professor Yoshio Karasawa, for his endless support, direction, and encouragement during my pursuit of M.E. and Ph.D. at UEC. Without Professor Karasawa's unwavering encouragement and patience, I would have never reached this point. Throughout the long journey of my Ph.D. work, he always welcomed my visits with a big smile on his face, answered my questions and listened to my ideas with unlimited enthusiasm and support. It has been a great privilege and rewarding experience to work with him. I would like to thank Professor Hashimoto, Professor Nobuo Nakajima, Professor Yasushi Yamao and Asso. Professor Takeo Fujii for serving on my Ph.D. committee and their valuable comments on the dissertation. I also would like to thank Dr. Tetsuki Taniguchi for many valuable discussions during the course of work. Working together with him is my pleasure. I would like further to thank Dr. Xuan Nam Tran, Asst. Professor at Le Qui Don Technical University, Vietnam for his helpful discussions during the beginning of this research. Thanks also go to members of Karasawa Laboratory for theirs useful discussions, supports, and fun that I had while working together with them.

This work would be impossible without the financial support. My graduate education has been supported in part by the Japanese Government Scholarship from Ministry of Education, Culture, Sport, Science and Technology (MEXT) of Japan, Panasonic Scholarship of Panasonic Ltd., and Telekom Malaysia (TM) Berhad Scholarship. At the same time, I would like to thank my employer, TM for giving me the chances to do this study in Japan.

Finally, I am grateful to my dearest parents for providing me with the best educational opportunities. They have been a vital source driving me to all accomplishments and success. I am thankful to my wife, Rosmawati Binti Ismail for being together with me in Japan, giving me love and encouragement during the most important time of this work. I am also owe a million of thanks to my lovely sons, Faris Aiman and Asyraf Danial, for their loves and fun that I have received everyday after school. Special thanks go to all of them listed above, which I could not done this work without supports from all of them. Thank you.

special dedicated to
my beloved wife
my beloved kids
my parents
my family

Contents

List of Tables

List of Figures

List of Abbreviations

BPSK	Binary phase shift keying
QPSK	Quaternary phase shift keying
FFT	Fast Fourier Transform
IFFT	inverse fast Fourier transform
i.i.d.	independent and identically distributed
STBC	Space-time block coding
STTC	Space-time trellis coding
TDLAA	Tapped delay line adaptive array
SBAA	Subband adaptive array
CP	Cyclic prefix
ISI	intersymbol interference
ICI	interchip interference
CCI	co-channel interference
MAI	multiple access interference
MMSE	minimum mean square error
MLSE	maximum likelihood sequence estimator
ZF	zero forcing
LMS	least mean square
SMI	sample matrix inversion
RLS	recursice least square
SNR	signal to noise ratio
BER	Bit error rate
SINR	signal to interference plus noise ratio
CSI	Channel State Information
BLAST	Bell Laboratories Layered Space-time
2D-RAKE	Two-dimensional RAKE
OFDM	Orthogonal Frequency Division Multiplexing
DS	Direct Sequence
CDMA	Code Division Multiple Access
HSPDA	High Speed Packet Data Access
LDR	Low data rate
HDR	High data rate

List of Mathematical Notations

General notations

s	scalar S
$\boldsymbol{s}$	vector $\boldsymbol{s}$
$\boldsymbol{S}$	matrix $\boldsymbol{S}$
$\mathbf{S}$	constant matrix $\mathbf{S}$
$\boldsymbol{S}_{M\times N}$	matrix $\boldsymbol{S}$ with M rows and N columns
$\mathbf{I}$	identity matrix $\mathbf{I}$

Mathematical operation

T_b	block duration
T_s	symbol duration
δ	Dirac delta function
$(\cdot)^*$	complex conjugate
$(\cdot)^T$	vector or matrix transpose operation
$(\cdot)^H$	complex vector or matrix Hermitian operation
$\det(\cdot)$	matrix determinant operation
$\mathrm{E}(\cdot)$	expectation operation
$\bigtriangledown$	gradient operation
$\downarrow K$	decimating factor
$\uparrow K$	expanding factor
P	total number of users
$\mathcal{F}_{u,q}$	FFT operation
$\boldsymbol{R}_{rr}$	Autocorrelation of r
$\boldsymbol{X}_{rd}$	Cross-correlation of r and d

Chapter 1

Introduction

1.1 Introduction

The use of antenna array is one of the frontiers that promise substantial increase in capacity of wireless systems. Antenna arrays offer the ability to suppress interfering signals, to improve signal reception capability, and to increase data rates [1–4]. Over the last decade, the field of wireless communications has expanded explosively in terms of the number of portable devices around the globe, allowing ubiquitous communications in voice and data services and indoor and outdoor environments. Advancements in RF circuit technologies and in large-scale integrated processing platforms facilitate the implementation of sophisticated signal processing algorithms that improve the reliability and data rate of current wireless networks. Multimedia applications represent a challenging task for system designers in the 21st century, as they require broadening of currently narrow and condensed wireless pipe. Sparked by a new class of codes, termed space-time codes (STC), it has been shown that we can exploit spatial and temporal characteristics of the multiple-input multiple-output (MIMO)[1] channel [4], with improvements in throughput and link reliability.

In this chapter, a brief review of wireless communication history of the past, present and future is discussed. Furthermore, we explain the role of diversity, overview the space-time processing and adaptive array. The context and motivation of the work throughout this dissertation is also highlighted and we conclude this chapter with the purpose and outline of the dissertation.

[1]The MIMO channel corresponds to the use of multiple element arrays in both end of the wireless links.

1.2 Wireless Communications: Past, Present, & Future

The gradual evolution of mobile communication systems follows the demand for high data rates, measured in *bits/sec (bps)*, and for a high spectral efficiency, measured in *bps/Hz*. The first mobile communications systems were analogue and are today referred to as systems of the *first generation* (1G). At the beginning of 1990s, the first digital systems emerged, referred to *second generation* (2G) systems. In Europe, the most popular 2G system introduced was the *global system for mobile communications (GSM)*, which operated in the 900 MHz and the 1800 MHz bands, and supported data rates up to 22.8 kbps. In the United States, the most popular 2G system is *TDMA/136*, while in Japan it was *Personal Digital Communications* (PDC). To accomplish higher data rates, two add-ons were developed for GSM, namely the *high speed circuit switched data (HSCSD)* and *general packet radio system (GPRS)*, providing data rates up to 38.4 kbps and 172.2 kbps, respectively.

The demand for yet higher data rates forced the development of a new generation of wireless systems, the so-called *third generation (3G)*. 3G systems are characterized by a maximum data rate of at least 384 kbps for mobile and 2 Mbps for indoors. One of the leading technologies is the *universal mobile telephone system (UMTS)*[2]. UMTS represents an evolution in terms of services and data speeds from today's 2G mobile networks. As a key member of the global family of 3G mobile technologies identified by International Telecommunication Union (ITU), UMTS is natural evolutionary choice for operators of GSM networks. UMTS is already in reality. Japan launched world's first W-CDMA network in October 2001, and it is now operating commercially throughout the world. Compared to 2G technologies, UMTS is based on a novel technology. To yield on 3G data rates, an alternative approach was made with *enhanced data rates for GSM evolution (EDGE)* concept. The EDGE system is based on GSM and operates in the same frequency bands. The significantly enhanced data rates are obtained by means of a new modulation scheme, which is more efficient than GSM modulation scheme.

The new IEEE and High Performance Radio Local Area Network (HIPERLAN) standards specify data rates of up to 54 Mbps, although 24 Mbps will be the typical rate used in most applications. Such high data rates impose large bandwidths, thus pushing carrier frequencies for values higher than the UHF band. HIPERLAN has frequencies allocated in the $5 \sim 17$ GHz bands; multimedia broadcasting (MBS) will occupy the $40 \sim 60$ GHz bands; even the infrared band is being considered for broadband wired local area networks (WLANs).

The goal of the next generation of wireless system - the *fourth generation* (4G) is to provide data rates yet higher than the ones of 3G while granting the same degree of user mobility. 4G services are expected to be introduced first in Japan, as early as 2010. The major distinction of 4G over 3G communications is increased data rates, just as it is for 3G over 2G. 3G rates reached the speed of 200 times higher of 9.6 kbps (2G

[2]Also known as wideband code division multiple access (W-CDMA) or UTRA FDD/TDD.

data rates (theoretically)) [5, 6], and 4G to yield further increases, reaching $20 \sim 40$ Mbps (about $10 \sim 20$ times of current ADSL services). 4G is expected to deliver a more advanced version of the improvements promised by 3G, such as enhanced multimedia, smooth streaming video, universal access, and portability across all type of devices. As projected by 3G system, 4G might actually connect the entire globe and be accessed from any location. This aspect makes it different from the technologies developed above. These technologies were built for or overlaid onto proprietary networking equipment. In fact, the outlook for 3G is uncertain. In contrast, 4G wireless networks that are Internet Protocol (IP)-based have an intrinsic advantage over their predecessors. IP tolerates a variety of radio protocols, and allow to design a network that gives a complete flexibility as to what shape the access network will be. One can support a diverse technologies like 802.11, W-CDMA, Bluetooth, HIPERLAN and so on, as well as some new CDMA protocols.

The first 4G system are likely to be an integration of 3G systems and WLAN systems [7–9]. By this means, considerable data rates can be granted at hot. On the other hand, the inter-working of WLAN and 3G systems will provide a good degree of mobility, given that seamless handover is accomplished between several heterogeneous system. However, in order to protect the operator and vendor investments, the performance gain of any proposed update to or evolution of 3G radio access or radio access network (RAN) must always be traded off against its impact on already made investment [7–9]. The hottest candidates for 4G appear to be as follows:-

a. BWIF: The Broadband Wireless Internet Forum (BWIF) [10] is the principle organization chartered with creating and developing next generation fixed wireless standards. The broadband wireless specifications are based on the *vector orthogonal frequency division multiplexing (OFDM)* technology and *data over cable service interface specification* (DOCSIS).

b. TD-SCDMA: Time division synchronous CDMA (TD-SCDMA) [11] is the Chinese contribution to the ITU's IMT-2000 specification for 3G wireless mobile services. It endeavors to integrate with the existing GSM system. TD-SCDMA combines two leading technologies - an advanced TDMA system with an adaptive CDMA component.

c. HSDPA: High-speed downlink packet access (HSDPA) [12] is a packet based data services in WCDMA downlink with data transmission up to $8 - 10$ Mbps (20 Mbps for MIMO systems) over a 5 MHz bandwidth in WCDMA downlink. HSDPA implementations include adaptive modulation and coding (AMC), MIMO, hybrid automatic request (HARQ), fast cell search, and advanced receiver design. MIMO system will support even higher data rate transmission up to 20 Mbps. Comparing to the other candidates, HSPDA based on W-CDMA system, can protect the investment and backward compatibility to the current technology.

A comparison between several systems based on mobility and data rate is shown in Fig. 1.1. A common theme of this evolution has been the need for more capacity, which motivates the exploration of MIMO techniques in this dissertation.

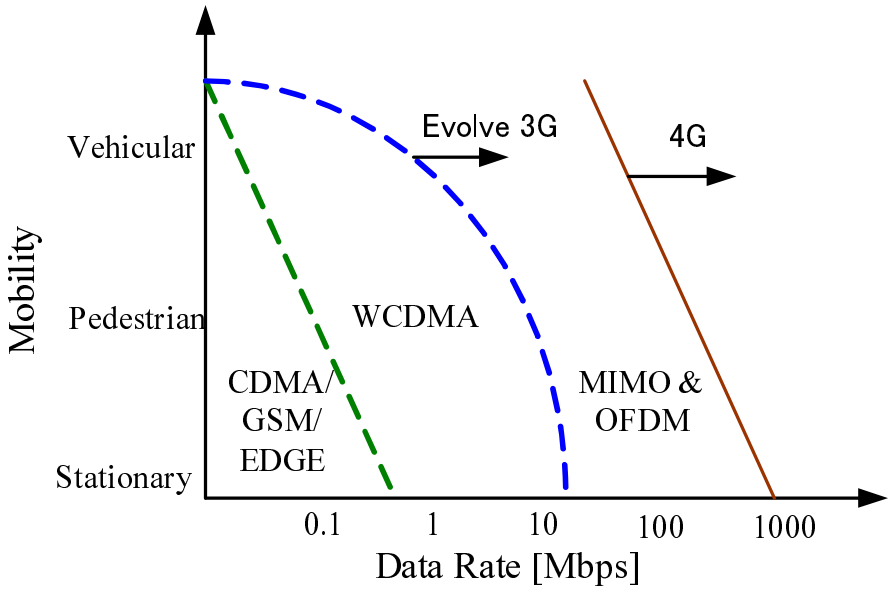

Figure 1.1: The comparison between technologies and their ability.

1.3 The Role of Diversity

Compared to the Gaussian channel, fading channel introduces severe performance degradation to a digital communication receiver, measured in tens of decibels, in terms of the mean signal-to-noise ratio (SNR) required to achieve bit error probability within given specifications. Increasing the transmitter power or size of the antennas are not economically feasible approaches for combating this problem. One widely used example is multiple receive antenna combining techniques, categorized as *spatial diversity* techniques. Another example is error correction codes with interleaving, which provide a form of *time diversity*. In this dissertation, *diversity order* is frequently used as a term which refers to the negative power of SNR in the error rate expressions. That is, the asymptotic slope of the error rate curves when plotted versus SNR in decibels. The principle of diversity is aimed towards reducing the probability of near zero fades, or "deep fades" as often used. It is important to note that large scale fading channel, corresponding to movement of the terminal over large areas can not be compensated by the use of diversity. This is due to the fact that all diversity channels are affected identically by the large scale fading channel. The goal is to compensate or mitigate the small fading effects. The following are various forms of diversity which have been proposed in the literature.

1. **Spatial Diversity** - is based on reception or transmission via multiple antenna elements along with appropriate signal processing that combines the signals from the various antennas. The effect of spatial diversity with multiple receive antenna elements was observed originally in 1927 during experiments with spatially separated receive antennas at High Frequency (HF) [13]. It was observed that with

sufficient spacing between antennas, the fading fluctuations of the received signals are independent of one another. It was then demonstrated that appropriate switching between the two replicas of the received signal greatly reduces the probability of having a "deep fade". The concept of "switched diversity", known later as selection diversity, assumes that at each instant in time, the best signal is selected. Note that the term "instant" refers to the time constant in the order of the estimation process involved in the combiner, which should be shorter than the coherence time of the channel. Extension of the selection diversity to linear combining yields the well known maximal-ratio combining (MRC) approach. This technique weights the signal received by each diversity branch according to the actual channel estimates in order to maximize SNR at the combiner output. MRC is known to be optimal in the SNR sense. Equal gain combining (EGC) is a degenerated form of MRC in which equal weights are assigned to all diversity branches. It is suboptimal but simple to implement as it does not depend on channel estimation.

2. **Frequency (Multipath) Diversity** - In frequency selective fading channel[3], transmission of a signal in sufficiently spaced carrier frequencies allows reception independently faded replicas of the signal, thus a form of frequency diversity. To obtain relatively high decorrelation, it is desirable to space the carriers an order of magnitude larger than the coherent bandwidth. The bandwidth of each carrier can be narrow enough such that fading channel is flat on each individual branch. The cost of the frequency diversity lies in the increased bandwidth occupancy, the multiple transmitter and receivers per user, and overall lower efficiency in usage of spectrum. Wideband communications (e.g. spread spectrum) exploits the form of frequency diversity as the channel introduces resolvable multipath that can be coherently combined using Rake receiver. From frequency domain perspective, the channel exhibits different responses for different frequencies. In the time domain, this translates to time dispersion or channel induced inter-symbol-interference (ISI).

3. **Time Diversity** - is achieved by employing error correction code with interleaving such that errors occurring in the channel are well separated compared with the reciprocal of the average fading rate. Since the fade levels associated with various repetition of the information bits are essentially independent, an appropriate decoding of these repetitions provides a diversity effect. The use of error correction codes to achieve temporal diversity results in bandwidth expansion due to the transmission of redundant bits.

4. **Polarization Diversity** - implies a single polarization at the transmitter, with depolarization in the propagation medium. The receiver is composed two orthogonal polarization such that the two resulting signals do not fade in a correlated manner. For the practical applications, the diversity is limited to dual diversity as any third is a linear combination of the other two and hence can not contribute to the diversity effectiveness.

[3]Also known as time dispersive channels.

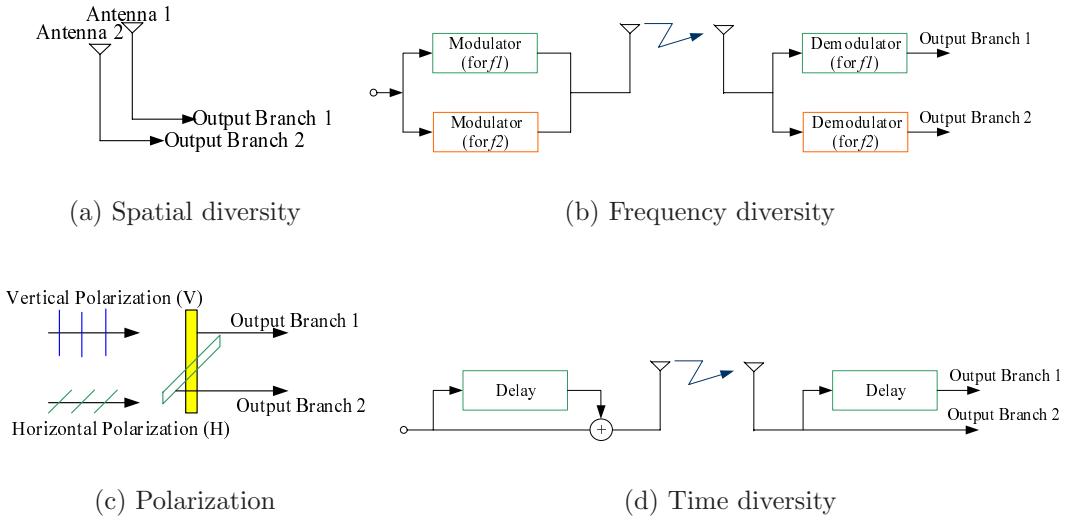

(a) Spatial diversity

(b) Frequency diversity

(c) Polarization

(d) Time diversity

Figure 1.2: Diversity methods.

5. **Angle Diversity** - requires antenna beamwidth that are narrow compared to the transmitted beamwidth, such that the two beams are oriented towards different portions of the transmitted signal, and thus the signals received via the multiple beams appear to be de-correlated.

In summary, diversity techniques play a significant role in the design of wireless systems. Although it can take in multiple forms (time, frequency, space, polarization, etc), not all forms of diversity are possible at all times. For example, Rake reception is effective only if frequency selective such that multipath component are resolvable. Time diversity is not effective for delay-sensitive applications, operating in slow fading channels. In this dissertation, it will be shown that it is beneficial to combine different forms of diversity in a joint design rather than employing these techniques independently.

1.4 Space-Time Coding and MIMO Channels: An Overview

With the integration of Internet and multimedia applications in the next generation wireless communications, the demand for a reliable high data rate services are rapidly growing. The MIMO channel model in wireless communications corresponds to the use of antenna arrays at both ends of the wireless link [2, 14]. Space-time coding exploits the diversity provided by the MIMO channel in both space (antenna) and time domains, thus significantly increasing capacity as well as improving reliability of the wireless link.

Current cellular systems use antenna diversity at the base station for improving the reception and capacity of the uplink channel. However, it becomes apparent that the weak

link is the downlink channel. Furthermore, as data type services continue to evolve, the requirements for throughput in a cellular system are asymmetrical. In data applications, users frequently access the wireless network with relatively short messaging requesting large amounts of data to be sent. This leads to the question of how to broaden the band-limited wireless pipe for the downlink channel. In many applications, antenna receive diversity at the mobile handset is not a feasible option due to limitations on the simplicity, size and cost of the handset. Moreover, implementation of multiple antenna elements at the handset is often difficult, resulting in non-equal gain and correlated channels, which lead to ineffective diversity mechanisms. This has motivated researchers and wireless designers to propose solutions in the form of transmit diversity where multiple antenna elements (possibly the same physical elements used for reception) are used in conjunction with appropriate signal processing at the receiver to achieve higher spectral efficiency, diversity advantage and possibly coding gain.

Information theoretic aspect of transmit diversity were addressed by Foschini and Gans [4], Telatar [14], Marzetta [15], and Narula, Trott and Wornell in [16]. In [14], capacity of MIMO channels as compared with the capacity for Single-Input Single-Output (SISO) channel. It was shown in [4] that capacity grows at least linearly with the number of transmit antennas as long as the number of receive antennas is greater than or equal to the number of transmit antennas. This framework has led to the development of many transmit-receive diversity architectures, space-time codes (STCs) and advanced signal processing technique - all aiming to exploit the unprecedented capacity offered by the MIMO channel. Major approaches that exploit capabilities of MIMO channels are as follows.

i. Bell Labs Layered Space-Time Architecure (BLAST), proposed by Foschini et al. [4]

ii. Space-Time Trellis Codes (STTC), proposed by Tarokh et al. [19]

iii. Space-Time Block Codes (STBC), proposed by Alamouti [17].

The BLAST test bed system (with 8 and 16 antenna elements at each side of the wireless link) was the first prototype to prove the significant capacity enhancements of wireless systems in indoor environments. In BLAST, the receiver applies multi-user detection techniques preceded by a sorting algorithm in order to decouple successively the sub-channels arriving from different antenna elements. The BLAST transmitter does not introduce any orthogonality across multiple transmit antennas. The propagation environment itself, which is assumed to exhibit significant multipath, is exploited to separate signals at the receiver. It was demonstrated that over "rich scattering" indoors environment, the BLAST system achieves a throughput of 621 kbps over a narrowband channel of 30 kHz bandwidth. Thus, unprecedented spectral efficiency is achieved. It has been shown that the main problem in BLAST is its poor energy efficiency [18], requiring very high SNR to guarantee acceptable level of error probability.

Space-time trellis coding (STTC) [19–24] is a class of signaling techniques that combines the design of the channel code with transmit (and optionally receive antenna) diversity. Coding theory suggests [2] that in random channels, even if there is not any a-priori

channel state information (CSI) at the transmitter, a single channel code can cope well with a broad range of channel realizations. In this context, the term outage probability is used to describe the extent of channel realizations in which the code performs well. The transmit diversity advantage offered by STTC is equivalent to receiver antenna diversity with maximal ratio combining (MRC). In addition to the diversity advantage, a certain amount of coding gain can be achieved by a well-constructed STTC.

In order to reduce the exponential decoder complexity of STTC, Alamouti proposed a simple transmit diversity scheme [17], namely space-time block code (STBC), which was later expanded by Tarokh. et al. [19, 21] for an arbitrary number of array elements to form the class of STBC. The STBCs achieve the same diversity advantage as maximal ratio receive combining (MRRC). STBCs are defined by a mapping operation of block of input symbols into space and time domains, creating orthogonal[4] sequences that are transmitted from different transmit antennas. The receiver is composed of a channel estimator, a combining procedure (in both space and time), and a maximal likelihood (ML) symbol-by-symbol detector. The STBC allows remarkably simple receiver structure and yet achieves the same diversity advantage as that of MRRC. Note that there is no memory between consecutive blocks and the typical block length is very short. Thus, a very limited coding gain is expected. Also, the low decoder complexity lends itself naturally to concatenation with a powerful outer error correction code [26]. In order to relax the requirement for instantaneous channel estimation at the receiver, a differential STBC (D-STBC) technique was proposed in [24]. The performance of D-STBC is inferior to the performance of coherent STBC (C-STBC) by 3 dB under ideal conditions but is much more robust to frequency and phase errors and does not rely on instantaneous tracking of CSI.

The development of STC for MIMO channels brings a new paradigm for combining the benefits of coded modulation with full diversity gains over wireless links. If this technology is to be incorporated in the next generation wireless systems, many issues need to be investigated. Active research areas include: performance evaluation over correlated fading paths, performance evaluation over flat and frequency selective channels in conjunction with channel estimation techniques, characterization of space-time channel vector models, performance evaluation in the presence of MAI, hybrid space-time coding with beamforming and implementation issues on reconfigurable hardware and DSP platforms. Also, possible integrations of STC schemes with other known techniques such as: turbo codes and iterative decoding [26], multi-user interference rejection [89] and OFDM [58] are under intensive investigation.

1.5 Overview of Adaptive Arrays

An array comprises of a set of sensors, the outputs of which are combined in some way to produce a desired effect, e.g. a set of beams "looking" in various directions. The sensors may be of many forms, e.g. acoustic transducers for sonar, monopole aerials for

[4]This codes is known as orthogonal STBC.

H.F. reception, microwave horns in a radar system, the influence of the application on the processing required concerns the technology rather than principles. Array processing systems [1] which can respond to an unknown interference environment are currently of considerable interest.

In land mobile communications, a user signal transmitted by a mobile station is reflected and scattered by surroundings before arriving at a base station, creating a multipath fading problem. As the demand for multimedia communications is increasing, mobile communication technology is developing towards high speed digital wireless networks, where the communication channels are frequency-selective, and the ISI is highly pronounced. Another source of channel distortion and signal impairment is cochannel interference (CCI), which is generated due to frequency reuse in cellular systems.

Adaptive arrays implementing spatial or spatial-temporal equalizations have shown to be useful in suppressing both ISI and CCI, leading to increased capacity and range [27–32, 90]. Spatial-temporal equalizations can be achieved by space-time adaptive processing (STAP), which is composed of an integrated adaptive array and temporal filters. However, solving both the CCI and the ISI problems simultaneously by conventional STAP methods remains difficult, as these methods require either large scale matrix inversion or recursive computation, or a cascaded form of CCI and ISI cancellers [3, 31, 32].

In the next subsection, the purpose and outline of this dissertation is presented, emphasizing original contributions to the areas of SBTC and adaptive array.

1.6 Context of the works

In this dissertation, assuming that the CSI is unknown at both transmitter and receiver while a pilot signal is available during the training period, we propose a MIMO transmission scheme using STBC by adopting subband adaptive array (SBAA) processing at the receiver. The received signals are converted into the frequency domain and adaptive processing is done in each subband. A novel construction of SBAA is introduced to process received signals based on STBC in each subband, and two weight vectors are needed to detect each user's desired signals. In addition, to improve the performance of STBC-SBAA, cyclic prefix (CP) [49] was also adopted in STBC-SBAA. Simulation is brought to show the efficiency of the proposed scheme over frequency selective fading channels. Simulation results demonstrate that the proposed scheme has a better performance compare to the conventional STBC[5], and has a better performance and less computational load compare to tapped delay line adaptive array (TDLAA) for STBC (STBC-TDLAA). Furthermore, we show the performance comparison for SIMO-SBAA, STBC-SBAA, SIMO-OFDM, and STBC-OFDM.

Next step, we extend the proposed method to uplink multi-user STBC code division multiple access (CDMA) system. The proposed scheme utilizes CDMA system with STBC and a receive array antenna with SBAA processing at the receiver. The received signal is converted into the frequency domain before de-spreading and adaptive processing is

[5]Conventional STBC refers to the STBC proposed by Alamouti et al. [17] with MLD.

performed for each subband for each user. A novel SBAA construction is introduced to process CDMA signals based on STBC for mitigating the effects of inter-chip interference (ICI), and multiple access interference (MAI). To improve the performance of the proposed scheme, we introduce a STBC-SBAA using CP. Simulation results demonstrate an improved performance of the proposed system for single and multi-user environments compare to competing related techniques. Moreover, we also evaluate the STBC-SBAA for the multi-code multi-rate CDMA system for high data rate transmission. Here, we present a novel multirate multicode CDMA system using SBAA designed for STBC transmission over frequency selective fading channel, which allows the flexible data rate transmission with affordable complexity. Here, we propose a joint equalization scheme which utilizes a STBC as transmit diversity and receive antenna with SBAA. At the receiver, a novel construction of SBAA to process multirate multicode CDMA signal based on STBC is introduced. Simulation results demonstrate the effectiveness of STBC-SBAA for multicode multirate CDMA system over the frequency selective fading channel.

Finally, we study on the performance improvement of multi-user STBC transmission using STBC-TDLAA[6] [61] by proposing the Modified STBC-TDLAA. In STBC-TDLAA, *one symbol delay* would destroy the orthogonality of STBC, which we refer it as *codes synchronization error*. In [61], synchronous STBC transmission with TDLAA at the receiver was proposed to overcome the ISI and CCIs. However, the author only consider the detection and equalization for odd and even signal without consider the delayed signal. Therefore, we present a modified spatio-temporal adaptive array for multiuser STBC (Modified STBC-TDLAA) transmission over frequency selective fading channel with the presence of CCIs. This method based on the transversal filter[7] adaptive array performing the joint interference suppression and equalization to overcome the problem of *one symbol delay*. The presented Modified STBC-TDLAA can maximize the transmission efficiency by incorporating the receive signal component for both non-conjugated and the complex conjugated version of desired signal in the received signal, which is not only dispersed in space, but also in the time. Furthermore, Modified STBC-TDLAA overcomes the multiuser timing errors by re-aligning the asynchronous multiuser signal to undergo the synchronous joint interference suppression and equalization. Simulation results show that our proposed scheme has a better performance than the conventional STBC-TDLAA over frequency selective fading channel. The performance of proposed method developed in this dissertation are validated by computer simulations.

It is noting that there is an extensive literature in frequency domain equalizations and echo-cancellation method using single sensor receivers (see, e.g. [36, 74, 91] and references therein). The method provide a fundamental development in the theory of subband processing. However, importance differences exist between single and multi-sensor systems in both formulations and performances. The inclusion of the spatial domain to subband signal processing affects both the processing structure and the performances. Single antenna receivers cannot deal with the cancellation of CCIs.

[6] In chapter 7, STBC-TDLAA was renamed as STBC-STAA for simplicity.

[7] Also known as temporal finite impulse responde (FIR) filter.

1.7 Original Contributions

Several contributions on subband adaptive array for space-time block coding and its application have been made in this work. The following summarizes the main contributions within the scope of the work.

1. First, the Chapter 4 describes the introduction of SBAA for STBC in order to suppress the ISI due to frequency selective fading channel. This work was published in the *IEICE Trans. Fundamentals, vol.E89-A, no.11, pp.3103-3113, Sept 2006* and also presented at *2004 International Symposium. on Antennas & Propagation (ISAP'04), Sendai, Japan, vol.1, pp.289-292, Aug.17-21, 2004.*

2. Second, the work on STBC-SBAA for CDMA system to overcome the ICI and MAI in frequency selective fading channel has been presented in Chapter 5. This work was published in *IEICE Trans. Fundamentals, vol.E90-A, no.10, pp.2309-2317, Oct 2007* and also presented at*14th European Signal Processing Conference(EUSIPCO), Firenze, Italia, September 2006.*

3. Third, we perform the performance evaluation of STBC-SBAA for multicode multirate transmission in CDMA system as presented in Chapter 6. This work was presented at *International Symposium on Advanced ICT (AICT), Tokyo, Japan* and also presented at *2006 International Symposium. on Antennas & Propagation (ISAP'06), Singapore Nov.1-4, 2006.*

4. Fourth, the Chapter 7 presents the performance improvement for multiuser STBC transmission with modified spatio-temporal adaptive array by introducing the new structure of detector at the receiver. This work was partly submitted for revision process in *IEICE Trans. Fundamentals*, and also has been accepted for presentation and publication to *The 3rd International Symposium on Communications, Control and Signal Processing (ISCCSP 2008), Malta, 12-14 March, 2008.*

1.8 Structure of the dissertation

This dissertation is composed of eight chapter. The organization of this dissertation are as follows.

Chapter 1 gives the overview of this dissertation including the introduction of the general of wireless communication and background of our research, purposes and contributions.

Chapter 2 gives the description on MIMO and STC. First, we provide the MIMO channel capacity based on the case of CSI known at both end and, the case of CSI unknown to the transmitter, but known at the receiver. Next, the explanation on STC which divided into STBC, STTC , BLAST are given. Moreover, we describe the problem of STBC in frequency selective fading channel.

Chapter 3 provides the overview of adaptive array technology. The adaptive array model for a single and multipath with the introduction of beamforming method is given. Furthermore, we provide the brief introduction on MMSE (Minimum Mean Square Error), the optimization method to decide the optimal weight. Moreover, we give the basic idea of adaptive algorithm such as LMS (Least Mean Squares), SMI (Sample Matrix Inversion), and RLS (Recursive Least Squares). Here, we also introduce the conventional TDLAA and SBAA and its benefits.

Chapter 4 presents a diversity transmission using STBC shows a degraded performance over frequency selective fading channel. In this chapter, assuming the CSI is unknown at both transmitter and receiver while a pilot signal is available during the training period, we propose a MIMO transmission scheme using STBC by adopting SBAA processing. The receive signal is converted into the frequency-domain and adaptive processing is done at each subband. A novel construction of SBAA is introduced to process received signal based on STBC. Simulation results demonstrate that the proposed scheme has a better performance compare to conventional STBC, and has a better performance and less computational load compare to STBC-TDLAA.

Chapter 5 presents interference suppression using a SBAA for uplink STBC CDMA system over a frequency selective fading channel. The proposed scheme utilizes CDMA system with STBC and a receive array antenna with SBAA processing at the receiver. The received signal is converted into the frequency domain before despreading and adaptive processing is performed for each subband. A novel SBAA construction is introduced to process CDMA signals based on STBC. To improve the performance of the proposed scheme, we evaluate STBC-SBAA using CP. Simulation results demonstrate an improved performance of the proposed system for single and multiuser environments compared to competing related techniques.

Chapter 6 presents an interference suppression using SBAA for STBC with multirate multicode CDMA system under the frequency selective fading channel. The proposed scheme has a flexible configuration which allows base station (BS) to dynamically adapt to multirate transmission requests from mobile stations (MS). At the receiver, the received signal undergoes STBC based subband adaptive array processing at each subband to suppress the inter ICI, multicode interference (MCI) and MAI simultaneously. The proposed system is simulated under different channel conditions and is compared against conventional SBAA.

Chapter 7 presents a new structure of STBC-TDLAA for maximizing the transmission efficiency by overcoming the *one symbol delay* problem. Although the spatio-temporal equalization achieved by the STBC-TDLAA approach reduces ISI significantly, there always is some residual ISI due to *one-symbol delay*, namely the *codes synchronization error*. This would destroy the orthogonality imposed on the transmitted signals by STBC. The impact of residual ISI will be more crucial in higher order constellations required for higher data rate in a band-limited channel. Here, we present a modified spatio-temporal adaptive array for multiuser space-time block codes (Modified STBC-TDLAA) transmission in frequency selective fading channel with the presence of CCIs. This method based on the transversal filter adaptive array perform the joint interference suppression and equaliza-

tion. The presented Modified STBC-TDLAA can maximize the transmission efficiency by incorporating the receive signal component for both non-conjugated and the complex conjugated version of desired signal, which is dispersed in the received signal. Furthermore, Modified STBC-TDLAA overcomes the multiuser timing errors by realigning the asynchronous multiuser signal to undergo the synchronous joint interference suppression and equalization. Simulation results show that Modified STBC-TDLAA scheme has a better performance than conventional STBC-TDLAA over frequency selective fading channel with affordable complexity.

Chapter 8 concludes the dissertation and gives topics for future research.

Chapter 2

Multiantenna System & Space-Time Codes for Wireless Communications

In this chapter, we present an overview of the multiantenna system and space-time processing for wireless communications. We discuss the basic ideas and performance of space-time codes which are divided into space-time block coding (STBC), space-time trellis coding (STTC), and Bell Laboratories Layered Space Time (BLAST). Furthermore, we elaborate the problem on the STBC transmission over frequency selective fading channel.

2.1 Wireless Radio Channel

Communicating over wireless channel is highly challenging due to complex characteristics and time-varying propagation medium. Consider a wireless link with a transmitter and receiver as shown in Fig. 2.1. The transmitted signal that is launched into the wireless environment arrives at the receiver along a number of distinct paths. The paths arise from scattering and reflection of the radiated energy by objects such as buildings, hills, and trees. Each of these paths has a distinct and path delay, angle of arrival, and signal power. Due to constructive and destructive interference of these paths, the received signal can vary as a function of frequency and time. These variations are collectively referred to as *fading* and cause deteriorate link quality.

2.1.1 Multipath Propagation Model

Let the transmitted signal be a complex bandpass signal $s(t) = s_0(t)e^{j2\pi f_c t}$, where B is the bandwidth, $s_0(t) : \{t \in \mathbb{Z}\}$ is input data signal, f_c is the carrier frequency, and t denotes time. Ignoring the additive white Gaussian noise (AWGN) at the receiver, the corresponding receive signal $x(t)$, is the sum of all multipath components given as

$$x(t) = \sum_{l=0}^{L-1} \alpha_l(t) s(t - \tau_l) e^{j2\pi[f_d cos(\theta_l)t - f\tau_l]} \tag{2.1}$$

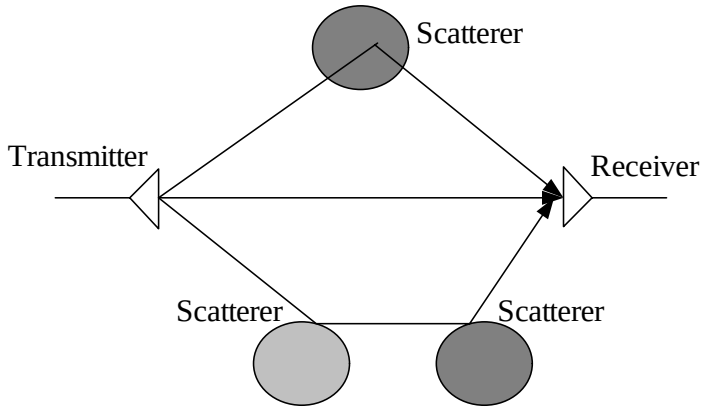

Figure 2.1: Radio channel model

where L is the number of multipaths, $\alpha_l(t)$ is the received amplitude, θ_l is the direction of lth scatterer from the receiver, $\tau_l(t)$ is the delay of lth multipath, and f_d is the maximum Doppler shift which is a function of the receiver speed and carrier frequency.

The multipath delay spread is given as $\kappa_{\tau_l} = \max_l[\tau_l(t)] - \min_l[\tau_l(t)]$. If this delay spread δ_τ, is much less than the symbol period T_s of the transmit signal, i.e., $\delta_\tau \ll T_s, \tau_l \simeq \tau_0$, then (2.1) can be written as

$$x(t) \simeq s(t-\tau_0)\left[\sum_{l=0}^{L-1}\alpha_l(t)e^{j\phi_l(t)}\right] = h(t,\tau)s(t-\tau_0), \tag{2.2}$$

where $h(t,\tau) = \alpha(t)e^{j\phi(t)}\delta(\tau-\tau_0)$, and $\phi_l(t) = 2\pi(f_d cos(\theta_l)t - f\tau_l)$ and $h(t)s(t-\tau_0)$. The channel is then a *frequency flat* fading channel, which is invariant across the bandwidth $B(=1/T_s)$ of the signal. When there are a large number of paths with similar gains and the phase is uniformly distributed between 0 and 2π, it can be shown that the received signal $|x(t)|$ is Rayleigh distributed [5, 87]. When the signal bandwidth B, increases (or alternatively, when the symbol period T_s decreases), $\delta_\tau \leq T_s$ is no longer true. The received signal is then a sum of copies of the original signal, where each copy is delayed in time by τ_l. The channel $h(t,\tau)$ at time t to an impulse at time $t-\tau$ is now given as

$$h(t,\tau) = \sum_{l=0}^{L-1}\delta(\tau-\tau_l(t))\alpha_l(t)e^{j\phi_l(t)}, \tag{2.3}$$

and referred to as a delay-spread channel with L taps. In the frequency domain, the channel response fluctuates across the signal bandwidth and hence such a channel is called *frequency selective* fading channel. *Coherence bandwidth* C_B, is (approximately) inversely proportional to the delay spread, i.e., $C_B \simeq \alpha\frac{1}{\delta_\tau}$.

Coherence bandwidth and frequency selectivity are important parameters that affect system performance. In multicarrier systems employing orthogonal frequency division multiplexing (OFDM) modulation, the total bandwidth is divided into smaller frequency

bins over which signal transmitted. A frequency selective fading channel with small coherence bandwidth implies that difference frequency bins experience different fades. Techniques such as coding and interleaving across these frequency bins can be employed to get frequency diversity and improve system performance. In single carrier systems, frequency selectivity introduces inter-symbol interference (ISI). This causes distortion of the received signal and may lower the system performance. Time domain equalization of the channel taps are typically employed to mitigate ISI and get multipath diversity. Frequency domain equalization is also popular to mitigate ISI and enhance multipath diversity.

Frequency Selective Fading Channels

A frequency selective fading channel can be modeled as a causal continuous time linear system with an impulse response $h_{cont}(t), 0 \leq t \leq \infty$, which consist of a number of impulses with coefficient $\{h^l\}$ and relative delay τ_l:

$$h_{cont}(t) = \sum_{l=0}^{L-1} h^l \delta(t - \tau_l) \tag{2.4}$$

The transfer function of this channel is

$$\bar{H}_{cont}(\omega) = \int_{-\infty}^{\infty} h_{cont}(t) e^{-i\omega t} dt \tag{2.5}$$

Let τ be the sampling period, and suppose that the transmitted signal is ideally band limited to the Nyquist frequency $1/2\tau$; hence we can assume that the channel is band limited to $1/2\tau$ as well. Then assuming that the sampling timing is chosen such that a sample is taken at $t = 0$, the sample impulse response of the channel becomes as

$$\begin{aligned} h(n\tau) &= \int_{-\infty}^{\infty} h_{cont}(n\tau - t) \frac{\sin(\pi t/\tau)}{\pi t/\tau} dt \\ &= \int_{-\infty}^{\infty} \{\sum_k h_k \delta(n\tau - \tau_k - t)\}. \frac{\sin(\pi t/\tau)}{\pi t/\tau} dt \qquad (2.6) \\ &= \sum_k h_k \frac{\sin(\pi(n - \tau_k/\tau))}{\pi(n - \tau_k/\tau)} dt. \qquad (2.7) \end{aligned}$$

Note that for frequency flat fading channel, $h_{cont} \approx h_0 \delta(t)$. Let $L + 1$ be the number of significant taps of the channel. Then, we arrive at the following causal finite impulse response (FIR) channel model.

$$H(z^{-1}) = \sum_{l=0}^{L-1} h^l z^{-l} \tag{2.8}$$

where h^l are the channel coefficient corresponding to the delays $l = 0, 1, \ldots, L-1$. Note that L can be interpreted as the *delay spread* of the channel (in units of symbol interval). The transfer function associated with $H(z^{-1})$ is

$$H(\omega) = \sum_{l=0}^{L-1} H^l e^{-iwl}. \tag{2.9}$$

2.2 Space-Time Processing

Consider a wireless link with one transmitter and one receiver. The transmitted signal that is launched into the wireless environment arrives at the receiver along a number of distinct paths. These variations are collectively referred to *fading*, which the signal amplitude can experience deep nulls leading to a highly unreliable link. Space-time processing is a useful tool to provide a reliable communication over fading channels. In this technology, multi element antennas (MEA), (i.e., known also as multiple input multiple output (MIMO))[1] and space-time modems are employed at the transmitter and/or at the receiver for *array gain*, *interference cancellation*, *diversity gain* and *multiplexing* [2, 14, 48]. The concept of *array gain*, *diversity gain*, and *interference reduction* have been studied for many decades. Actually, such schemes typically required state information (CSI) at the receiver. The receiver uses the received signal to estimate the channel. On the other hands, the concept of *transmit diversity* [3, 4, 17, 19–22, 51, 52, 55] and *spatial multiplexing* [2] have attracted wide-spread attention. Both schemes do not require channel knowledge at the transmitter, but assume perfect channel knowledge at the receiver.

2.2.1 MIMO Propagation Channel

In communication theory, MIMO refers to radio links with multiple antennas at the transmitter and the receiver side. The MIMO system recently has been receiving significant attentions in wireless communication due to its promised capacity in a fading channel. While capacity of a frequency flat fading MIMO channel is proportional to the number of antennas [14, 51], frequency selective fading MIMO channel has been shown to offer even more diversity gain in capacity [36]. Here, we describe briefly about the capacity of MIMO in Rayleigh fading channel. Consider a narrowband MIMO channel as follows. A narrowband point-to-point communication system of M transmit and N receive antennas is shown in Fig. 2.2. This system can be represented by the following discrete time model:

$$\begin{bmatrix} y_1 \\ \vdots \\ y_N \end{bmatrix} = \begin{bmatrix} h_{11} & \ldots & h_{1M} \\ \vdots & \ddots & \ldots \\ h_{N1} & \ldots & h_{NM} \end{bmatrix} \begin{bmatrix} x_1 \\ \vdots \\ x_M \end{bmatrix} + \begin{bmatrix} n_1 \\ \vdots \\ n_N \end{bmatrix} \tag{2.10}$$

[1]The MIMO channel corresponds to the use of multiple element arrays in both end of the wireless links.

or simply as $\boldsymbol{y} = \boldsymbol{H}\boldsymbol{x} + \boldsymbol{n}$. Here $\boldsymbol{x}$ represents the M-dimensional transmitted symbol, $\boldsymbol{n}$ is the N dimensional noise vector, and $\boldsymbol{H}$ is the $N \times M$ matrix of channel gains h_{ji} representing the gain from transmit antenna i to receive antenna j. We assume a channel bandwidth of B and complex Gaussian noise with zero mean and covariance matrix $\sigma 2n\boldsymbol{I}_N$, where typically $\sigma_n^2 = \mathcal{N}_0 B$. For simplicity, given a transmit power constraint P we will assume an equivalent model with a noise power of unity and transmit power $P/\sigma_n^2 = \rho$, where ρ can be interpreted as the average SNR per receive antenna under unity channel gain. This power constraint implies that the input symbols satisfy

$$\sum_{i=1}^{M} E[x_i x_i^*] = \rho, \tag{2.11}$$

or, equivalently, that $Tr(R_{xx}) = \rho$, where $Tr(R_{xx})$ is the trace of the input covariance matrix $R_{xx} = E[\boldsymbol{x}\boldsymbol{x}^T]$.

Different assumptions can be made about the knowledge of the channel gain matrix $\boldsymbol{H}$ at the transmitter and receiver, referred to as CSI at the transmitter.

Given a MIMO channel as shown in Fig. 2.2. MIMO system can be categorized as

- Flat or frequency selective fading channel
- With full, limited or without transmitter CSI.

Here, a full CSI means the knowledge of the complete MIMO channel transfer function. In a time- division duplex (TDD) system with a duplex delay less than the coherence time of the channel, full CSI is available at the transmitter, since then the channel is reciprocal. In frequency division duplex (FDD) systems, there commonly exists a feedback channel from the receiver to the transmitter that provides the transmitter with some partial CSI. This could be an information on which subgroup of antennas to be used or which eigenmode of the channel is the strongest. It is also possible to achieve a highly robust wireless link without any CSI at the transmitter, by using transmit diversity. Diversity can be achieved through so called space-time codes, like the Alamouti code for two transmit antennas, and a high bit rate is achieved by spatial multiplexing systems, like BLAST.

If a broadband wireless connection is desired, the symbol rate must be increased further which at some point will lead to a frequency selective channel. Then, there are two ways to go, either we employ a single-carrier transmission with pre- or post-equalization or we employ multicarrier transmission like OFDM, and transmit data on these sub streams without the need for channel equalization.

2.2.2 Flat Fading MIMO Channel Capacity

Given a frequency flat MIMO channel with M transmit antenna and N receive antennas as illustrated in Fig. 2.2, the channel impulse response is represented as

$$\boldsymbol{H} = \begin{bmatrix} h_{11} & \cdots & h_{1M} \\ \vdots & \ddots & \vdots \\ h_{N1} & \cdots & h_{NM} \end{bmatrix} \tag{2.12}$$

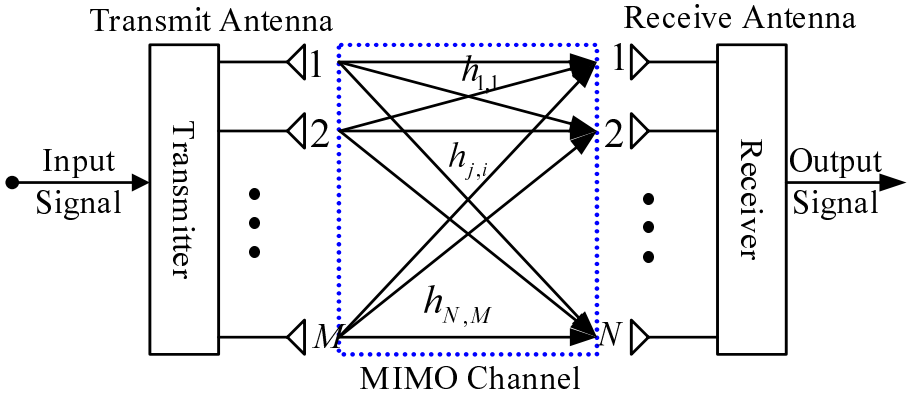

Figure 2.2: MIMO channel with M transmit and N receive antennas.

where h_{ji} is the path from antenna transmit antenna i $(= 1, 2, \ldots, M)$ to the receive antenna j $(= 1, 2, \ldots, N)$.

For $M = N = 1$, channel capacity is given as [5]

$$C = \log_2(1 + \zeta) \text{ [bit/s/Hz]} \tag{2.13}$$

where ζ is the SNR. This capacity formula assumes complete CSI both at transmitter and receiver. Capacity of MIMO system can be also derived when CSI is unknown at the transmitter.

Capacity of the MIMO channel with no CSI at the transmitter

When the channel matrix is totally unknown, uncorrelated channel inputs give capacity as C_1,

$$C_1 = \log_2|(I + \frac{\zeta_0}{M}\boldsymbol{H}\boldsymbol{H}^H)| \tag{2.14}$$

$$= \sum_{i=1}^{M} \log_2(1 + \frac{\lambda_i \zeta_0}{M}) \text{ [bit/s/Hz]} \tag{2.15}$$

where λ_i are the eigenvalues of the channel and ζ_0 is the total transmit SNR at transmitter. When the CSI is unknown at transmitter, the transmitter will transmit at the same power which been divided equally for all the available paths. When the channel matrix is totally unknown, uncorrelated channel inputs give capacity and mutual information can be maximized, As the result, capacity and mutual information can be maximized.

Capacity of the MIMO channel with full CSI at the transmitter

When a full CSI is available at the transmitter, it is possible to transmit data on the MIMO channel eigenmodes [14,48,49]. A MIMO system with M transmit antennas and N receive

antennas has $\min(M, N)$ eigenmodes. The gain of each eigenmode is proportional to the associated singular value. In this case, channel capacity is represented as

$$\begin{aligned} C_{WF} &= \max_{\sum_{i=1}^{M_0} \zeta_i = \zeta_0} \sum_{i=1}^{M_0} \log_2(1 + \frac{\lambda_i \zeta_i}{M}) \text{ [bit/s/Hz]} \\ \text{where, } M_0 &= \min[M, N]. \end{aligned} \tag{2.16}$$

By using a *waterfilling* method [14, 48] which achieves channel capacity by optimizing the power allocation in transmitter.

On the other hand, if the total power ζ_0 is allocated to the largest eigenvalues λ_1, MRC [49] transmission achieves. Achievable information rate of MRC is given by

$$C_{MRC} = \log_2(1 + \frac{\lambda_1}{\zeta_0} \text{ [bit/s/Hz]}. \tag{2.17}$$

In Fig. 2.3, we show the comparison of achievable information rate (bit/s/Hz) for three methods which are given by (2.15), (2.17), (2.17). Here, we assume an independent and identically distributed (i.i.d.) Rayleigh fading channels and the analysis is done for three different SNRs -10 dB[2], 0 dB, and 10 dB. From the figure, we can conclude that at the lowest SNR, all the transmit power will be allocated to the largest eigenvalues to achieve capacity. On the other hand, at the highest SNR, we can attain channel capacity by allocating the transmit power to all the available eigenvalues. In Fig. 2.4, the achievable information rates for 1×1 SISO, and 2×2, 4×4 and 8×8 MIMO systems are given as the function of SNR. It is shown that the achievable rates when the CSI known to the transmitter is always higher than unknown, and this advantages reduces at high SNRs.

2.2.3 Frequency Selective Fading MIMO Channels

In the frequency selective fading MIMO channel, channel capacity can be achieve by subdividing the wideband channel to V narrow band ones, and then summing the information rates of these V frequency flat channel. Let the bandwidth of these sub-channels be B/V Hz, where B is the overall channel bandwidth. Taking the vth sub-channel, the receive signal is given as

$$\boldsymbol{y}_v = \boldsymbol{H}_v \boldsymbol{x}_v + \boldsymbol{n}_v \tag{2.18}$$

where $\boldsymbol{r}_v$ is the $N \times 1$ received signal vector, $\boldsymbol{H}_v$ is $N \times M$ channel matrix for vth sub-channel, $\boldsymbol{x}_v$ is the $M \times 1$ transmitted signal vector, and $\boldsymbol{n}_v$ is the $N \times 1$ noise vector for the vth sub-channel. Hence the overall received signal can be represented as

$$\mathbf{Y} = \mathbf{HX} + \mathbf{N} \tag{2.19}$$

where $\mathbf{Y} = [\boldsymbol{y}_1^T \boldsymbol{y}_2^T \dots \boldsymbol{y}_V^T]^T$ is an $NV \times 1$ vector, $\mathbf{X} = [\boldsymbol{x}_1^T \boldsymbol{x}_2^T \dots \boldsymbol{x}_V^T]^T$ is an $MV \times 1$ vector, $\mathbf{N} = [\boldsymbol{n}_1^T \boldsymbol{n}_2^T \dots \boldsymbol{n}_V^T]^T$ is $NV \times 1$ vector, and $\mathbf{H}$ is an $V \times V$ block diagonal matrix with $N \times M$

[2]dB: decibel

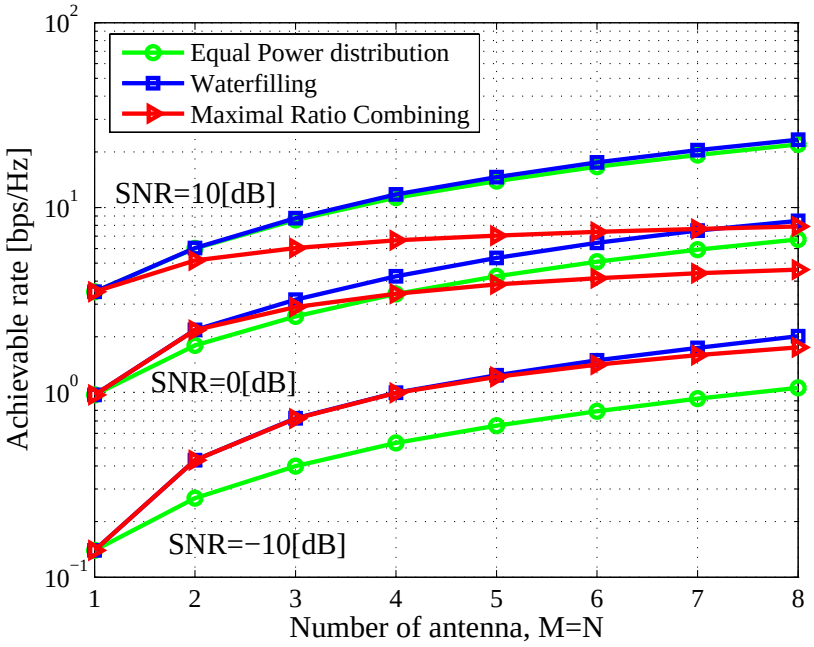

Figure 2.3: Capacity of MIMO channels at $M = N$.

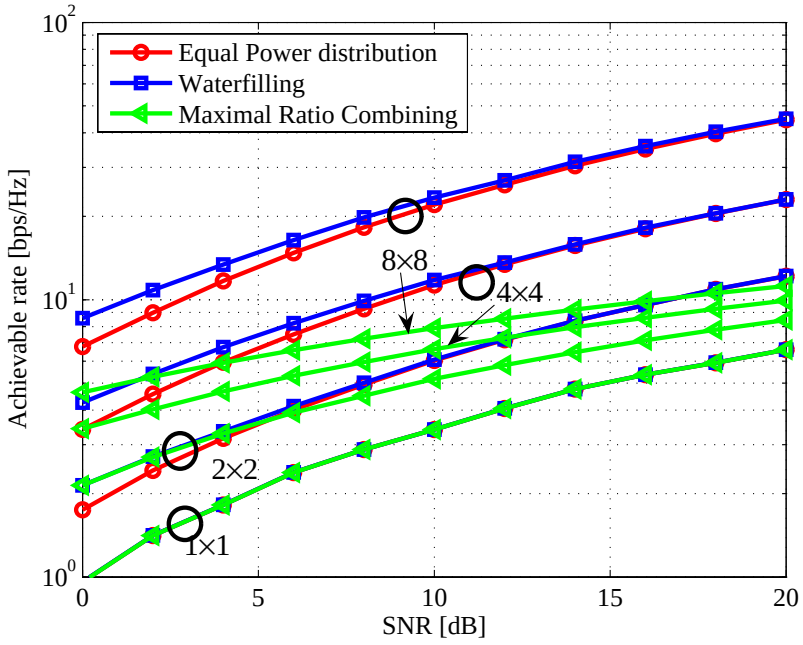

Figure 2.4: Capacity of MIMO channels as a function of SNR.

matrices of $\boldsymbol{H}_v$ as block diagonal elements. $\mathbf{R}_{xx} = \mathrm{E}[\mathbf{X}\mathbf{X}^H]$ is the covariance matrix of $\mathbf{X}$. We assume that the total transmit power constrained to $E_s = \mathrm{Trace}(\mathbf{R}_{xx}) = VM$. Capacity of the frequency selective fading MIMO channel is given by

$$C_{FSF} = \frac{B}{V} \max_{\mathrm{Trace}(\mathbf{R}_{xx})=VM} \log_2 \det \left\{ \mathbf{I}_{MV} + \frac{E_s}{M\mathcal{N}_0} \mathbf{H}\mathbf{R}_{xx}\mathbf{H}^H \right\} \text{bit/sec/Hz.} \quad (2.20)$$

Channel Unknown to the transmitter

In this case, $\mathbf{R}_{xx} = \mathbf{I}_{MV}$ achieves channel capacity, which implies the covariance matrix is of full rank (no correlation) and this in turn means that transmit power is allocated evenly across space (transmit antennas) and frequency (subchannels). Capacity is given as

$$C_{FSF} \approx \frac{B}{V} \sum_{v=1}^{V} \log_2 \det \left\{ \mathbf{I}_N + \frac{E_s}{M\mathcal{N}_0} \mathbf{H}_v \mathbf{H}_v^H \right\} \text{bit/sec/Hz.} \quad (2.21)$$

If the channel is flat, that is, $\boldsymbol{H}_v = \mathbf{H}$, where$v = \{1, 2, \ldots, V\}$, then

$$C_{FF} = \log_2 \det \left\{ \mathbf{I}_N + \frac{E_s}{M\mathcal{N}_0} \mathbf{H}\mathbf{H}^H \right\} \text{bit/sec/Hz.} \quad (2.22)$$

Channel known to the Transmitter

In this case, the ideas are similar to what was done for frequency flat fading channels, and the channel capacity is given as (2.20).

2.3 Space-Time Coding for Wireless Communications

Space-Time Coding (STC) techniques are categorized as an open loop architecture. They do not require a feedback link and are not based on measuring information at the receiver prior to transmission. STC introduces a signal structure that is exploited at the receiver to offer spatial diversity. Unlike the traditional error correction codes, the redundant information is distributed over space (antenna) and time domains, thus leading to an increased bandwidth efficiency. Since in a space-time coded system the transmit antenna array emits waveforms that operate over the same frequency and time, a superposition of signals appear at the receiver coupled with noise. The underlying question is how to decouple this superposition such that each sub-stream can be decoded. One approach might be introducing linear processing at the transmitter to map information across antennas. The mapping rule may introduce orthogonality across sequences transmitted from distinct antenna elements, which can be exploited at the receiver with an appropriate combing rule [17]. The receiver carries out linear processing followed by maximum likelihood decoding (MLD). This technique is known as the class of STBC. The orthogonality can be also implemented via time multiplexing [52], frequency multiplexing [53] or by using orthogonal spreading sequences for different antennas [54]. The time multiplexing approach is the delay diversity scheme, originally proposed by Seshadri and Winters [52].

In this scheme, delayed replicas of the same symbol are transmitted through different antenna elements such that a flat fading channel is transformed into a frequency selective fading channel. The receiver uses a maximum likelihood sequence estimator (MLSE) equalizer to offer a diversity order similar to MRC. Tarokh and Calderbank extended the delay-diversity approach to the joint design of error-correction codes, modulation and array processing [20]. These codes are known as Space-Time Trellis Codes (STTCs), which achieve both diversity gain and coding gain and lead to an increased bandwidth efficiency. In space-time coded systems, there is not a mandatory requirement for multiple antenna elements at the receiver. The design and structure of STTC and STBC, and BLAST is the topic of the following sections.

2.3.1 Space-Time Block Codes (STBCs)

Seeking a low decoder complexity, Alamouti in [17] proposed a simple dual transmit diversity scheme that achieves the same diversity gain as the dual branch receiver with MRC. The scheme was generalized by Tarokh et al. in [19] for arbitrary number of transmit antennas elements by applying the theory of orthogonal design. The orthogonality of STBC allows a simple receiver structure of maximum likelihood decision, which is preceded by linear processing only. The scheme is defined by its encoder matrix, which maps k input $\mathcal{M}$-ary symbols into $\mathcal{M}$ orthogonal sequences of length p, thus creating a rate $r = k/p$ code. The encoder matrix, denoted by G_M, is called the STBC for the orthogonality property across its columns. A block diagram of the full rate orthogonal STBC scheme with two transmit and one receive antenna elements (G_2) is illustrated in Fig. 2.5. The orthogonality across the sequences of symbols, transmitted simultaneously form the two antenna elements, is exploited at the receiver by the combining rule. The objectives of this combiner are two fold:
1) decouple the received superposition of symbols to create separate decision statistics, and
2) coherently combine the fade coefficients associated with each transmitted symbol to allow for diversity order.
The derived decision statistics are fed into a symbol-by symbol MLD. It is noted that the STBC scheme relies on "quasi-static" of the channel conditions, or a slow time-varying channel such that the coherence time of the channel is greater than the duration of a block (p consecutive symbols). This is a reasonable assumption in most practical systems since the block length of STBC is relatively short.

Coherent Space-Time Block Coding (C-STBC)

Encoding Algorithm

Each set of b bits is mapped to form a $\mathcal{M}$-ary PSK or QAM symbol with cardinality 2^b. The space-time block encoding algorithm of Fig. 2.5 is described by the encoder matrix G_2, which maps a block of $k = 2$ symbols into $M = 2$ sequences of length $p = 2$ each. G_2

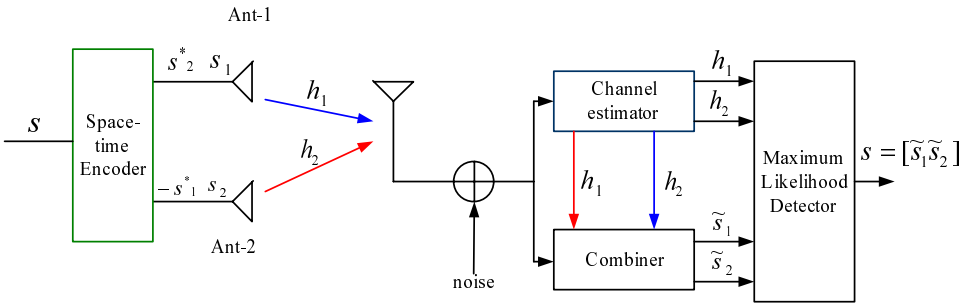

Figure 2.5: Illustration of Alamouti's two antenna transmit diversity scheme.

is given by

$$G_2 = \begin{bmatrix} s_1 & s_2 \\ -s_2^* & s_1^* \end{bmatrix}, \tag{2.23}$$

where s_1 and s_2 denote a pair of symbols at the encoder input. The encoder output is denoted by s_t^i, where $1 \leq t \leq p$ corresponds to the time instant within a block of length p symbols and i corresponds to the ith antenna element at the transmitter. The G_2 matrix implies a rate 1 ($r = k/p$) code that does not expand bandwidth to transmit the redundant information. The first and second rows of the encoder matrix are transmitted at times t and $t + T$ from the two antennas, respectively. The orthogonality criteria corresponds to a zero inner product of the two columns.

Decoding Algorithm

The received signal at receive antenna j at time t is modeled by,

$$r_t^j = \sum_{i=1}^{N} \alpha_{i,j} s_t^i + n_t^j, \tag{2.24}$$

where n_t^j denotes the AWGN term and is modeled as independent samples of a zero mean complex Gaussian random variable with variance $[\frac{\mathcal{N}_0}{2}]$ per dimension. Assuming ideal CSI at the receiver, the following decision metric is evaluated

$$\sum_{t=1}^{p} \sum_{j=1}^{N} \mid r_t^j - \sum_{j=1}^{M} \alpha_{i,j} s_t^j \mid^2 \tag{2.25}$$

In the case of G_2 matrix, the ML detection rule is the minimization process of the following decision metric:

$$\sum_{j=1}^{N} (|r_1^j - \alpha_{1,j} s_1 - \alpha_{2,j} s_2|^2 + |r_2^j - \alpha_{1,j} s_2^* - \alpha_{2,j} s_1^*|^2). \tag{2.26}$$

Note that the fade coefficients are assumed to be constant over the block duration of $p = 2$ symbols. This is a reasonable assumption for typical coherence time and baud rate of practical systems. Expanding the above metric and simplifying, the minimization of (2.26) is equivalent to the following two separate minimization processes:

$$\left|\left[\sum_{j=1}^{N}(|r_1^j\alpha_{1,j}^* + (r_2^j)^*\alpha_{2,j} \right] - s_1\right|^2 + \left(-1 + \sum_{j=1}^{N}\sum_{i=1}^{2}|\alpha_{i,j}^2| \right)|s_1|^2 \tag{2.27}$$

for decoding s_1, and

$$\left|\left[\sum_{j=1}^{N}(|r_1^j\alpha_{2,j}^* - (r_2^j)^*\alpha_{1,j} \right] - s_2\right|^2 + \left(-1 + \sum_{j=1}^{N}\sum_{i=1}^{2}|\alpha_{i,j}^2| \right)|s_2|^2 \tag{2.28}$$

for decoding s_2.

Thus, the receiver structure for STBC includes channel estimates of the fade coefficients in the following linear processing rule:

$$\tilde{s}_1 = \sum_{j=1}^{N}(|\alpha_{1,j}^* r_1^j + \alpha_{2,j}(r_2)^*) \tag{2.29}$$

$$\tilde{s}_2 = \sum_{j=1}^{N}(|\alpha_{2,j}^* r_1^j - \alpha_{1,j}(r_2)^*) \tag{2.30}$$

Using the combining rule of (2.29) yields,

$$\tilde{s}_1 = \left| \sum_{j=1}^{N}\sum_{i=1}^{N}|\alpha_{i,j}|^2 \right) s_1 + \grave{n}_1 \tag{2.31}$$

$$\tilde{s}_2 = \left| \sum_{j=1}^{N}\sum_{i=1}^{N}|\alpha_{i,j}|^2 \right) s_2 + \grave{n}_2 \tag{2.32}$$

where $\grave{n}_1$ and $\grave{n}_2$ are the noise terms given by

$$\grave{n}_1 = \sum_{j=1}^{N}(\alpha_{1,j}^* n_1^j + \alpha_{2,j}(n_2^j)^*), \tag{2.33}$$

$$\grave{n}_2 = \sum_{j=1}^{N}(-\alpha_{1,j}(n_1^j)^* + \alpha_{2,j}^* n_1^j) \tag{2.34}$$

Note that the fade coefficients are added coherently, yielding optimal combining and diversity order of $2 \times N$. Also, note that the linear combining rule takes advantage of the orthogonality of the columns of G_2 in order to decouple the estimates for s_1 and s_2. Once decision statistics for s_1 and s_2 are obtained, the optimum detection rule is described by: Choose $s_1 = s_i; i = [1, \ldots, 2b]$ if and only if

$$\left(-1 + \sum_{j=1}^{N}\sum_{i=1}^{2}|\alpha_{i,j}|^2 \right)|s_1|^2 + d^2(\tilde{s}_1, s_i) \leq \left| -1 + \sum_{j=1}^{N}\sum_{i=1}^{2}|\alpha_{i,j}|^2 \right)|s_k|^2 + d^2(\tilde{s}_2, s_i), \forall i \neq k. \tag{2.35}$$

Table 2.1: Orthogonal designs for STBC.

Orthogonal Design	*N*	*Rate*	*k input block length*	*p output block length*
G_2	2	1	2	2
G_3	3	1/2	4	8
G_4	4/2	1/2	4	8
H_3	3	3/4	3	4
H_4	4	3/4	3	4

For phase shift keying (PSK) signals (equal energy constellations) the decision rule in (2.35) is simplified to:
Choose $s_1 = s_i$ if and only if

$$d^2(\tilde{s}_1, s_i) \leq d^2(\tilde{s}_1, s_k), \forall i \neq k, \tag{2.36}$$

and a separate identical decision rule for s_2:
Choose $s_2 = s_i$ if and only if

$$d^2(\tilde{s}_2, s_i) \leq d^2(\tilde{s}_2, s_k), \forall i \neq k. \tag{2.37}$$

Orthogonal Designs

A complex orthogonal design G is defined as a $p \times N$ orthogonal transmission matrix with entries the indeterminants $[\pm x_1, \pm x_2, \ldots, \pm x_n]$, their conjugates $[\pm x_1^*, \pm x_2^*, \ldots, \pm x_n^*]$ and the superposition of those. In the previous section, a full rate (G_2, $r = 1$) complex orthogonal design was described for 2 transmit antenna elements. Following the theory of orthogonal design by Radon and Hurwitz, Tarokh et al. generalized in [19] these schemes for an arbitrary number of antenna elements. While a full rate orthogonal design exists for real alphabets (i.e., pulse amplitude modulation (PAM)) with arbitrary number of elements, it does not exist for an arbitrary complex alphabet (i.e., PSK or quadrature amplitude modulation (QAM)) with more than 2 antenna elements. This has motivated researchers to search for sporadic complex orthogonal designs, which accommodate rates as close to one as possible, yet achieve full spatial diversity order. Table 2.1 summarizes the characteristics of few sporadic complex orthogonal designs, proposed originally in [19], for $2, 3$ and 4 transmit antenna elements. Following Table 2.1, the orthogonal transmission matrices are described.

1. Orthogonal Design I: 2 transmit antenna elements, $r = 1$.

$$G_2 = \begin{bmatrix} s_1 & s_2 \\ -s_2^* & s_1^* \end{bmatrix} \tag{2.38}$$

2. Orthogonal Design IIa: 3 transmit antenna elements, $r = 1/2$.

$$G_3 = \begin{bmatrix} s_1 & s_2 & s_3 \\ -s_2 & s_1 & -s_4 \\ -s_3 & s_4 & s_1 \\ -s_4 & -s_3 & s_2 \\ s_1^* & s_2^* & s_3^* \\ -s_2^* & s_1^* & -s_4^* \\ -s_3^* & s_4^* & s_1^* \\ -s_4^* & -s_3^* & s_2^* \end{bmatrix} \tag{2.39}$$

3. Orthogonal Design IIb: 3 transmit antenna elements, $r = 3/4$.

$$H_3 = \begin{bmatrix} s_1 & s_2 & s_3/\sqrt{(}2) \\ -s_2^* & s_1^* & s_3/\sqrt{(}2) \\ -s_3^*/2 & s_3^*/2 & (-s_1 - s_1^* + s_2 - s_2^*)/2 \\ -s_3^*/2 & -s_3^*/2 & (s_2 + s_2^* + s_1 - s_1^*)/2 \end{bmatrix} \tag{2.40}$$

4. Orthogonal Design IIIa: t transmit antenna elements, $r = 1/2$.

$$G_4 = \begin{bmatrix} s_1 & s_2 & s_3 & s_4 \\ -s_2 & s_1 & -s_4 & s_3 \\ -s_3 & s_4 & s_1 & -s_2 \\ -s_4 & -s_3 & s_2 & s_1 \\ s_1^* & s_2^* & s_3^* & s_4^* \\ -s_2^* & s_1^* & -s_4^* & s_3^* \\ -s_3^* & s_4^* & s_1^* & -s_2^* \\ -s_4^* & -s_3^* & s_2^* & s_1^* \end{bmatrix} \tag{2.41}$$

5. Orthogonal Design IIIb: 4 transmit antenna elements, $r = 3/4$.

$$H_4 = \begin{bmatrix} s_1 & s_2 & s_3/\sqrt{(}2) & s_4/\sqrt{(}2) \\ -s_2^* & s_1^* & s_3/\sqrt{(}2) & -s_3/\sqrt{(}2) \\ s_3^*/2 & s_3^*/2 & (-s_1 - s_1^* + s_2 - s_2^*)/2 & (-s_2 - s_2^* + s_1 - s_1^*)/2 \\ s_3^*/2 & -s_3^*/2 & (s_2 + s_2^* + s_1 - s_1^*)/2 & -(s_1 + s_1^* + s_2 - s_2^*)/2 \end{bmatrix} \tag{2.42}$$

It can be verified that the columns of these matrices meet the orthogonality requirement. These codes have a simple linear processing rule, followed by a maximum likelihood decoder. As an example, the decoder for G_3 minimizes the following decision metrics:

$$\left| \left[\sum_{j=1}^{N} (|r_1^j \alpha_{1,j}^* + (r_2^j)\alpha_{2,j}^* + r_3^j \alpha_{3,j}^* + (r_5^j)^* \alpha_{1,j} + (r_6^j)^* \alpha_{2,j} + (r_7^j)^* \alpha_{3,j} \right] - s_1 \right|^2 + \left(-1 + \sum_{j=1}^{N} \sum_{i=1}^{3} |\alpha_{i,j}^2| \right) |s_1|^2 \tag{2.43}$$

for decoding s_1, and,

$$\left|\left[\sum_{j=1}^{N}(|r_1^j\alpha_{2,j}^* - (r_2^j)\alpha_{1,j}^* + r_4^j\alpha_{3,j}^* + (r_5^j)^*\alpha_{2,j} - (r_6^j)^*\alpha_{1,j} + (r_8^j)^*\alpha_{3,j} \right] - s_2\right|^2 + \left(-1 + \sum_{j=1}^{N}\sum_{i=1}^{3}|\alpha_{i,j}^2| \right)|s_2|^2 \quad (2.44)$$

for decoding s_2, and,

$$\left|\left[\sum_{j=1}^{N}(|r_1^j\alpha_{3,j}^* - (r_3^j)\alpha_{1,j}^* - r_4^j\alpha_{2,j}^* + (r_5^j)^*\alpha_{3,j} - (r_7^j)^*\alpha_{1,j} - (r_8^j)^*\alpha_{2,j} \right] - s_3\right|^2 + \left(-1 + \sum_{j=1}^{N}\sum_{i=1}^{3}|\alpha_{i,j}^2| \right)|s_3|^2 \quad (2.45)$$

for decoding s_3, and,

$$\left|\left[\sum_{j=1}^{N}(|-r_2^j\alpha_{3,j}^* + (r_3^j)\alpha_{2,j}^* - r_4^j\alpha_{1,j}^* - (r_6^j)^*\alpha_{3,j} + (r_7^j)^*\alpha_{2,j} - (r_8^j)^*\alpha_{1,j} \right] - s_3\right|^2 + \left(-1 + \sum_{j=1}^{N}\sum_{i=1}^{3}|\alpha_{i,j}^2| \right)|s_4|^2 \quad (2.46)$$

for decoding s_4.

Performance of G_2 codes with 4-ary PSK in the frequency flat and frequency selective fading channel are given in Fig. 2.6. It is shown that STBC work very well in the flat fading, however the bit error rate (BER) degraded in the frequency selective fading channel, due to the the presence of ISI. We will focus on this problem in the next chapter by giving the countermeasures to suppress the ISI, as well the co-channel interference (CCI) (or multiple access interference (MAI) in CDMA network.) in the following chapter.

Differential Space-Time Coding

Differential demodulation techniques are widely used in contemporary communications systems, offering robust performance in the presence of unknown phase and CSI. In contrast, coherent demodulation implies stringent requirements for accurate carrier recovery and channel estimation in order to compensate the instantaneous phase and allow for optimal detection. Carrier recovery and channel estimation can be performed with data-aided type techniques (i.e., transmission of pilot symbols) or non data-aided (blind) techniques. In the former, additional overhead is introduced to provide robust tracking of signal parameters, while in the latter additional complexity is added to the system. In addition, instantaneous tracking of phase and CSI is a challenging task in time varying channels. Under ideal conditions, coherent demodulation outperforms differential demodulation by approximately 3 dB [17, 24, 25]. In differential modulation schemes, the information is carried out in the phase difference between consecutive symbols rather than in the absolute phase. Demodulation is performed by using the previous received symbol as a noisy reference signal to the incoming current symbol. Since both previous and current symbols undergo the same channel conditions, the demodulator extracts the difference

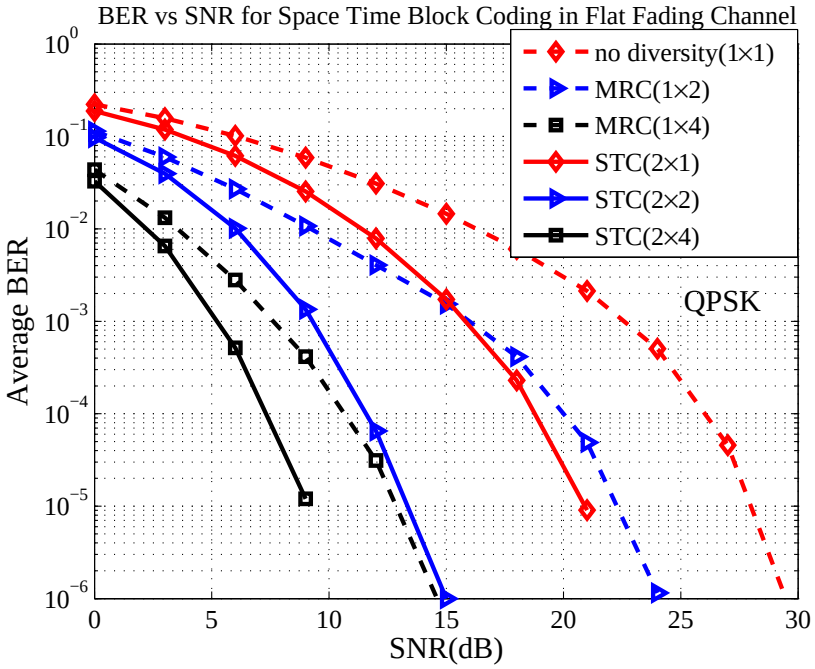

(a) BER

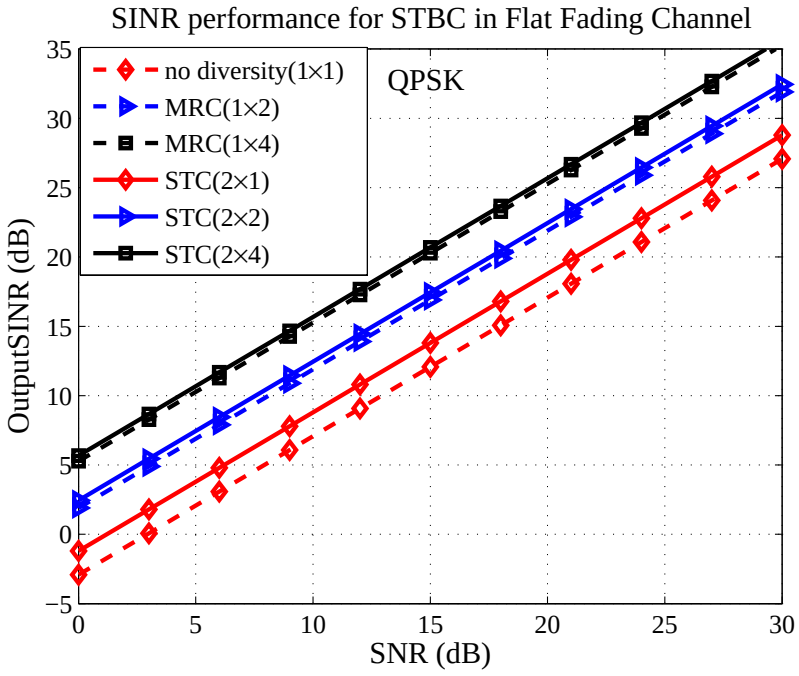

(b) Output SINR

Figure 2.6: The comparison of BER and output SINR for STBC and MRC in frequency flat fading channels.

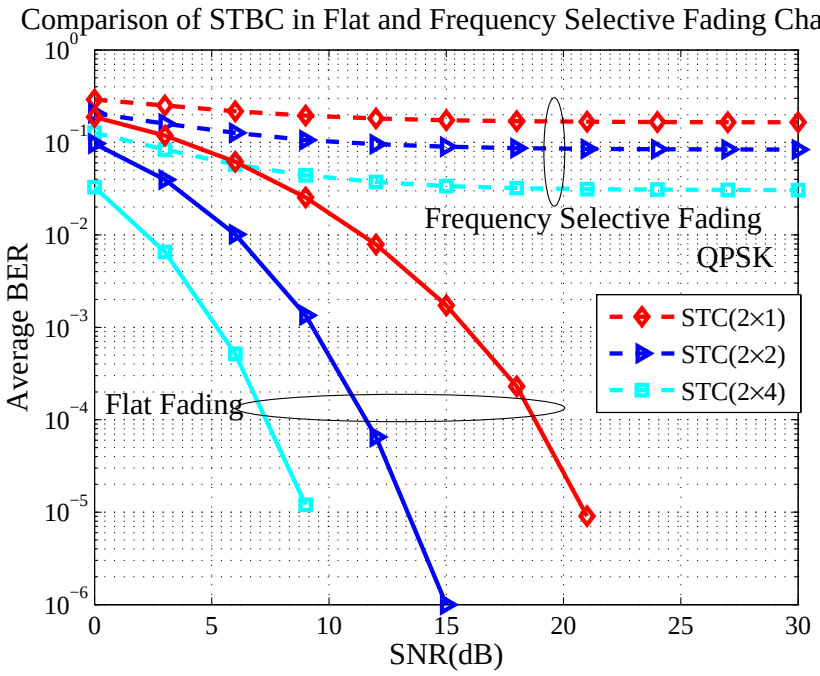

(a) BER

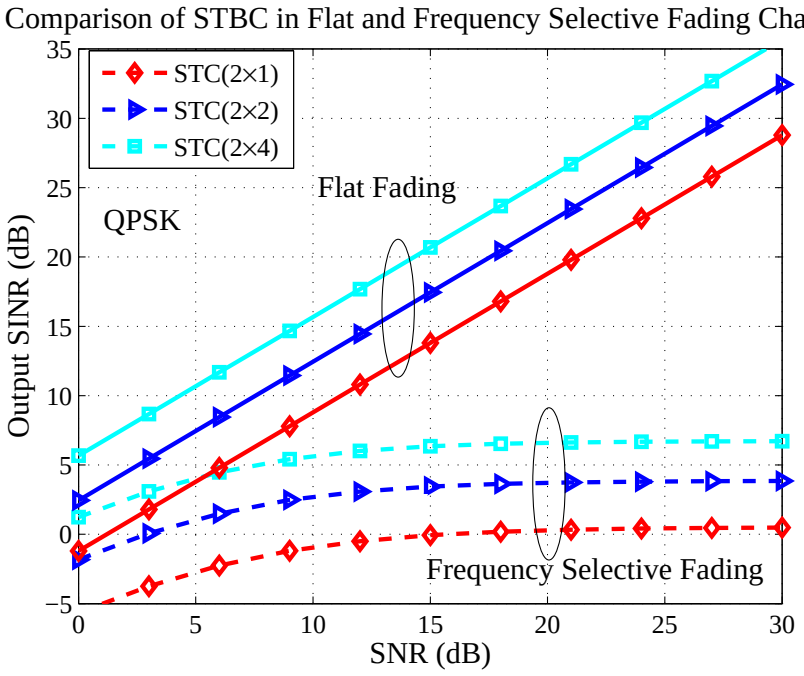

(b) Output SINR

Figure 2.7: Performance comparison of STBC in flat and frequency selective fading channels.

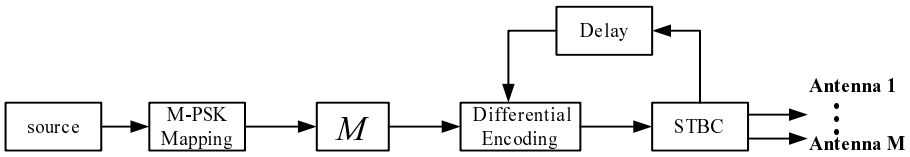

(a) D-STBC encoding

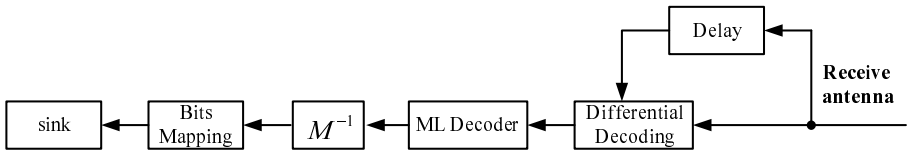

(b) D-STBC decoding

Figure 2.8: Block diagrams of D-STBC encoding and decoding.

between consecutive phases to yield the information sequence. This process causes error propagation, which leads to degradation in performance as compared with coherent demodulation. While differential demodulation has been primarily used in single transmit antenna systems, the concept can be also applied to transmit diversity schemes to solve practical issues such as the need for accurate channel estimation at the receiver and carrier recovery. Differential space-time modulation approaches have been proposed and investigated in [24, 25]. Here, we adopt the scheme proposed in [24] as an extension to the family of space-time block codes.

The Encoding Algorithm

The transmitter block diagram for D-STBC is illustrated in Fig. 2.8(a). The information bits are packed into groups of b bits each and mapped by the following $\mathcal{M}$-ary PSK mapper:

$$A = \{\frac{1}{\sqrt{(2)}} \exp \frac{j2\pi k}{\mathcal{M}}\} \tag{2.47}$$

We denote (a_1, a_2) as our reference pair (constant and known at the receiver) or $\mathcal{M}$-ary PSK symbols. Grouping a pair of new $\mathcal{M}$-ary PSK constellation symbols, denoted as (a_3, a_4), the mapping M performs change of basis according to Alamouti's orthogonal design. That is, the column of G_2, $(-x_2^*, x_1^*)$, are used as orthonormal vectors to span the new basis. The pair of symbols (a_3, a_4) in the new basis are denoted by (A, B) and given by

$$A = a_3 a_1^* + a_4 a_2^*, \tag{2.48}$$

$$B = -a_{3a2} + a_4 a_1. \tag{2.49}$$

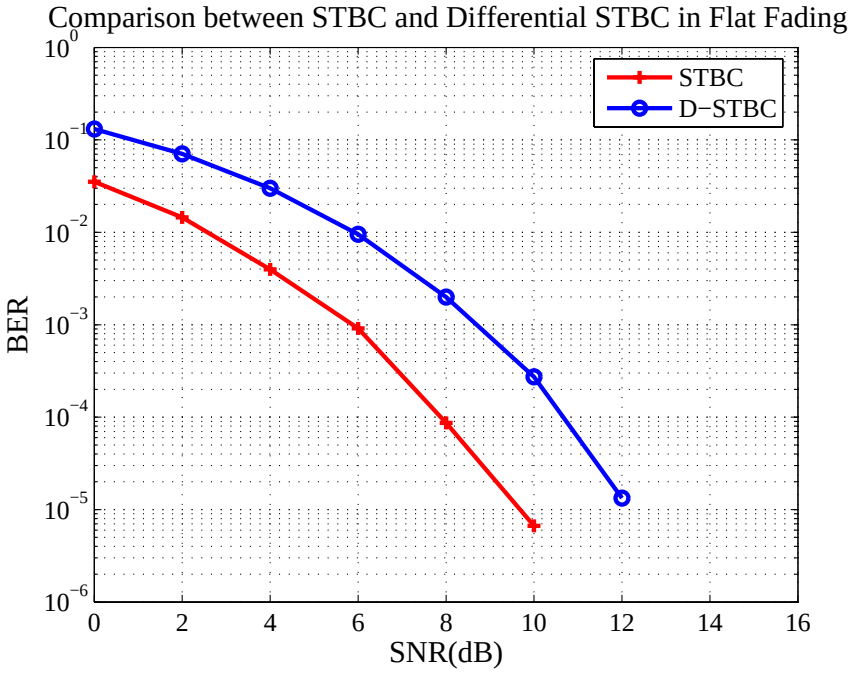

Figure 2.9: Performance comparison of STBC and Differential STBC in flat fading channel with BPSK modulation.

Note that this mapping is an isometric mapping, thus preserving distance properties. Thus, the distance between two vectors in the natural basis is equal to distance between vectors in the new basis. This property will be used by performing maximal likelihood decoding over the vector (A, B) to decode for the pair (a_3, a_4). Next, differential encoding is performed across set of symbols:

$$s(2t+1) = As(2t-1) - Bs(2t)^*, \tag{2.50}$$
$$s(2t+2) = As(2t) + Bs(2t-1)^*, \tag{2.51}$$

where (A, B) is the pair of new symbols in the G_2 basis, $(s(2t), s(2t-1))$ is the previously transmitted pair of symbols from antenna 1 and 2 respectively, at time $(2t-1)$, and $(s(2t+1), s(2t+2))$ is the current differentially encoded pair of symbols to be transmitted text. This new pair of symbols is fed into the space-time block encoder, described by G_2, to create the following two pairs of symbols: $(s(2t+1), -s(2t+2)^*)$ and $(s(2t+2), s(2t+1)^*)$ that are transmitted from antennas 1 and 2 respectively at times $(2t+1)$ and $(2t+2)$. The pair $(s(2t+1), s(2t+2))$ is fed back to the differential encoder for the next iteration where the set $(s(2t+3), s(2t+4))$ is produced. This process continues in an inductive manner until the end of the frame.

The Decoding Algorithm

The receiver block diagram for differential STBC is illustrated in Fig. 2.8(b). Let us assume that the receiver is equipped with a single antenna element. The extension to N receive antenna element is straightforward. Let us denote $r(2t-1), r(2t), r(2t+1), r(2t+2)$ as four consecutive samples at the matched filter output. In quasi-static frequency flat fading channel, the received signals are modeled by:

$$\begin{aligned} r(2t-1) &= h_{11}s(2t-1) - h_{12}s(2t) + n(2t-1), \\ r(2t) &= -h_{11}s(2t)^* + h_{12}s(2t-1)^* + n(2t), \\ r(2t+1) &= h_{11}s(2t+1) - h_{12}s(2t+2) + n(2t+1), \\ r(2t+2) &= -h_{11}s(2t+2)^* + h_{12}s(2t+1)^* + n(2t+2). \end{aligned} \tag{2.52}$$

where $n(i), i = [2t-1, 2t, 2t+1, 2t+2]$ represents the AWGN term in consecutive time samples. Differential decoding is performed by the following operations:

$$\begin{aligned} R_1 &= r(2t+1)r(2t-1)^* + r(2t+2)r(2t)^*, \\ R_2 &= r(2t+1)r(2t)^* - r(2t+2)r(2t-1)^*. \end{aligned} \tag{2.53}$$

Plugging Eq. (2.52) into Eq. (2.53) and some algebraic manipulations, R_1 and R_2 are simplified to:

$$\begin{aligned} R_1 &= (|h_{11}|^2 + |h_{12}|^2)A + \mathcal{N}_1 \\ R_2 &= (|h_{11}|^2 + |h_{12}|^2)B + \mathcal{N}_2. \end{aligned} \tag{2.54}$$

where $\mathcal{N}_1$ and $\mathcal{N}_2$ represent the effective noise terms (composed of noise cross signal terms and noise cross noise terms) of the decision statistics R_1 and R_2. Thus, differential decoding procedure, described by Eq. (2.53), performs decoupling of the pair of symbols and yields separate decision statistics for A and B, respectively. Moreover, observing Eq. (2.54), we see the optimal combining of the fade coefficients, similar to 2-fold diversity of maximal ratio combining (MRCC). Since the vector (A, B) has a unit length regardless if the sequence if $2b$ information bits associated with it, a maximum likelihood decision rule is applied by choosing the closest vector(A, B) to (R_1, R_2) out of the 2^{2b} possible candidates. The decision $(\tilde{A}, \tilde{B})$ is transformed back to $2b$ decoded bits by inverse M-mapping rule. The differential decoding followed by MLD rule continues in an inductive manner until all frame components are decoded.

The extension to N elements at the receiver is performed by following equal gain combining rule over the decision statistics:

$$\begin{aligned} \tilde{R}_1 &= \textstyle\sum_{j=1}^{N} R_1^j, \\ \tilde{R}_2 &= \textstyle\sum_{j=1}^{N} R_2^j. \end{aligned} \tag{2.55}$$

where R_1^j and R_2^j are computed per receive antenna j using (2.53). $(\tilde{R}_1, \tilde{R}_2)$ is the combined decision statistics vector which can be described by

$$\begin{aligned} \tilde{R}_1 &= (\textstyle\sum_{j=1}^{N} \sum_{i=1}^{2} |h_{j,i}|^2)A + \tilde{N}_1, \\ \tilde{R}_2 &= (\textstyle\sum_{j=1}^{N} \sum_{i=1}^{2} |h_{j,i}|^2)B + \tilde{N}_2. \end{aligned} \tag{2.56}$$

Thus, diversity advantages of $2 \times N$ is achieved. Note that, the decoding scheme is not based on knowledge of tracking of the fade coefficients.

Figure 2.3.1 show the performance comparison between STBC and D-STBC in the frequency flat fading channel (for BPSK modulated signal with 2×2 MIMO system).

2.3.2 Space-Time Trellis Codes (STTCs)

Encoding and Decoding Algorithms

A system model for a STTC is given in Fig. 2.3.2. STTC scheme contain M transmit antennas and possibly N receive antenna elements. The data stream is encoded by the channel code and then split into M parallel transmission chains. The channel code creates the inter-relations between signals in the space-domain (different antenna elements) and signals in the time domain (consecutive time symbols). A STTC encoder maps each k input bits into M $\mathcal{M}$-ary symbol which are simultaneously transmitted using M transmit antennas. Each transition in the trellis diagram corresponds to M symbols that are transmitted simultaneously over the channel. The values of $\mathcal{M}$-ary symbol are based on the k input bits, v state bits and generator polynomial $g_i, i = [i, 2, \ldots, M]$. Thus, a generator matrix with the size $(k + v) \times M$ can entirely define the STTC. In Fig. 2.3.2, $c_t^i, i = [1, 2, \ldots, M]$ are the M symbols that are simultaneously transmitted at symbol time t over the wireless link. As example, trellis diagram of STTC with 4 or 8 state, QPSK modulation, and 2 transmit antenna elements are described in Fig. 2.3.2. Note that each trellis transition is labeled with a pair of QPSK symbol that are transmitted simultaneously from antenna 1 and 2, respectively. Also, the four transition that diverge from and merge into each node correspond to all possible combinations of 2 information bits.

Assuming a frequency flat fading channel, the signal at each receive antenna $j, \ := \{1, 2, \ldots, N\}$, is a linear superposition of the N simultaneously received signals, weighted by fading coefficients and corrupted by noise. The signal received by antenna j, at time t, can be modeled as:

$$r_j^t = \sum_{i=1}^{M} h_{j,i} c_t^i + n_t^j \tag{2.57}$$

where n_t^j denotes the AWGN term and is modeled as independent samples of a zero mean complex Gaussian random variable with $\frac{\mathcal{N}_0}{2}$ per dimension.

The channel is modeled by $N \times M$ matrix $\boldsymbol{H} = [h_{j,i}]$, whose the $h_{j,i}$ represents the complex fade coefficient for the path from transmit antenna i to receive antenna j. These coefficients are assumed to be independent complex Gaussian random variables with possibly nonzero complex mean and variance 0.5 per dimension. The channel is assumed to be quasi-static, flat fading channel such that no channel induced the ISI.

The receiver is based upon estimation of the channel coefficients followed by a MLSE decoder, which computes the lowest accumulated square Euclidean distance metric to extract the most likely transmitted sequence. The branch metric of the MLSE decoder is

based on the squared Euclidean distance between the received signal and each candidate set of M transmitted codeword, denoted $e_t^i, i = [1, 2, \ldots, M]$. Assuming perfect knowledge of CSI (the $h_{j,i}$) at the receiver, this metric is given by,

$$\sum_{j}^{N} |r_j^t - \sum_{i=1}^{M} h_{j,i} e_t^i|^2. \tag{2.58}$$

Note that, the receiver diversity takes the form of equal gain combining. Figure 2.3.2 shows the performance of 4 and 8 state STTC for 2×1 and 2×2 MIMO in flat fading channel.

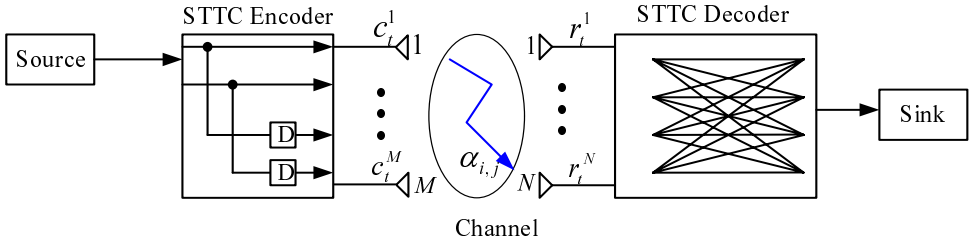

Figure 2.10: STTC system model.

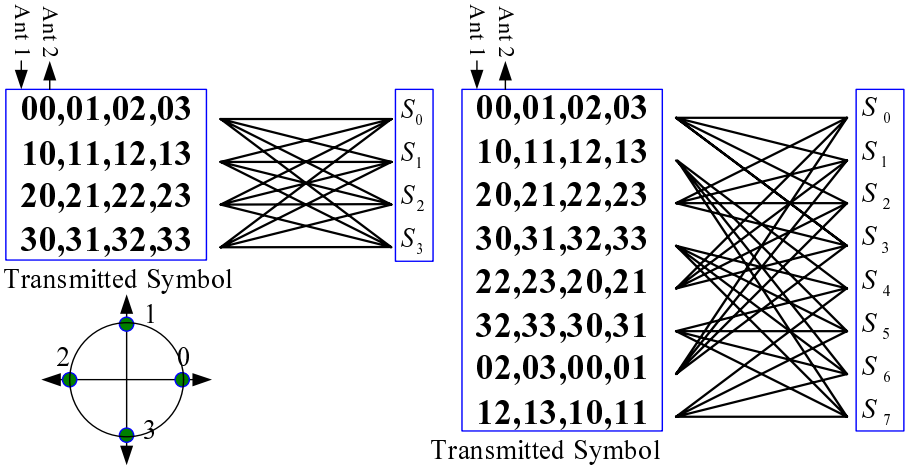

Figure 2.11: 4 and 8 state STTC with QPSK modulation.

2.3.3 Bell Labs Layered Space-Time Architecture (BLAST)

The design of the BLAST test bed system was motivated by the information theoretic results of Foschini and Gans in [4], showing the enormous capacity growth with the use

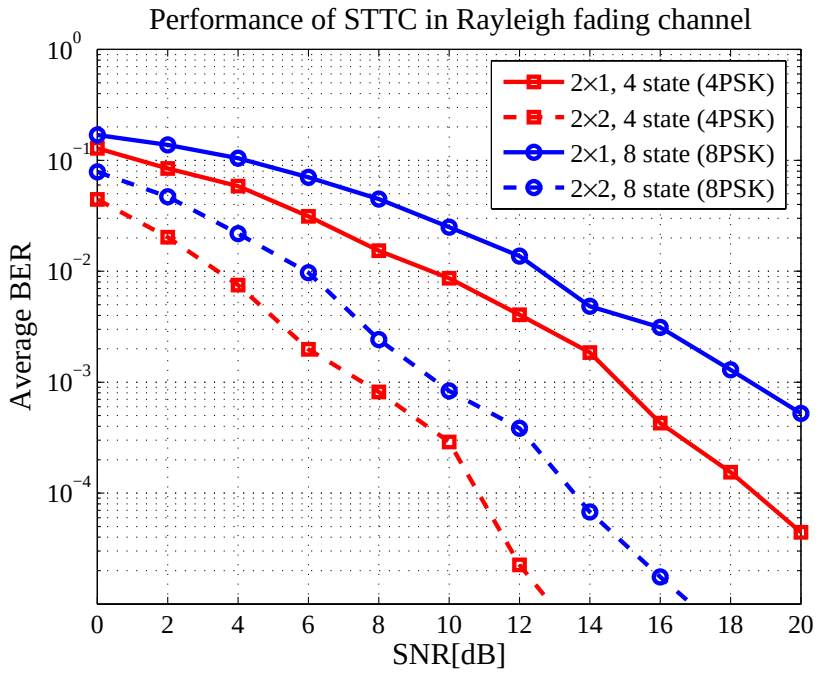

Figure 2.12: Performance of 4 and 8 state STTC for 2×1 and 2×2 MIMO in flat fading channel.

of multiple element array technology. The BLAST architecture (with 8 or 16 antenna elements in both ends of the wireless link) demonstrates unprecedented data rates over a rich scattering environment such as indoor wireless channel. A throughput of 621 kbps over a narrow band channel of 30 kHz was demonstrated in an indoor environments. Thus, spectral efficiencies at the order of 20 bps/Hz was achieved. An essential feature of BLAST is that there is no mechanism, such as *time, frequency or code-division multiplexing* that assures an orthogonality across sequences transmitted from the different transmitter antenna elements. Rather, the propagation environment itself, which is assumed to exhibit significant multipath, is exploited to separate the signals at the receiver. Two main BLAST schemes were proposed in the literature. The V-BLAST scheme [47] known as the vertical BLAST and corresponds to a vertical mapping of symbols onto the space domain such that a simultaneous transmission from all transmit antennas is performed without any sub-stream coding. That is, each transmitter operates as a conventional QAM transmitter. The second scheme, known as D-BLAST [2], is a diagonally layered space time architecture, in which inter sub-stream coding is introduced across diagonals in space-time. Here, only the V-BLAST is considered.

Figure 2.3.2 show the block diagram of V-BLAST. The received signal vector is given by following matrix equation:

$$\boldsymbol{r} = \boldsymbol{H}\boldsymbol{a} + \boldsymbol{n} \tag{2.59}$$

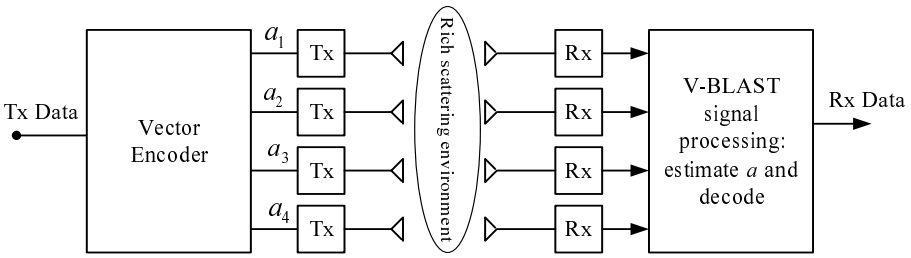

Figure 2.13: V-BLAST system.

where $\boldsymbol{H}$ represents the channel coefficient matrix with size $N \times M$, $\boldsymbol{a}$ is the transmitted vector with size $M \times 1$, which composed of a set of symbols, each of which is a member of QAM constellation. $\boldsymbol{n}$ represents a vector of independent samples of AWGN over N receive antennas. The V-BLAST receiver performs channel estimation based on pilot symbols and then sorts the channel on these channel estimates. The sorting algorithm determines the order in which the various transmitted component will be decoded. Nulling is performed by linearly weighting the received signals in order to minimize a given cost function, such as the mean minimum square error (MMSE) or zero forcing (ZF) detector. As an example, ZF nulling is performed by finding the weight vector, $\tilde{\boldsymbol{w}}_i$ which satisfies:

$$\boldsymbol{w}_i^T \boldsymbol{H}_j = \delta_{i,j} \tag{2.60}$$

where $\boldsymbol{H}_j$ is the jth column of the channel matrix $\boldsymbol{H}$, and $\delta_{i,j}$ is the Kronecker delta function. Thus the decision statistics for the ith sub-stream (signal from transmit antenna i) is given by:

$$\boldsymbol{y}_i = \boldsymbol{w}_i^T \boldsymbol{r}. \tag{2.61}$$

Next the receiver slice $\boldsymbol{y}_i$ to perform decision for $\boldsymbol{a}_i$ and regenerates the contribution of $\boldsymbol{a}_i$ in order to subtract it from the received vector, which can be shown as:

$$\boldsymbol{r}_{i+1} = \boldsymbol{r}_i - \hat{\boldsymbol{a}}_i \boldsymbol{H}_i \tag{2.62}$$

where $\hat{\boldsymbol{a}}_i$ are the decisions of $\boldsymbol{a}_i$. The process of linear nulling decision rule and symbol cancellation is performed successively until all components of the $\boldsymbol{a}$ vector are recovered. Note that, the sorting algorithm is performed each iteration and enhances system performance.

Figure 2.3.2 shows the comparative simulation results for maximum likelihood (ML), MMSE, and ZF using V-BLAST systems. This was 2×2 system with QPSK modulation. The results show that ML is the best in performance followed by MMSE and ZF. The power is normalized across the transmit antennas and the channel is a slow Rayleigh fading channel.

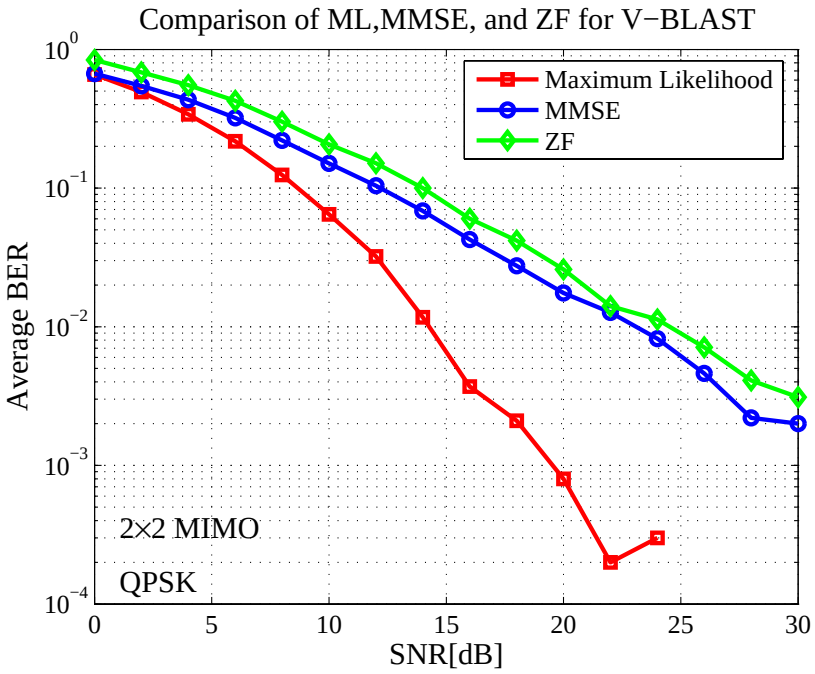

Figure 2.14: Performance comparison of ML , MMSE and ZF for 2×2 V-BLAST using QPSK modulation in Rayleigh channel.

2.4 Conclusion

Fundamentals of space-time coding techniques were introduced in this chapter. The class of space-time block coding was shown to be a simple transmit diversity mechanism that achieves the same diversity advantage of MRC. STBC is composed of three stages: encoding procedure which is based on orthogonal design, a combining procedure in time domain that decouples the symbols associated with the received superposition and a symbol-by-symbol ML detection rule. Orthogonal designs for more than two antenna elements at the transmitter were presented. From the performance evaluation, it is shown that STBC is working very well in flat fading channel, however the performance degradation is shown over frequency selective fading channel, due to the presence of ISI. Moreover, Differential STBC was introduced as an option for transmit diversity scheme that does not require explicit knowledge of CSI and is robust to carrier recovery mismatch. The encoding and decoding mechanisms of space-time trellis codes were described followed by performance evaluation. Finally, the BLAST architecture was presented, achieving high data rates using multiple antenna array technology.

Armed with the fundamentals of space-time coding techniques, we will focus on STBC. In the following chapters of this dissertation, we introduce original contributions to overcome the ISI and MAI.

Chapter 3

Fundamentals of Adaptive Arrays

This chapter presents the principal concepts of adaptive array. In particular, this chapter covers array signal models, types of beamforming, optimization criteria, and adaptive signal processing algorithms for adaptive arrays. The benefits of using adaptive arrays in wireless communications are also discussed. Furthermore, the conventional applications of adaptive arrays to exploit diversity gain, namely TDLAA and SBAA, are introduced.

3.1 Basic Concepts of Adaptive Arrays

An adaptive arrays [37,50,56,57,75] is a system consisting of an array of antenna elements and a real-time adaptive processor which control the beamforming network to automatically adjust its control weights toward optimization of a certain criterion. Sometimes adaptive arrays also are referred to as *adaptive antennas* or *smart antennas*. An adaptive array is illustrated in the Fig. 3.1.

Consider a uniform spaced linear array with N elements illustrated in Fig. 3.2, with antenna separation d. Assume that a plane wave incident at the array forms a direction θ off the broadside. The angle θ, measured clockwise from the array broadside, is called the direction of arrival (DOA) or angle of arrival (AOA). The wavefront at the $(j+1)$th element is later than at the jth element with the different distance of $d \sin\theta$.

Let us take the first element as the reference element and let the signal at the reference element as $x(t)$, then the phase delay of the signal at the element j relative to element 1 is $(j-1)kd \sin\theta$, where $k = \frac{2\pi}{\lambda}$ is the wave number and λ is the wavelength. The receive signal $y_m(t)$, at the jth element is given as

$$y_m(t) = x(t)e^{-\mathrm{j}\frac{2\pi}{\lambda}(j-1)d\sin\theta} \tag{3.1}$$

for $j = 1, 2, \ldots, N$, and $x(t)$ is a complex sinusoidal wave signal. It should be noted that (3.1) holds for signals with bandwidth much smaller than the reciprocal of the propagation time across the array. Any signal satisfies this condition is referred to as the *narrowband*, otherwise it is called *wideband* as shown below.

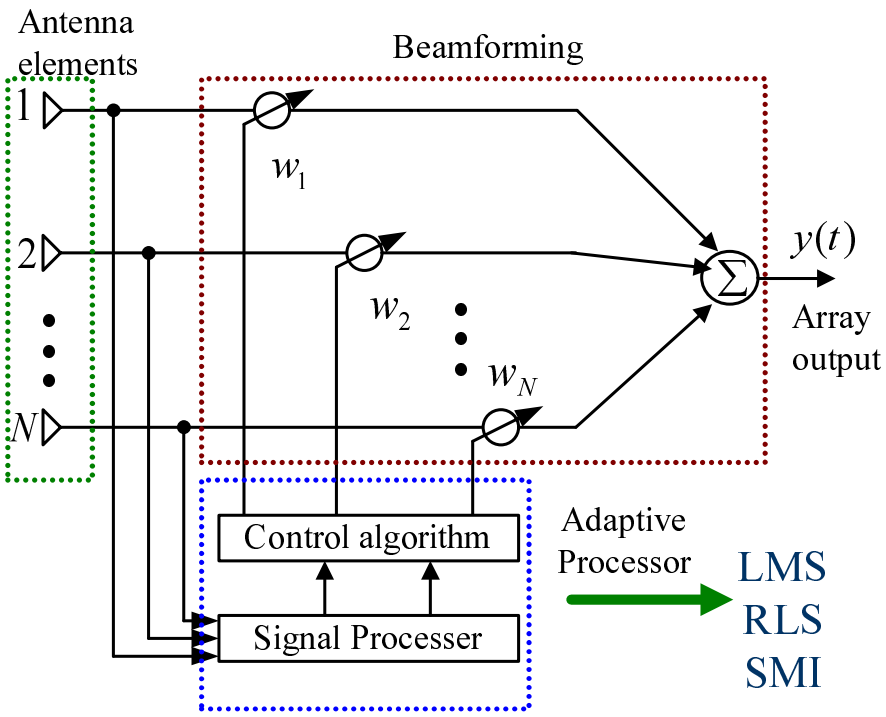

Figure 3.1: An adaptive array with N elements.

We introduce the vector as

$$\boldsymbol{y}(t) = [y_1(t)\ y_2(t)\ \ \ldots y_N(t)]^T \tag{3.2}$$

and let

$$\boldsymbol{a}(\theta) = [1\ e^{-\mathrm{j}\frac{2\pi}{\lambda}d\sin\theta}\ \ \ldots\ \ e^{-\mathrm{j}\frac{2\pi}{\lambda}(N-1)d\sin\theta}]^T. \tag{3.3}$$

Then (3.2) can be expressed as

$$\boldsymbol{y}(t) = x(t)\boldsymbol{a}(\theta). \tag{3.4}$$

Here, vector $\boldsymbol{y}(t)$ is called the array *input signal* and $\boldsymbol{a}(\theta)$ is called the *array response vector* or the *steering vector*. The array response vector depends only on the AOA. In general, it may also depend on the individual element response, the array geometry, and signal frequency. The set of array response vectors over all directions and frequencies is known as the *array manifold*. For simple array such as uniformly spaced linear array as considered here, the array manifold can be analytically computed. In practice, however it is measured as point source responses over various directions and various frequencies and this process of obtaining the array manifold is referred to as *array calibration*.

Considering the noise in the receiver, the input data vector at the receiver will become as

$$\boldsymbol{y}(t) = x(t)\boldsymbol{a}(\theta) + \boldsymbol{n}(t), \tag{3.5}$$

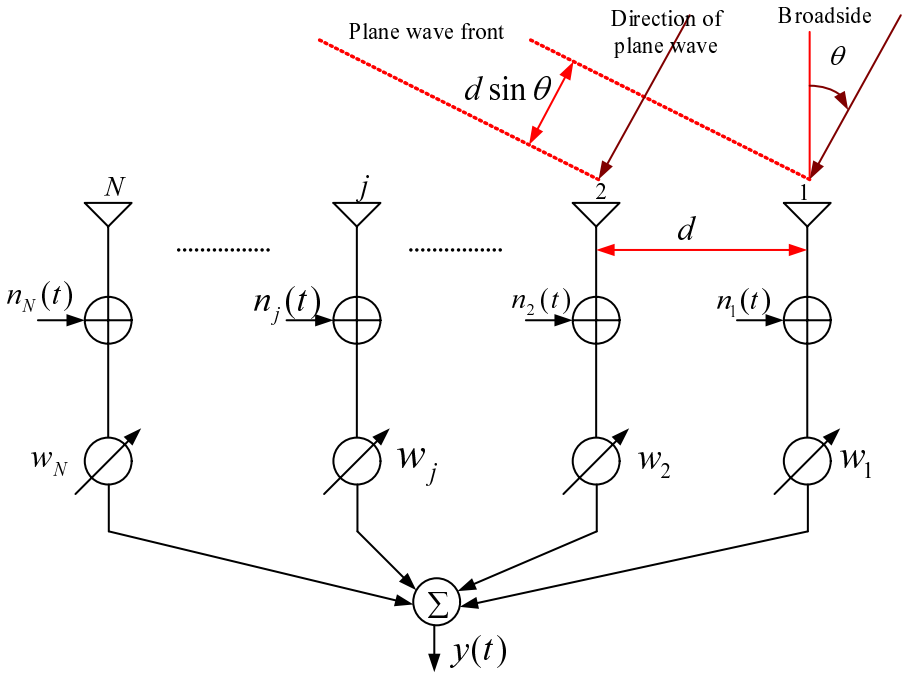

Figure 3.2: Model of adaptive array.

where $\boldsymbol{n}(t)$ has been defined as

$$\boldsymbol{n}(t) = [n_1(t)\ n_2(t)\ \ldots n_N(t)]^T. \tag{3.6}$$

We now consider the array signal for more general case with multipath and multiuser effects. Let $p = \{1, 2, \ldots, P\}$, and let P denote the total number of users with signals impinging on array, and let us assume that the incident signal of the pth user $x_p(t)$ contains L_p multipaths with complex amplitudes $\vartheta_{p,l}$, angles of arrival $\theta_{p,l}$, and path delays $\tau_{p,l}$, where l is the path index and $l = 1, 2, \ldots, L_p$. The received signal vector for the pth user can be expressed as

$$\boldsymbol{x}_p(t) = \sum_{l}^{L_p} \vartheta_{p,l}\boldsymbol{a}(\theta_{p,l})s_{p,l}(t - \tau_{p,l}). \tag{3.7}$$

Considering the effects of P users and noise, the receive vector can be written in a generalized form as

$$\boldsymbol{y}(t) = \sum_{p=1}^{P}\sum_{l=1}^{L_p} \vartheta_{p,l}\boldsymbol{a}(\theta_{p,l})x_{p,l}(t - \tau_{p,l}) + \boldsymbol{n}(t). \tag{3.8}$$

Equation (3.7) and (3.8) are called the spatial signature vector of pth user.

3.1.1 Adaptive Beamforming and Spatial Filtering

Beamforming is one type of signal processing used to focus the array beams toward the desired signal sources while simultaneously create null toward interferences. This process of separating desired user from the interferences based on their spatial positions is called *spatial filtering*. In the reverse link or uplink (from mobile to base-station), the objective of beamforming is to maximize the signal to interference plus noise ratio (SINR) of the received desired signal. Similarly, for the forward link or downlink (from base station to mobile), beamforming is utilized to maximize the transmit power of the base station to desired mobile, thereby maximizing the SINR of the downlink. When beamforming is controlled with adaptive signal processing, it is called *adaptive beamforming*.

A *beamformer* is a processer used in conjunction with an array to perform spatial filtering [38], which can be categorized as *narrowband beamformer* and *wideband beamformer*. A narrowband beamformer samples input signals in spatial domain and typically used to process narrowband signals. The configuration of a narrowband beamformer is depicted in Fig. 3.3. The output of the narrowband beamformer are weighted and combined as

$$y(t) = \boldsymbol{w}^H \boldsymbol{x}(t), \tag{3.9}$$

where $\boldsymbol{x}(t)$ is received data vector, and $\boldsymbol{w}$ is the complex weight vector which is defined as

$$\boldsymbol{w} = [w_1 \; w_2 \; \ldots \; w_N]^T. \tag{3.10}$$

Different from the narrowband beamformer, a wideband beamformer samples input signals in both spatial and temporal domains and is employed to process wideband signals. It is also called *spatio-temporal processor* or *spatio-temporal equalizer*. The structure of a wideband beamformer contains tapped delayed lines (TDLs) or also called transversal filters in individual array elements. If the tap spacing is sufficiently small and the number of taps is large, the TDL approximates an ideal filter that allows exact control of gain and phase at each frequency within the band of interest [39]. The TDL is not only useful for providing desired adjustment to gain and phase over the frequency band of interest in wideband signal, but also suited for other purposes such as mitigation of multipath fading and compensation for effects of finite array propagation delay and interchannel mismatch [50]. A typical tapped delayed line beamformer is shown in Fig. 3.4. The TDLs beamformer (also known as *Tapped Delayed Line Adaptive Array*) is arrange with L_r TDL-taps of antenna m as

$$\begin{aligned} \acute{\boldsymbol{x}}(t) &= [x_m(t) \; x_m(t - T_s) \; \ldots \; x_m(t - [L_r - 1]T_s)]^T & (3.11) \\ \acute{\boldsymbol{w}}_m &= [w_{m1} \; w_{m2} \; \ldots \; w_{mK}]^T, & (3.12) \end{aligned}$$

and the receive signal will be given as

$$\begin{aligned} \boldsymbol{x}(t) &= [\acute{\boldsymbol{x}}_1^T(t) \; \acute{\boldsymbol{x}}_2^T(t) \; \ldots \; \acute{\boldsymbol{x}}_N^T(t)]^T & (3.13) \\ \boldsymbol{w}_m &= [\acute{\boldsymbol{w}}_1^T \; \acute{\boldsymbol{w}}_2^T \; \ldots \; \acute{\boldsymbol{w}}_N^T]^T. & (3.14) \end{aligned}$$

The output of the wideband beamformer can be expressed as below.

$$y(t) = \boldsymbol{w}^H \boldsymbol{x}(t). \tag{3.15}$$

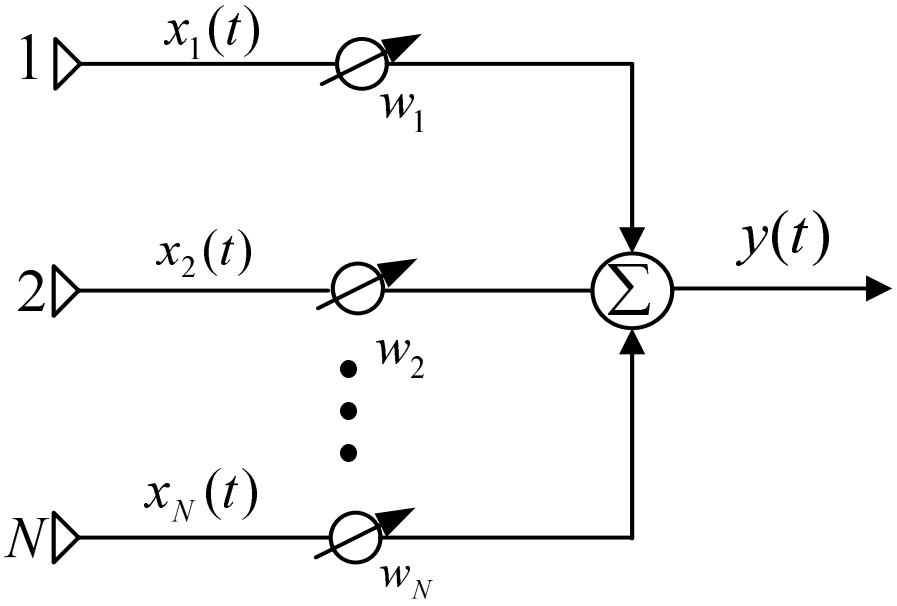

Figure 3.3: Configuration of an adaptive narrowband beamformer.

The wideband beamformer using TDLs considered so far is a classical time domain processor. Recently, fast Fourier transform (FFT) has been used to replace TDLs in the beamformer configuration resulting in an equivalent frequency domain wideband beamformer as shown in Fig. 3.5 [38, 40]. The advantage of the frequency domain approach is achievement of reduced computational load and increased convergence rate. Since the control weights are obtained independently for each subband (frequency bin), the process of selecting the weights can be performed in parallel, leading to faster weight update. Moreover, when adaptive algorithm such as the least mean square (LMS) is used, different step sizes can be applied to different subbands, resulting in faster convergence.

Weight optimization

As mentioned in the previous section, the adaptive processor controls the beamforming network to optimize the beamforming weights according to a criterion. There are four criteria commonly used in wireless communication to optimize the weight: minimum mean square error (MMSE), Maximum Signal to Interference plus Noise Ratio (MSINR), Minimum Variance (MV) and Maximum Likelihood (ML). Since we will adapt the MMSE in this work, here we only describe the MMSE.

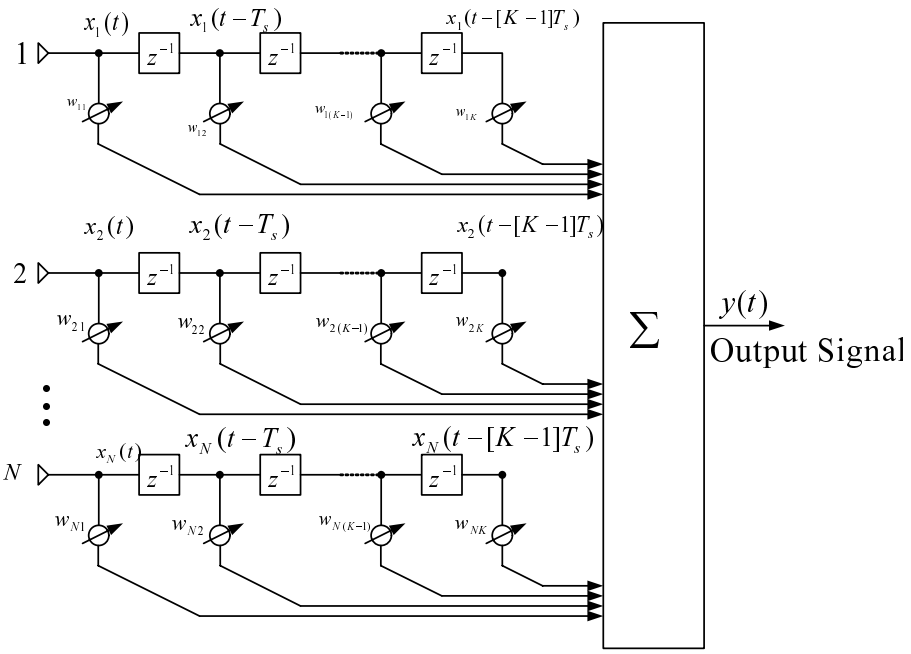

Figure 3.4: Wideband beamformer using tapped delay lines.

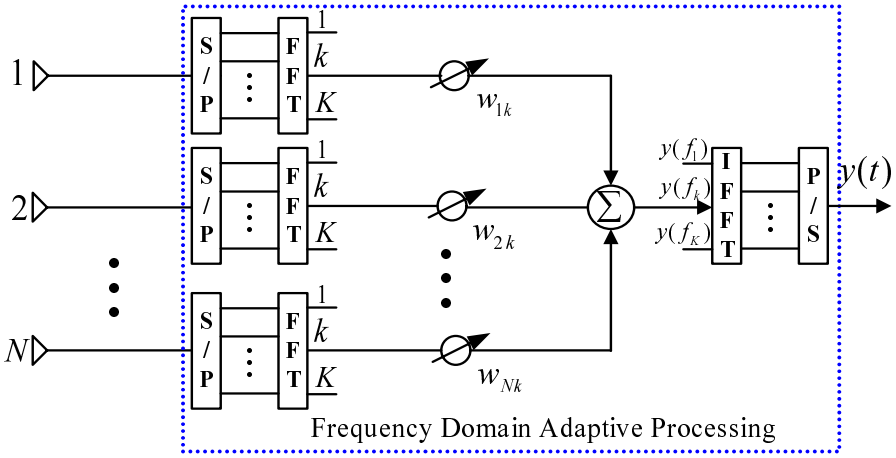

Figure 3.5: Frequency domain beamformer using FFT/IFFT.

The MMSE criterion is first considered by Widrow *et al.* in [50]. The criterion make the array strive to minimize the error between the array output signal $y(t)$ and the desired signal $s(t)$. In practice, the desired signal $s(t)$ is unknown. However, using some techniques such as training method or estimation based on the desired signal characteristics, one can generate the *reference signal* $r(t)$ that closely approximates the desired signal to a certain extent.

Consider the input signal vector given by

$$\begin{aligned} \boldsymbol{x}(t) &= s(t)\boldsymbol{a}(\theta) + \boldsymbol{n}(t) && (3.16)\\ &= \boldsymbol{s}(t) + \boldsymbol{n}(t), && (3.17) \end{aligned}$$

where $\boldsymbol{a}(\theta)$ is the array response and $\boldsymbol{n}(t)$ is a vector containing zero mean noise and uncorrelated interferences. For a narrowband adaptive array, the output signal is recalled from (3.9),

$$y(t) = \boldsymbol{w}^H \boldsymbol{x}(t). \tag{3.18}$$

The error signal is defined as

$$\begin{aligned} \epsilon(t) &= r(t) - y(t) && (3.19)\\ &= r(t) - \boldsymbol{w}^H \boldsymbol{x}(t), && (3.20) \end{aligned}$$

and the weights are chosen to minimize the mean square error (MSE), which is given by

$$E[|\epsilon(t)|^2] = E[|r(t) - y(t)|^2]. \tag{3.21}$$

Expanding (3.21),

$$\begin{aligned} E[|\epsilon(t)|^2] &= E[|r(t)|^2] - \boldsymbol{w}^T E[\boldsymbol{x}^*(t) r(t)] - \boldsymbol{w}^H E[\boldsymbol{x}(t) r^*(t)] + \boldsymbol{w}^H E[\boldsymbol{x}(t)\boldsymbol{x}^H(t)]\boldsymbol{w} \\ &= E[|r(t)|^2] - \boldsymbol{w}^T \boldsymbol{r}_{xr}^* - \boldsymbol{w}^H \boldsymbol{r}_{xr} + \boldsymbol{w}^H \boldsymbol{R}_{xx} \boldsymbol{w} && (3.22) \end{aligned}$$

where $\boldsymbol{r}_{xr} = E[\boldsymbol{x}(t) r^*(t)]$ and $\boldsymbol{R}_{xx} = E[\boldsymbol{x}(t)\boldsymbol{x}^H(t)]$ are called the *correlation vector* and *covariance matrix*, respectively. The optimum weight can be found by setteing the gradient of (3.22) with respect to $\boldsymbol{w}$ equal to zero [37] as

$$\bigtriangledown_{\boldsymbol{w}} E[|\epsilon(t)|^2] = -2\boldsymbol{r}_{xr} + 2\boldsymbol{R}_{xx}\boldsymbol{w} = 0, \tag{3.23}$$

which gives the solution

$$\boldsymbol{w}_{MMSE} = \boldsymbol{w}_{opt} = \boldsymbol{R}_{xx}^{-1} \boldsymbol{r}_{xr}. \tag{3.24}$$

Equation (3.24) is often referred to as the *Wiener-Hopf equation* or the *optimum Wiener solution*. By substituting (3.24) into (3.22), we have the MMSE

$$MMSE = E[|\epsilon(t)|^2] = E[|r(t)|^2] - \boldsymbol{r}_{xr}^H \boldsymbol{R}_{xx} \boldsymbol{r}_{xr}. \tag{3.25}$$

3.1.2 Adaptive Algorithm

Least Mean Square (LMS)

The least mean squares (LMS) is the most popular adaptive algorithm for continuous adaptation [50,56]. The algorithm is based on the steepest descent method, which choose the weight vector to minimize the ensemble average of the error squares toward the MSE. Using the steepest descent method, the updated weight vector at time $(n+1)$ is given by

$$\boldsymbol{w}(n+1) \quad = \boldsymbol{w}(n) - \tfrac{\mu}{2} \bigtriangledown \mathrm{E}[\epsilon^2(n)], \tag{3.26}$$

where μ is the step size which control the convergence characteristics of $\boldsymbol{w}(n)$

$$0 < \mu < \frac{1}{\lambda_{max}} \tag{3.27}$$

Here λ_{max} is the largest eigenvalue of the covariance matrix $\boldsymbol{R}_{xx}$. From (3.23), we have

$$\bigtriangledown \boldsymbol{w} \mathrm{E}[|\epsilon(t)|^2] \quad = \quad -2\boldsymbol{r}_{xr} + 2\boldsymbol{R}_{xx}\boldsymbol{w}(n) \tag{3.28}$$

Substituting (3.28) into (3.26), we have

$$\boldsymbol{w}(n+1) \quad = \boldsymbol{w}(n) + \mu[\boldsymbol{r}_{xr} + \boldsymbol{R}_{xx}\boldsymbol{w}(n)]. \tag{3.29}$$

In order to update the optimum weight using (3.29), it is necessary to know in advance both $\boldsymbol{R}_{xx}$ and $\boldsymbol{r}_{xr}$, and it is better to use their instantaneous values

$$\begin{aligned} \boldsymbol{R}_{xx} &= \boldsymbol{x}(n)\boldsymbol{x}^H(n), \\ \boldsymbol{r}_{xr} &= \boldsymbol{x}(n)r^*(n). \end{aligned} \tag{3.30}$$

Thus, (3.29) will become

$$\begin{aligned} \boldsymbol{w}(n+1) &= \boldsymbol{w}(n) + \mu\boldsymbol{x}(n)[r^*(n) - \boldsymbol{x}^H(n)\boldsymbol{w}(n)] \\ \boldsymbol{w}(n+1) &= \boldsymbol{w}(n) + \mu\boldsymbol{x}(n)[r^*(n) - y^*(n)] \\ \boldsymbol{w}(n+1) &= \boldsymbol{w}(n) + \mu\boldsymbol{x}(n)\epsilon^*(n). \end{aligned} \tag{3.31}$$

It is noted that the convergence rate of the LMS algorithm depends on the step size μ and correspondingly on the eigenvalue spread of the covariance matrix $\boldsymbol{R}_{xx}$. An example illustrating the LMS convergence characteristics (learning curve) is shown in Fig. 3.6(a) for different μ.

Recursive Least Squares (RLS)

The RLS algorithm uses least squares to estimate the weight vector, that is, to choose the weight vector that minimizes the cost function of the sum of squared errors over a time window

$$Q(n) = \sum_{i=1}^{n} \alpha^{n-i}|\epsilon(i)|^2, \tag{3.32}$$

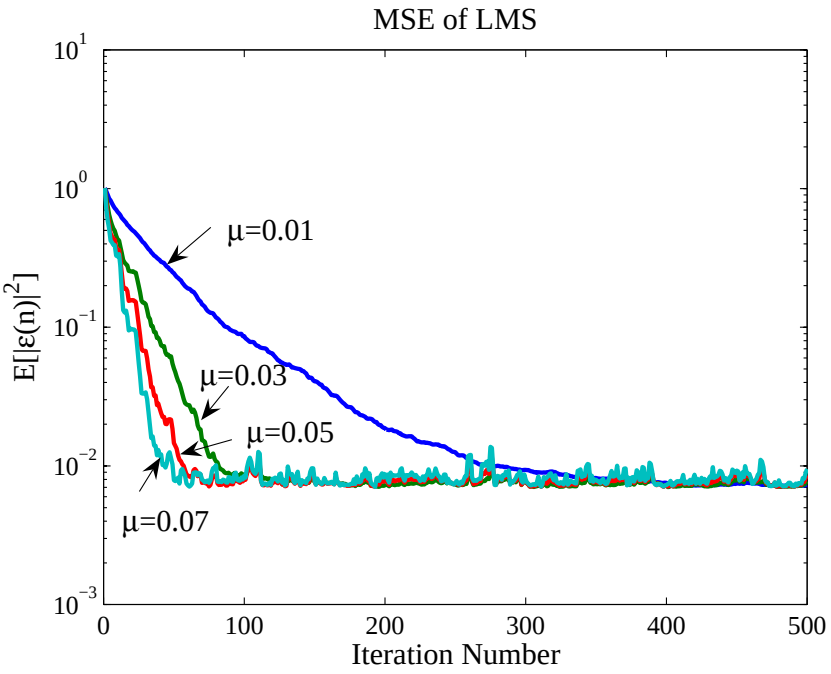

(a) MSE of LMS

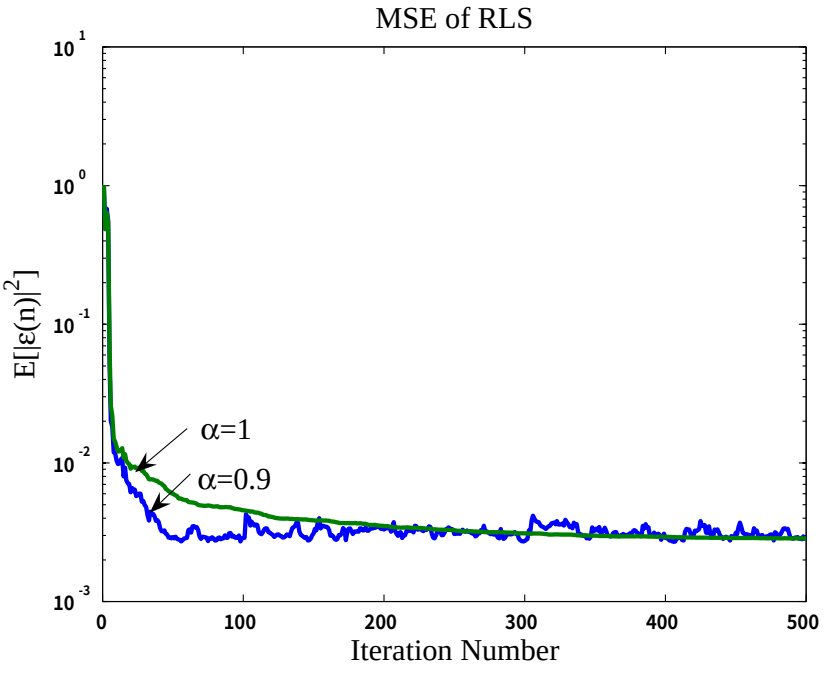

(b) MSE of RLS

Figure 3.6: Learning curve for the (a) LMS and (b) RLS algorithm. Linear array antenna with $d = \lambda/2$, $m = 2$, and input SNR=20dB were assumed.

where the error function $\epsilon(i)$ is defined in (3.19) and $0 < \alpha < 1$ is the forgetting factor. Using the least squares method, the covariance matrix and correlation vector is given by [1]

$$\boldsymbol{R}_{xx}(n) = \sum_{i=1}^{n} \alpha^{n-i} \boldsymbol{x}(i)\boldsymbol{x}^H(i) \tag{3.33}$$

$$\boldsymbol{r}_{xr}(n) = \sum_{i=1}^{n} \alpha^{n-1} \boldsymbol{x}(i)r^*(i). \tag{3.34}$$

Factoring out the terms corresponding to $i = n$, (3.33) and (3.34) become

$$\boldsymbol{R}_{xx}(n) = \sum_{i=1}^{n-1} \alpha^{(n-1)-i}\alpha\boldsymbol{x}(i)\boldsymbol{x}^H(i) + \boldsymbol{x}(i)\boldsymbol{x}^H(i) = \alpha\boldsymbol{R}_{xx}(n-1) + \boldsymbol{x}(n)\boldsymbol{x}^H(n) \tag{3.35}$$

$$\boldsymbol{r}_{xr}(n) = \sum_{i=1}^{n-1} \alpha^{(n-1)-i}\alpha\boldsymbol{x}(i)r^*(i) + \boldsymbol{x}(i)r^*(i) = \alpha\boldsymbol{r}_{xr}(n-1) + \boldsymbol{x}(n)r^*(n). \tag{3.36}$$

Applying Woodbury's identity, we obtain the inversion of the covariance matrix as follows [1]

$$\boldsymbol{R}_{xx}^{-1}(n) = \alpha^{-1}[\boldsymbol{R}_{xx}^{-1}(n-1) - \boldsymbol{q}(n)\boldsymbol{x}(n)\boldsymbol{R}_{xx}^{-1}(n-1)], \tag{3.37}$$

where

$$\boldsymbol{q}(n) = \frac{\alpha^{-1}\boldsymbol{R}_{xx}^{-1}(n-1)\boldsymbol{x}(n)}{1 + \alpha^{-1}\boldsymbol{x}^H(n)\boldsymbol{R}_{xx}^{-1}(n-1)\boldsymbol{x}(n)}. \tag{3.38}$$

The estimated weight vector can be updated using (3.24) as

$$\begin{aligned} \boldsymbol{w}(n) &= \boldsymbol{R}_{xx}^{-1}\boldsymbol{r}_{xr} \\ &= \alpha^{-1}[\boldsymbol{R}_{xx}^{-1}(n-1) - \boldsymbol{q}(n)\boldsymbol{x}(n)\boldsymbol{R}_{xx}^{-1}(n-1)][\alpha\boldsymbol{r}_{xr}(n-1) + \boldsymbol{x}(n)r^*(n)] \end{aligned} \tag{3.39}$$

which finally gives us [1]

$$\boldsymbol{w}(n) = \boldsymbol{w}(n-1) + \boldsymbol{q}(n)[r^*(n) - \boldsymbol{w}(n-1)\boldsymbol{x}(n)]. \tag{3.40}$$

Since the RLS algorithm utilizes information from initial sample to estimate the weight, it is an order to magnitude faster than that of the LMS algorithm. However, this convergence improvement is achieved at the expense of the increased computational complexity. An example of the convergence characteristic of the RLS algorithm is depicted in Fig. 3.6(b).

Sample Matrix Inversion (SMI)

If the desired and reference signals are both known in*a priori*, then the optimal weights could be computed using the direct inversion if the covariance matrix $\boldsymbol{R}_{xx}$ as (3.24).

Since the desired and reference signals are not known in practice, it is possible to use their estimates from the input data vector as [56]

$$\begin{aligned} \boldsymbol{R}_{xx} &= \frac{1}{n}\sum_{i=1}^{n}\boldsymbol{x}(i)\boldsymbol{x}^H(i), \\ \boldsymbol{r}_{xr} &= \frac{1}{n}\sum_{i=1}^{n}\boldsymbol{x}(i)r^*(i). \end{aligned} \tag{3.41}$$

From (3.24), it follows that the estimated weight vector using SMI algorithm is given by

$$\boldsymbol{w} = \boldsymbol{R}_{xx}^{-1}\boldsymbol{r}_{xr}. \tag{3.42}$$

It is noted that the SMI is a block-adaptive algorithm and has been shown to be the fastest algorithm for estimating the optimum weight vector [1]. However, it suffers the problems of increased computational complexity and numerical instability due to inversion of a large matrix.

3.1.3 Benefits of Adaptive Array

The application of adaptive array brings various benefits for mobile communications and has been discussed and proved in the literature [1,56]. We summarize some of the benefits as follows:

Improved signal quality

The using multiple elements adaptive arrays provide additional array gain, which depends on the number of utilized array elements, which leads to improve the transmission performance. For a given SNR, if the number of interferences is smaller than the degree of freedom (DOF)=$N-1$, the ouput signal-to-interference-plus-noise ratio (SINR) in a single propagation environment (without multipath fading) can be found as [72, 88]

$$\text{SINR} = N \times \text{SNR} \tag{3.43}$$

or

$$\text{SINR [dB]} = 10\log_{10} N + \text{SNR [dB]}, \tag{3.44}$$

where N is the number of array elements.

In multipath fading environment, if signal processing is used in both the spatial and temporal domains such as the case of the wideband beamformer, more diversity gain could be achieved depending on the number of the taps in the employed TDLs and fading characteristics. For example, let consider a simple two path model which are uncorrelated, the output SINR is estimated as

$$\text{SINR [dB]} = 10\log_{10} N + 10\log_{10} 2 + \text{SNR [dB]}. \tag{3.45}$$

This means that additional 3 dB diversity gain has been obtained in multipath fading channel environment. Therefore, the richer fading channel environment us, the more diversity gain can be achieved.

Extended Coverage

From (3.44), it is clear that the array gain achieved by an adaptive array is (assuming an antenna efficiency of 100% and no mutual coupling) that can be achieved with an antenna array of N elements is

$$G = 10 \log_{10} N. \tag{3.46}$$

This additional gain allow to extend the coverage of the base station (BS). When the angular spread is small and path loss is modeled with exponent β, the range extension factor (REF) is given by [57]

$$\text{REF} = \frac{r_{array}}{r_{conv}} = N^{\frac{1}{\beta}}. \tag{3.47}$$

where r_{conv} and r_{array} are the range covered by the conventional antenna (single element) and the array antenna (multiple elements), respectively. The extended area coverage factor (ECF) is [57]

$$\text{ECF} = (\frac{r_{array}}{r_{conv}})^2 = \text{REF}^2. \tag{3.48}$$

Figure 3.7 shows that with six element arrays, the coverage area is double compared to single antenna case for $\beta = 5$. Since the inverse of the ECF represents the reduction factor in number of BS required to cover the same area using a single antenna [57], it is clear that using adaptive arrays can significantly reduce the number of required BS.

Increased in Channel Capacity

Capacity is related to the spectral efficiency of a system. The spectral efficiency $\mathcal{E}$ measured in channels/km^2/MHz [41, 42] is expressed as

$$\mathcal{E} = \frac{B_t/B_{ch}}{B_t N_c A_c} = \frac{1}{B_{ch} N_c A_c} \tag{3.49}$$

where B_t is the total bandwidth of the system available for voice channels in MHz, B_{ch} is the bandwidth per voice channel in MHz, N_c is the number of cells per cluster. The capacity of a system is measured in channels/km^2 and is given by [41, 42]

$$C = EB_t = \frac{B_t}{B_{ch} N_c A_c} = \frac{N_{ch}}{N_c A_c}, \tag{3.50}$$

where $N_{ch} = B_t/B_{ch}$ is the total number of available voice channels in the system.

Example 1

A system with $N_{ch} = 280$ channels and with conventional BS antennas uses a seven-cell frequency reuse pattern ($N_c = 7$). Each cell covers an area of $A_c = 50$ km^2. From (3.50), the capacity is $C_c = \frac{280}{7 \times 50} = 0.8$ channels/km^2. By using an adaptive array at the base station, ICI is reduced and N_c can be reduced to 4. The capacity is $C_a = \frac{280}{4 \times 50 = 1.4}$ channels/km^2.

It is clear that use of adaptive array can improve system capacity compared to the conventional system at the same range.

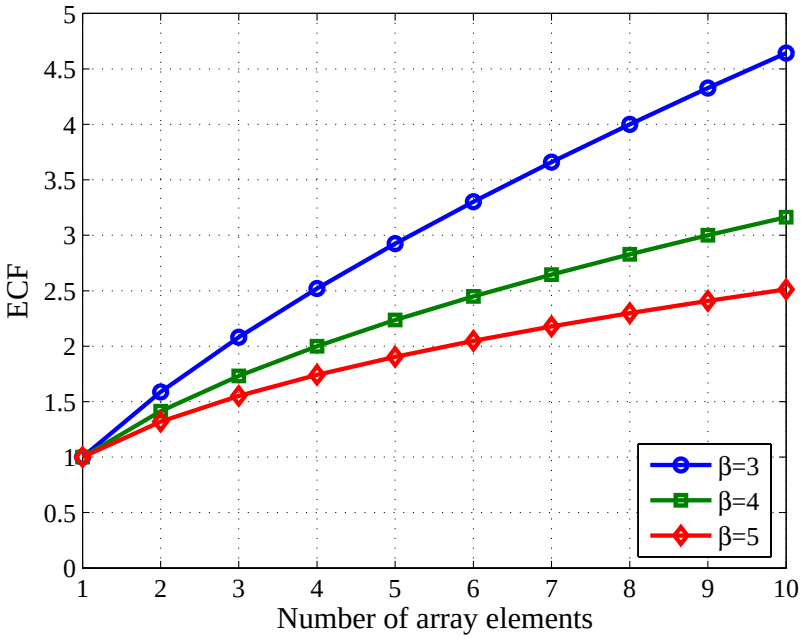

Figure 3.7: Improvement of area coverage by adaptive arrays.

Reduction in the Transmit Power

We have seen in Sec. 3.1.3 that the use of adaptive arrays can provide a large array gain, which leads to the reduction of required transmit power at the BS. If the required reception sensitivity is kept to the same, then the power requirement of the BS employed with Nth element array is reduced to N^{-1} and correspondingly the required output power of the BS power amplifier can be reduced to N^{-2} [57]. The reduction in the transmit power is beneficial to user's health and implementation cost since high frequency power amplifiers are often very expensive.

3.2 Adaptive array for the channel with delay spread.

As we have mentioned earlier, in mobile communications, ISI and CCI are two main factors which degrade the system performance. Here, we present the conventional method to mitigate the effects of ISI and CCI.

3.2.1 Tapped Delay Line Adaptive Array (TDLAA)

A TDLAA is using multiple temporal transversal filters as illustrated in Fig. 3.8. Assuming a TDLAA receiving L propagating waves $s_l(t), := \{0, 1, \ldots, L-1\}$, each coming from the direction of θ_l with respect to the array broadside. The input signal stored in the register of the L_rth order temporal filter following the jth element ($j = \{1, 2, \ldots, N\}$) of

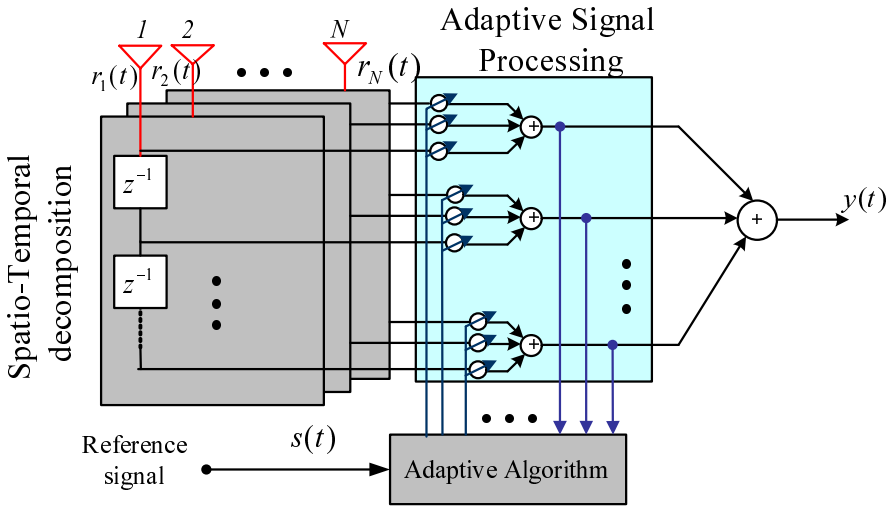

Figure 3.8: Tapped Delay Line Adaptive Array

the TDLAA is expressed at time t as

$$\boldsymbol{r}_j(t) = [r_j(t)\ r_j(t-1)\ \ldots\ r_j(t-(L_r-1))]^T, \tag{3.51}$$

and total input signal will be

$$\begin{aligned} \boldsymbol{r}(t) &= [\boldsymbol{r}_1^T(t)\ \boldsymbol{r}_2^T(t)\ \ldots\ \boldsymbol{r}_N^T(t)]^T & (3.52)\\ &= s(t)\boldsymbol{a}(\theta) + \boldsymbol{n}(t) & (3.53) \end{aligned}$$

where $\boldsymbol{a}(\theta) = [1\ e^{-\mathrm{j}\frac{2\pi}{\lambda}d\sin\theta}\ \ldots\ e^{-\mathrm{j}\frac{2\pi}{\lambda}(M-1)d\sin\theta}]^T$(as describe in (3.3)) is the steering vector. Here, $\boldsymbol{s}(t)$ and $\boldsymbol{u}$ are,

$$\begin{aligned} \boldsymbol{s}(t) &= [s_0^T(t), s_1^T(t), \ldots, s_{L-1}^T(t)]^T & (3.54)\\ \boldsymbol{n}(t) &= [n_1^T(t), n_2^T(t), \ldots, n_M^T(t)]^T. & (3.55) \end{aligned}$$

The optimum weight of the TDLAA can be calculated through

$$\boldsymbol{w}_{opt} = \boldsymbol{R}_{rr}^{-1} r_{rd}, \tag{3.56}$$

where $\boldsymbol{R}_{rr}^{-1} = E[\boldsymbol{r}^H(t)\boldsymbol{r}(t)]$ is the correlation matrix of the array input and $r_{rd} = E[\boldsymbol{r}(t)d^*(t)]$ is cross-correlation vector between array input signal and reference signal $d(t)$, respectively. The TDLAA output signal will be

$$y(t) = \boldsymbol{w}_{opt}^H \boldsymbol{r}(t). \tag{3.57}$$

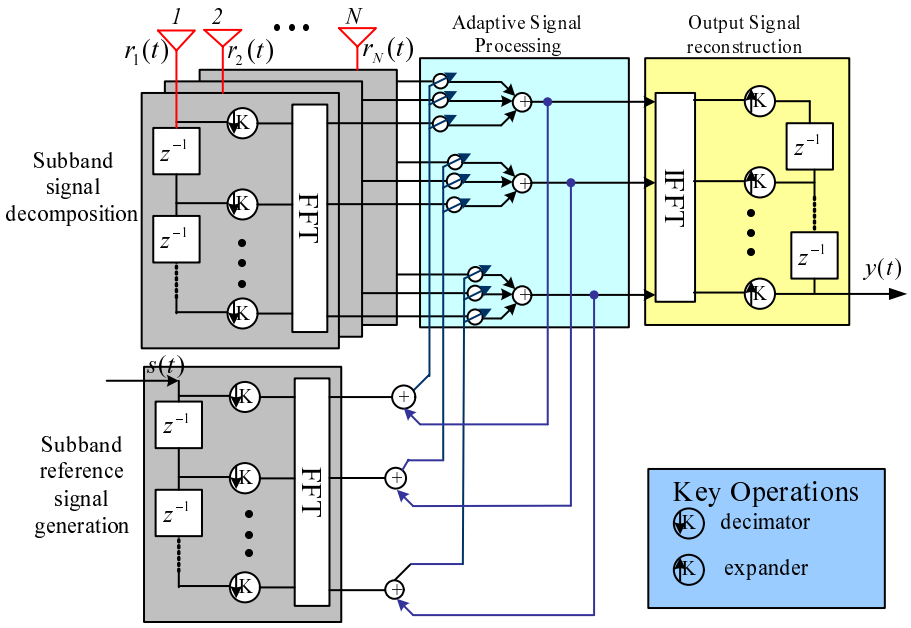

Figure 3.9: Subband adaptive array configuration

3.2.2 Subband Adaptive Array (SBAA)

Subband adaptive arrays are built on *multirate digital filters*, which comprise of *analysis* and *synthesis* parts [46]. The analysis part contains a bank of *decimator* $\downarrow K$ and *analysis filters*. The synthesis part, operated inversely, includes a *synthesis filter* and a bank of *expanders* $\uparrow K$.

A typical configuration of SBAA is illustrated in Fig. 3.9. The received signals from each array elements are first put through receive modules to convert to baseband and then converted into digital samples using analog-to-digital (A/D) converter. For simplicity, we have simplified the receive modules and A/D converter from the configuration of the SBAA. Also, to keep the signal model similar with that, we use t as the discrete time notation for SBAA. Denote the receive signal at the jth array element at time t as $x_m(t)$. Each signal $x_m(t)$ is decomposed into K subband signal and converted into the frequency domain using FFT filter bank. The adaptive signal processing is then carried out in subbands to obtain the optimum weight vector for each subband, $\boldsymbol{w}_{opt}^{(k)}$.

To do so the reference signal is also converted into the frequency domain subband signal using the same method for the received signal. After being multiplied with the optimum weights, the weighted samples are combined corresponding to each subband. The combined samples are then converted back into the time domain using the IFFT filter bank. Finally, the interpolation with the expansion rate K is applied to get the array output signal $y(t)$. The optimum weights are calculated in each subband by next equation

$$\boldsymbol{w}_{opt}^{(k)} = \boldsymbol{R}_{xx}^{-1}\boldsymbol{r}_{xd} \tag{3.58}$$

where $\boldsymbol{R}_{xx}^{-1} = E[\boldsymbol{x}^{(k)}(t)\boldsymbol{x}^{(k)H}(t)]$ and $\boldsymbol{r}_{xd}^{(k)} = E[\boldsymbol{x}^{(k)}(t)d^{(k)*}(t)]$ are the covariance matrix and correlation vector in kth subband, respectively. Here, $d(t)$ is the references signal. Finally, the array output signal $y(t)$ can be expressed by

$$y(t) \quad = \quad \boldsymbol{w}_{opt}^{(k)}\boldsymbol{x}^{k}. \tag{3.59}$$

Based on selection of the decimation rate, SBAA can be classified into the SBAA with decimation and SBAA without decimation. Similar to classification of the multirate filters, in the case of SBAAs with decimation, if the decimation rate is equal to the number of subbands, *i.e.*, $K = Q$, is then called the critical sampling SBAA, for $K < Q$, it is the oversampled SBAAs

Another method to classify SBAA is based on the definition of the feedback signal to update weights in subbands. According to this method, SBAAs are divided into three different groups: global feedback, local feedback, and partial feedback schemes. In the global feedback SBAAs, the feedback signal is taken from the array output signal, $y(t)$. Thus the reference signal in this case is not necessarily converted into subbands. This type of SBAAs, however, is only realized for the SBAA without decimation. When the feedback is extracted from the combined signal such as in Fig. 3.9, it is called the local feedback SBAA. The so-called partial feedback SBAA, is where a certain number of subbands are grouped with one another, is a generalization of both the local feedback abd global feedback schemes. As with the global feedback type, the partial feedback SBAA exists only for the SBAA without decimation.

In implementation when both the criteria are considered, the are four type s of SBAAs as summarized in Table 3.1.

Table 3.1: Classification of subband adaptive arrays

	Global	Local	Partial
Without Decimation	Type 1	Type 2	Type 3
With decimation	Not available	Type 4	Not realizable

3.2.3 Motivations

ISI and CCI mitigation capability

As we have mentioned earlier, in mobile communications, ISI and CCI are two main factors which degrade the system performance. Adaptive arrays as a spatial filter have been shown to have capability to suppress CCIs within the array degree of freedom (DOF) [1]. For an Nth element array, the DOF is given by

$$\text{DOF} \quad = \quad N - 1 \tag{3.60}$$

and the array can effectively cancel $(N-1)$ interferences. For ISIs, since the conventional adaptive arrays using narrowband beamforming process the input signal only in spatial

domain, they do not have capability to mitigate delay spread in the frequency selective channels. The solution is to use adaptive arrays in combination with temporal filters using TDLs such as wideband beamforming adaptive arrays [37, 39]. The TDL adaptive arrays (TDLAAs) work as spatio-temporal equalizer and thus can effectively suppress both ISIs and CCIs. However, resolving simultaneously both ISIs and CCIs is a difficult task for TDLAAs since it requires either inversion of large scale matrices or complex recursive computation [44]. Moreover, as the adative processing is done in full band, TDLAAs suffer slow convergence in searching the optimum weight [43]. In severe multipath fading environments these problems become even more serious as longer order temporal filters are required. In such cases, SBAA has been shown to outperform the conventional TDLAA [44, 45, 60, 72, 76, 84, 88].

A subband adaptive array, which is comprised of an integrated adaptive array and multirate filter banks, was shown to achieve the same objective as TDLAA while more efficient in implementation. In SBAA, the frequency band of the received signal is first decomposed into smaller subbands and then adaptive signal processing is performed in subbands to obtain the optimum weights. Due to the subband decomposition, the spatio-temporal equalization is converted into a number of simple spatial equalizers which can be implemented in parallel [44]. As a result, both the problems of slow convergence rate and the computational complexity can be resolved. Furthermore, if the multirate filter banks are properly designed then signal correlation can be significantly increased. This helps to mitigate the effect of multipath fading occurred in both the desired and interference signals [44].

Reduction in the computational complexity

The main different between TDLAA and SBAA is their processing modes. While TDLAA process the input signal in *sample-by-sample* basis, SBAA is done in *block-by-block* basis. As a result, SBAA requires less computational operations than TDLAA. For L_r tap and N elements array antenna, TDLAA employing the SMI requires $(L_rN)^3$ multiplications for each weight update. The SBA with K subbands, on the other hand, needs only KN^3 multiplication [37, 43]. As DFT/IDFT are often implemented using efficient FFT/IFFT filter banks, $2K\log_2 K$ more multiplications are needed by the SBAA. The total computational load required by the SBAA is $K(N^3 + 2\log_2 K)$. In wideband communications, the propagation channel often encounters multipath fading with large delay spread. This leads to the use of high order temporal filters, that is, with a large number of taps L_r. In this case, for $L_r = K$, $(L_rN)^3 \gg K(N^3 + 2\log_2 K)$ thus use of SBAA can help to reduce a significant amount of computational complexity. Fig 3.10 compares the computational complexity of the TDLAA and SBAA using SMI algorithm with $N = 4$. It is shown that SBAA requires less computational complexity compare to TDLAA.

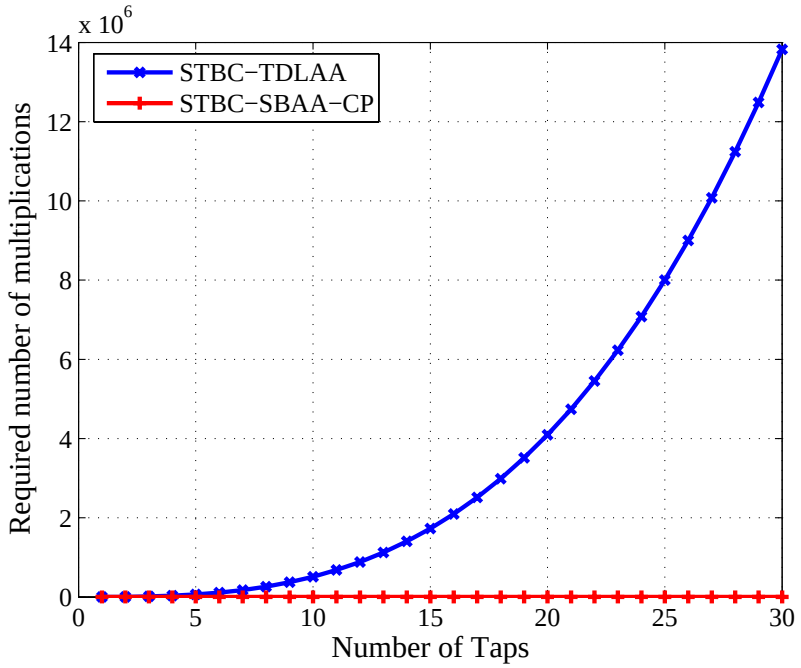

Figure 3.10: Computational complexity of TDLAA and SBAA ($N-4$, SMI algorithm).

3.3 Conclusion

In this chapter, a brief review on the basic concepts of adaptive array was provided. The array signal models for both single and multipath fading environment were developed and, the structure of the narrowband and wideband beamforming were described. It was shown that the array output of both beamformer can be expressed in the same multiplication form of the input signal and array weight vectors. The conventional time domain wideband beamforming was also shown to be equivalently replaced by frequency domain beamforming with less computational cost and fast convergence rate. The optimization criteria was given, namely MMSE which can be expressed in the form of well-known Wiener-Hopf equation. In additional, three common adaptive algorithm were discussed. Furthermore, basic operations and components of TDLAA and SBAA were presented. For SBAA, different configurations were reviewed, and it is shown for the case of critical sampling SBAA, only the local feedback is realizable. The critical sampling SBAA using local feedback scheme will be focused in this work. Moreover, the motivations of using SBAA in mobile communications were also discussed. It was shown that SBAA can effectively mitigate both ISI and CCI, while having greatly reduced computational complexity. Thus, the use of SBAA bring more benefits than TDLAA.

Finally, we describe that the use of adaptive array would bring great benefits for wireless communications.

Chapter 4

Subband Adaptive Array for Space-Time Block Coding

Diversity transmission using space-time block coding (STBC) shows a degraded performance in frequency selective fading channel. In this chapter, assuming the CSI is unknown at both transmitter and receiver while a pilot signal is available during the training period, we propose a MIMO transmission scheme using STBC by adopting subband adaptive array (SBAA) processing. The receive signal is converted into the frequency-domain and adaptive processing is done at each subband. A novel construction of SBAA is introduced to process received signal based on STBC. Simulation results demonstrate that the proposed scheme has a better performance compare to conventional STBC, and has a better performance and less computational load compare to STBC-TDLAA.

4.1 Introduction

The rapid growth of wireless subscribers, the Internet, and the increasing use of portable computing devices suggest that the high speed, high capacity and high quality wireless communications will grow to be a major area of telecommunications service. Third-generation (3G) wireless communication systems were initiated to meet this possible service. In this new wireless system, the communication channels are often frequency selective, which makes the ISI to be highly pronounced. Another important problem in mobile communication is the co-channel interference (CCI), which is the result of frequency reuse in cellular systems.

In order to fulfill the requirement of high speed, high capacity, and high quality transmission, the introduction of space-time coding [3, 17, 19] has became a promising method to make it happen. Diversity transmission using Alamouti's space time block coding (STBC) scheme [17] has been proposed in several wireless standards due to its many attractive features. First, it achieves full spatial diversity at full transmission rate for two transmit antennas and at any signal constellation. Second, it does not require channel state information (CSI) at the transmitter, and lastly, maximum likelihood decoding of

STBC requires only simple linear processing. However, this method which has been designed for flat Rayleigh fading channel does not work well in the presence of ISI due to frequency selective fading channel.

Orthogonal frequency division multiplexing (OFDM) is well known as a solution to overcome frequency selective fading channel. However, this method suffers from the peak to average power ratio (PAPR) problem and sensitivity to frequency offset as well as to Doppler spread. Tapped delay line adaptive array (TDLAA) [37, 61] is also a solution to overcome frequency selective fading channel since it utilizes the delayed signals to enhance the desired signal instead of excluding them as interferences. However, this method requires a large computational load compare to conventional adaptive array systems. The complexity of TDLAA grows exponentially with channel memory and spectral efficiency or requires very long finite impulse response (FIR) filters to achieve acceptable performance. Frequency-domain equalization (FDE) was shown in [34–36, 61] to be an attractive equalization scheme to overcome frequency selectivity, FDE has lower complexity, due to its use of the computationally-efficient fast Fourier transform (FFT) than TDLAA. Furthermore, this method has an advantage over OFDM and TDLAA in term of computational complexity and superiority to frequency offset as well as Doppler spread. In [34–36] there are proposals for a combined STBC with the SC-FDE scheme to overcome the frequency selectivity in the propagation channel, and it shows a great improvement in the performance. However, most of the authors of the work stated above was assumed full CSI known at receiver side.

In this chapter, assuming the CSI is unknown at both transmitter and receiver while a pilot signal is available during the training period, we propose a transmission scheme using STBC by adopting subband adaptive array (SBAA) processing. The proposed scheme utilizes a STBC as transmit diversity and at the receiver, a novel construction of SBAA to process received signal was introduced. The received signal is divided into two groups and adaptive processing is done to equalize and estimate the desired signal in frequency-domain. In addition, to improve the performance of STBC-SBAA, cyclic prefix (CP) [49] is also introduced. A simulation is brought to prove the efficiency of proposed scheme using frequency selective fading channels with uniform power delay profile and normalized exponential power profile distribution frequency selective fading channel.

We organized the remainder of this chapter as follows. As the preliminary, in the next section, we explain briefly the radio channels and assumption used in this chapter. Next, we briefly explain about the STBC in Section 4.3. In Section 4.4, we describe the configuration and operations of the proposed scheme. Simulation parameters and result for frequency selective fading channel are presented in Section 4.5 and this chapter is concluded in Section 4.6.

4.2 Channel Model and Assumptions

In this chapter, a MIMO transmission under the quasi-static frequency selective fading channel is assumed. The numbers of transmit and receive antennas are $M = 2$ and N,

respectively. The channel transfer function is modeled as follows:

$$\boldsymbol{H}_p(\tau) = \sum_{l=0}^{L-1} \boldsymbol{H}_p^l \delta(\tau - lT_s) \tag{4.1}$$

$$\boldsymbol{H}_p^l = \begin{bmatrix} h_{p,11}^l & h_{p,12}^l \\ h_{p,21} & h_{p,22}^l \\ \vdots & \vdots \\ h_{p,j1}^l & h_{p,j2}^l \\ \vdots & \vdots \\ h_{p,N1}^l & h_{p,N2}^l \end{bmatrix}, \tag{4.2}$$

where $h_{p,ji}^l$ is complex number expressing the channel between jth receive antenna and ith transmit antenna and, δ is the Dirac delta function, τ is the discrete time sequences of propagation delay for pth user ($p = \{1 \sim P\}$, P: total users). $\boldsymbol{H}_p^0$ is the channel state information of the preceding wave, while for $l = \{1, \ldots, L-1\}$, $\boldsymbol{H}_p^l$ is lth delayed channel information which causes ISI. Here, L and T_s are the length of the channel and symbol data duration, respectively.

4.3 Alamouti's STBC over a multipath channel

In this section, we explain the Alamouti's STBC scheme [17] with $M \times N$ MIMO transmission. The Alamouti's STBC with $M = 2$ is the only scheme which can provide data transmission at full rate and with full diversity at any signal constellations. Without the loss of generality, we shall restrict our attention to this type of STBC. Extension to more general type of STBC [19] is quite straight forward.

At the transmitter of Alamouti's STBC, input signal $s_p(t) : \{t \in \mathbb{Z}\}$ is divided into two groups as $s_p(2t-1)$ and $s_p(2t)$. Both signals are sent through two transmit antennas at different time. For each user, at time $2t-1$, first antenna transmits $s_p(2t-1)$ while second antenna transmits $s_p(2t)$, respectively. At the next symbol time $2t$, first antenna transmits $-s_p^*(2t)$ while second antenna transmits $s_p^*(t)$. The transmit signal at first antenna and second antenna will be summarized as follows. Note that $s_{k,i}(t)$ is the signal transmitted from antenna $i \in \{1, 2\}$, at time t of pth user..

$$s_{p,1}(2t-1) = s_p(2t-1), \quad s_{p,1}(2t) = -s_p^*(2t) \tag{4.3}$$

$$s_{p,2}(2t-1) = s_p(2t), \quad s_{p,2}(2t) = s_p^*(2t-1). \tag{4.4}$$

After the transmission through the frequency selective fading channel, the receive signal

by jth receive antenna at time $2t-1$ and $2t$ are given as follows:

$$r_j(2t-1) = \sum_{p=1}^{P}\sum_{l=0}^{L-1}\{h_{p,j1}^{l}s_{p,1}(2t-1-l) + h_{p,j2}^{l}s_{p,2}(2t-1-l)\} + n_j(2t-1) \quad (4.5)$$

$$r_j(2t) = \sum_{p=1}^{P}\sum_{l=0}^{L-1}\{h_{p,j1}^{l}s_{p,1}(2t-l) + h_{p,j,2}^{l}s_{p,2}(2t-l)\} + n_j(2t). \quad (4.6)$$

Here, $n_j(2t-1)$ and $n_j(2t)$ denote the complex additive white Gaussian noise (AWGN) with zero mean and variance σ_n^2 in each real dimension.

This method shows a significant performance improvement in the flat fading channel [17]. However, it cannot work well in the presence of multipath signal arriving with the longer delay than one symbol, which cause the ISI. Therefore, in the next section, we propose a strategy to improve the STBC transmission in the frequency selective fading channel.

4.4 Configuration and Signal Model of the Proposed Scheme

In this section, we propose a subband adaptive array for Alamouti-type STBC. Here we consider a system using STBC [17, 61] with $M = 2$ transmit antennas and N receive antennas for a single-user environment. For the comparison, we also describe the TDLAA for STBC data transmission (STBC-TDLAA)[1] [61].

4.4.1 STBC-TDLAA

The STBC-TDLAA system for $2 \times N$ MIMO system uses the transmitter as describe in Section 4.3. In Fig. 4.1, the configuration of the STBC-TDLAA's receiver is illustrated. The transmit signal will be the same as (4.3) and (4.4). At the receiver, the received signal in each antenna is then put through finite impulse responses (FIR) filters of length L_r for temporal equalization as shown in Fig. 4.2. STBC-TDLAA system uses spatial processing across the N receive antennas while temporal processing is done across the FIR filters.

The received signal at the receiver becomes as (4.5) and (4.6). Since the desired symbol of $s_p(2t-1)$ and $s_p(2t)$ are also contained in the received signal as a complex-conjugated form, we should incorporate the target component not only the received signal $r_j(t)$, but also in its complex-conjugated version of $r_j(t)$. Therefore, the output will be grouped into $r_j(t)$ and $r_j^*(t)$. Both sample signals are then put through FIR filters for temporal equalization and estimating $\tilde{s}_p(2t-1)$ and $\tilde{s}_p(2t)$, respectively.

[1]For simplicity, STBC-TDLAA was renamed as STBC-STAA in Chapter 7.

Now, we attempt to rewrite the receive signal in vector form. Let us define the following two channel coefficient vectors as

$$\boldsymbol{h}_{p,1}^{l} = [h_{p,11}^{l}\ h_{p,21}^{l}\ h_{p,31}^{l}\ \ldots\ h_{p,N1}^{l}]^{T} \tag{4.7}$$
$$\boldsymbol{h}_{p,2}^{l} = [h_{p,12}^{l}\ h_{p,22}^{l}\ h_{p,32}^{l}\ \ldots\ h_{p,N2}^{l}]^{T} \tag{4.8}$$

and then stack them to have

$$\tilde{\boldsymbol{H}}_{p}^{l} = \begin{bmatrix} \boldsymbol{h}_{p,1}^{l} & \boldsymbol{h}_{p,2}^{l} \\ \boldsymbol{h}_{p,2}^{l*} & -\boldsymbol{h}_{p,1}^{l*} \end{bmatrix} \tag{4.9}$$

Next, we define the following vectors

$$\hat{\boldsymbol{s}}_{p}(t) = \begin{bmatrix} s_{p}(2t-1) & s_{p}(2t) \end{bmatrix}^{T} \tag{4.10}$$
$$\boldsymbol{n}(v) = \begin{bmatrix} n_{1}(v) & n_{2}(v) & \ldots & n_{N}(v) \end{bmatrix}^{T} \tag{4.11}$$
$$\boldsymbol{r}(v) = \begin{bmatrix} r_{1}(v) & r_{2}(v) & \ldots & r_{N}(v) \end{bmatrix}^{T} \tag{4.12}$$

where $v \in \{(2t-1),(2t)\}$, and the $\boldsymbol{n}(v), \boldsymbol{r}(v)$ can be expressed as follows.

$$\hat{\boldsymbol{n}}(t) = \begin{bmatrix} \boldsymbol{n}(2t-1)^{T} & \boldsymbol{n}(2t)^{H} \end{bmatrix}^{T} \tag{4.13}$$
$$\hat{\boldsymbol{r}}(t) = \begin{bmatrix} \boldsymbol{r}(2t-1)^{H} & \boldsymbol{r}(2t)^{H} \end{bmatrix}^{T} \tag{4.14}$$

By using the notation from (4.7) to (4.14), we can rewrite the receive signal of STBC-TDLAA in the vector form as follows:

$$\hat{\boldsymbol{r}}(t) = \sum_{p=1}^{P} \sum_{l=0}^{L-1} \tilde{\boldsymbol{H}}_{p}^{l} \hat{\boldsymbol{s}}_{p}(t-l) + \hat{\boldsymbol{n}}(t) \tag{4.15}$$

The receive signals are then put into FIR filters such as at all taps of all $2N$ receive antenna branches is expressed as

$$\tilde{\boldsymbol{r}}(t) = [\hat{\boldsymbol{r}}(t)^{T}\ \ \hat{\boldsymbol{r}}(t - T_s)^{T}\ \ \ldots\ \ \hat{\boldsymbol{r}}(t - L_r T_s + T_s)^{T}]^{T} \tag{4.16}$$

where $\tilde{\boldsymbol{r}} \in \mathbb{C}^{2NL_r \times 1}$.

Assume the coefficients of FIR filter as

$$\boldsymbol{w}_{p,v,j} = [w_{p,v,j}(1)\ \ldots\ w_{p,v,j}(l_r)\ \ldots\ w_{p,v,j}(L_r)]^{T} \tag{4.17}$$

where $w_{p,v,j}(l_r)$ and $\boldsymbol{w}_{p,v,j}$ are the weight coefficient at l_rth tap and vector represents the weight coefficient of FIR filters at jth antenna, respectively ($v \in \{1,2\}$). Note that, $l_r = 1, 2, \ldots, L_r$ is the filter tap number. By considering all the receive antennas, the optimal weight $\tilde{\boldsymbol{w}}_{p,v}$ can be shown as follows:

$$\tilde{\boldsymbol{w}}_{p,v} = \begin{bmatrix} \boldsymbol{w}_{p,v,1}^{T} & \boldsymbol{w}_{p,v,2}^{T} & \ldots, \boldsymbol{w}_{p,v,j}^{T}, \ldots, \boldsymbol{w}_{p,v,N}^{T} \end{bmatrix}^{T} \tag{4.18}$$

The output signal is extracted by multiplying receiver weights $\boldsymbol{w}_{p,1}$ for odd signal $(2t-1)$, and $\boldsymbol{w}_{p,2}$ for even signal $(2t-1)$, with the dimension of $2NL_r \times 1$, for all the receive antennas. Using the minimum mean square error (MMSE) criterion, the optimal weights are decided for v as follows:

$$\tilde{\boldsymbol{w}}_{p,1} = \arg\min E[|d_p(2t-1) - \tilde{\boldsymbol{w}}_{p,1}^H \tilde{\boldsymbol{r}}(t)|^2] \tag{4.19}$$

$$\tilde{\boldsymbol{w}}_{p,2} = \arg\min E[|d_p(2t) - \tilde{\boldsymbol{w}}_{p,2}^H \tilde{\boldsymbol{r}}(t)|^2] \tag{4.20}$$

Solving (4.19) and (4.20), the optimal weight can be represented as below:

$$\tilde{\boldsymbol{w}}_{p,1} = \boldsymbol{R}_{\tilde{r}\tilde{r}}^{-1} \boldsymbol{X}_{rd,(2t-1)} \tag{4.21}$$

$$\tilde{\boldsymbol{w}}_{p,2} = \boldsymbol{R}_{\tilde{r}\tilde{r}}^{-1} \boldsymbol{X}_{rd,(2t)} \tag{4.22}$$

where, $\boldsymbol{R}_{\tilde{r}\tilde{r}} = E[\tilde{\boldsymbol{r}}(t)\tilde{\boldsymbol{r}}(t)^H] \in \mathbb{C}^{NL_r \times NL_r}$ is the covariance matrix of the receive signals, $\boldsymbol{X}_{rd,(2t-1)} = E[\tilde{\boldsymbol{r}}(t)d_p^*(2t-1)] \in \mathbb{C}^{NL_r \times 1}$ and $\boldsymbol{X}_{rd,(2t)} = E[\tilde{\boldsymbol{r}}(t)d_p^*(2t)] \in \mathbb{C}^{NL_r \times 1}$, are the correlation vector between receive signal and the reference signal. Here $d_p(2t-1)$ and $d_p(2t)$ are the reference signal at time $2t-1$ and time $2t$ for pth user, respectively. The reference signal is extracted from the pilot signal. Note that, in order to extract a higher array signal output, we use the same covariance matrix to calculate the optimal weight for $2t-1$ and $2t$. We prove it theoretically as shown in the Appendix A [72]. The output signal is extracted using (4.21) and (4.22) to be resulted as below.

$$\tilde{s}_p(2t-1) = (\tilde{\boldsymbol{w}}_{p,1})^H \tilde{\boldsymbol{r}}(t), \tag{4.23}$$

$$\tilde{s}_p(2t) = (\tilde{\boldsymbol{w}}_{p,2})^H \tilde{\boldsymbol{r}}(t). \tag{4.24}$$

4.4.2 STBC-SBAA

Next, we describe the proposed STBC-SBAA system. The configuration of transmitter and receiver is illustrated in Fig. 4.3. In the transmitter as shown in Fig. 4.3(a), we use Alamouti's STBC, but the transmission is done in a *blockwise*, not in *symbolwise* as the conventional STBC [17, 61]. In the frequency selective fading channel, the sequentially transmitted symbol will interfere with each other at the receiver, and therefore we need to consider a sequence, or block of symbol instead of single symbol at a time as described in Section 4.3. This operation is to realize an additional multipath diversity gain without sacrificing full spatial diversity [62]. Here, the signal is transmitted using the block transmission as illustrated in Fig. 4.4.

The signal of each user, $s_p(t)$ is then be divided into blocks of length Q symbol each. The $k^{th}(\in \mathbb{Z})$ block $\boldsymbol{s}_p^{(k)}[q] = [s_p(Qk), \ldots, s_p(qk), s_p(Qk + (Q-1))]^T$ contains Q symbol with the duration of T_s. Here, $\boldsymbol{s}_p^{(k)}[q]$ shows the input symbol of each block where $q \in \{0, 1, \ldots, Q-1\}$. The input block signal is encoded by space-time block encoder (STBE), where at the odd block $2k-1$, a pair of blocks $\boldsymbol{s}_p^{(2k-1)}[q]$ and $\boldsymbol{s}_p^{(2k)}[q]$ are transmitted from the first and second transmit antennas, respectively. Similarly, at the even block $2k$

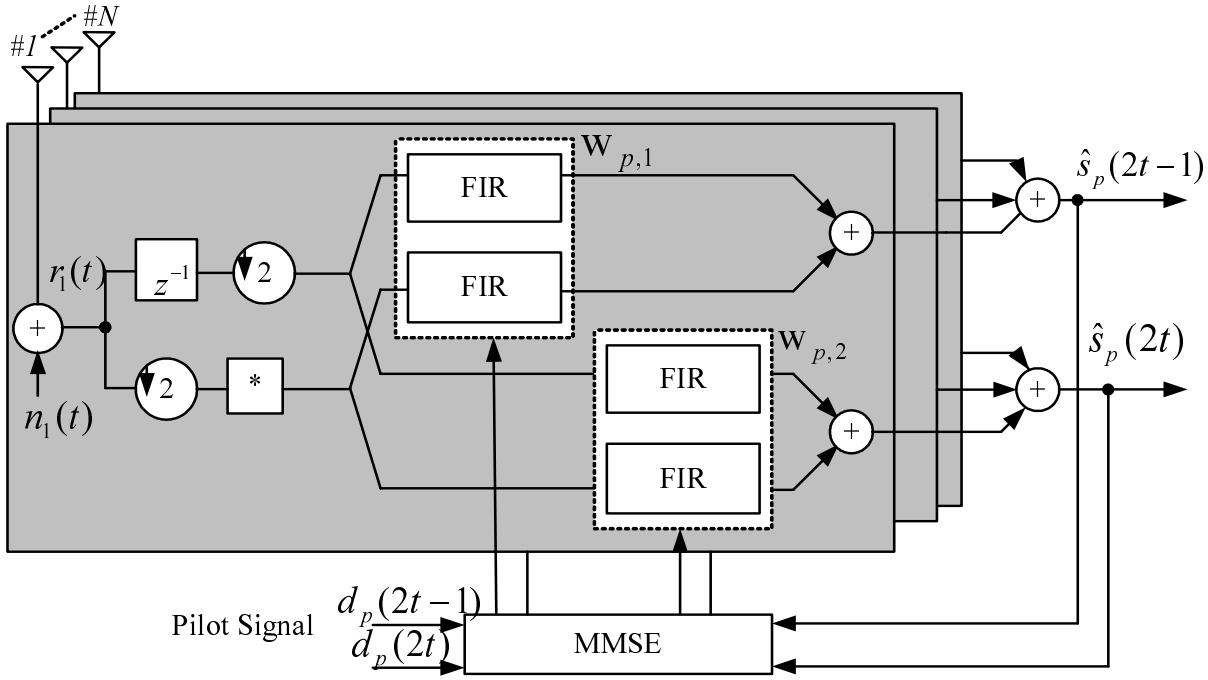

Figure 4.1: Configuration of the receiver of STBC-TDLAA [61].

transmission time, a pair of blocks $\bar{\boldsymbol{s}}_p^{(2k),*}[q]$ and $\bar{\boldsymbol{s}}_p^{(2k-1),*}[q]$ are transmitted at first and second antennas, respectively. The transmit signal at antenna i can be summarized as the following equations. Note that, $\boldsymbol{s}_{p,i}^{(k)}[q]$ is the transmit signal at antennas $i \in \{1,2\}$ for user p.

$$\boldsymbol{s}_{p,1}^{(2k-1)}[q] = \boldsymbol{s}_p^{(2k-1)}[q], \quad \boldsymbol{s}_{p,1}^{(2k)}[q] = -\bar{\boldsymbol{s}}_p^{(2k),*}[q] \tag{4.25}$$

$$\boldsymbol{s}_{p,2}^{(2k)}[q] = \boldsymbol{s}_p^{(2k)}[q], \quad \boldsymbol{s}_{p,2}^{(2k)}[q] = \bar{\boldsymbol{s}}_p^{(2k-1),*}[q]. \tag{4.26}$$

Here the notation $\bar{\boldsymbol{s}}_p^{(2k-1),*}[q]$ and $\bar{\boldsymbol{s}}_p^{(2k),*}[q]$ are time reversed complex-conjugated (TRCC) version of $\boldsymbol{s}_p^{(2k-1)}[q]$ and $\boldsymbol{s}_p^{(2k)}[q]$, respectively. Then, a CP [43, 49] is added, i.e., the last L_{CP} symbol of each block is copied and pasted at the top of each block as the guard interval (GI), to make the total length of $Q + L_{CP}$.

The signal is transmitted over the frequency selective fading channel and we assume the CP is chosen to satisfy $L_{CP} \geq L - 1$. At the receiver, after discarding the CP, the received signal by antenna $j(\{1, 2, .., N\})$ at block $2k-1$ and $2k$ as Fig. 4.3(b) are given

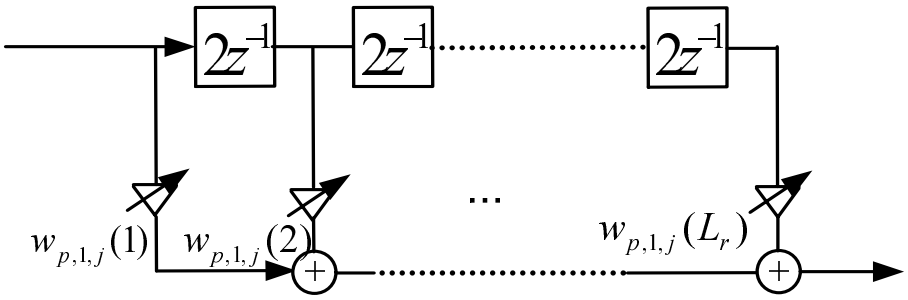

Figure 4.2: A finite impulse response (FIR) filter with controlling weights.

as follows:

$$\boldsymbol{r}_j^{(2k-1)}[q] = \sum_{p=1}^{P}\sum_{l=0}^{L-1}\{h_{p,j1}^{l}\boldsymbol{s}_{p,1}^{(2k-1)}[q-l] + h_{p,j2}^{l}\boldsymbol{s}_{p,2}^{(2k-1)}[q-l]\} + \boldsymbol{n}_j^{(2k-1)}[q] \tag{4.27}$$

$$\boldsymbol{r}_j^{(2k)}[q] = \sum_{p=1}^{P}\sum_{l=0}^{L-1}\{h_{p,j1}^{l}\boldsymbol{s}_{p,1}^{(2k)}[q-l] + h_{p,j2}^{l}\boldsymbol{s}_{p,2}^{(2k)}[q-l]\} + \boldsymbol{n}_j^{(2k)}[q]. \tag{4.28}$$

At the receiver, as shown in Fig. 4.5, the perfect symbol synchronization[2] is assumed. Then the first L_{CP} symbols corresponding to CP are removed from each block. By this operation, all the multipath signals having delays within the GI become equivalent in the frequency-domain with respect to the reference signal. This process will make the channel to be circulant.

The receive signal is then divided into two groups, and each group signal is then split into K subbands using filter banks [44, 46]. The signals in different subbands are processed separately. The filter banks, which are popularly used in SBAA, are realigned by fast Fourier transform (FFT) and inverse fast Fourier transform (IFFT). When critical sampling is used, the decimation rate in the filter banks Q is equal to the number of employed subbands K. In order to perform adaptive processing, the reference signal is also decomposed into subbands to get subband reference signals using the same analysis filter which used to decompose the receive signal. Therefore at the receiver, $\boldsymbol{r}_j^{(2k-1)}[q]$ is delayed about QT_s to synchronize with the next data data (even block). At the mean time, the even block is to be conjugated as $\boldsymbol{r}_j^{(2k)*}[q]$ to extract the component of $\boldsymbol{s}_p^{(2k-1)}[q]$ and $\boldsymbol{s}_p^{(2k)}[q]$ without conjugation. Then, the received signal is decimated with the maximal rate of Q.

MMSE Detection

We now present the theoretical model of proposed configuration of MMSE for STBC-SBAA system. We begin to describe the configuration by attempt to rewrite (4.27) and

[2]The effects of symbol synchronization problem will be discussed in Chapter 7.

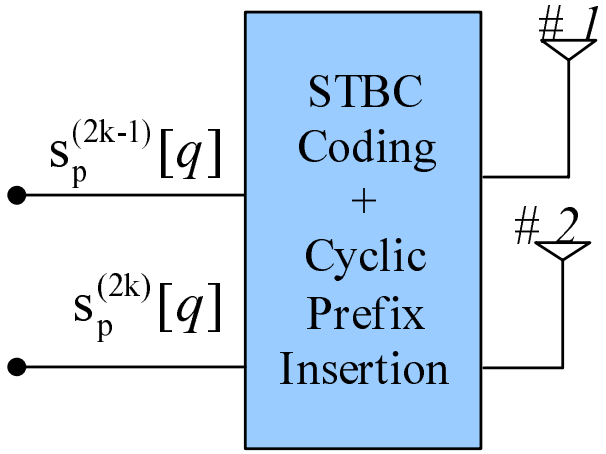

(a) Transmitter

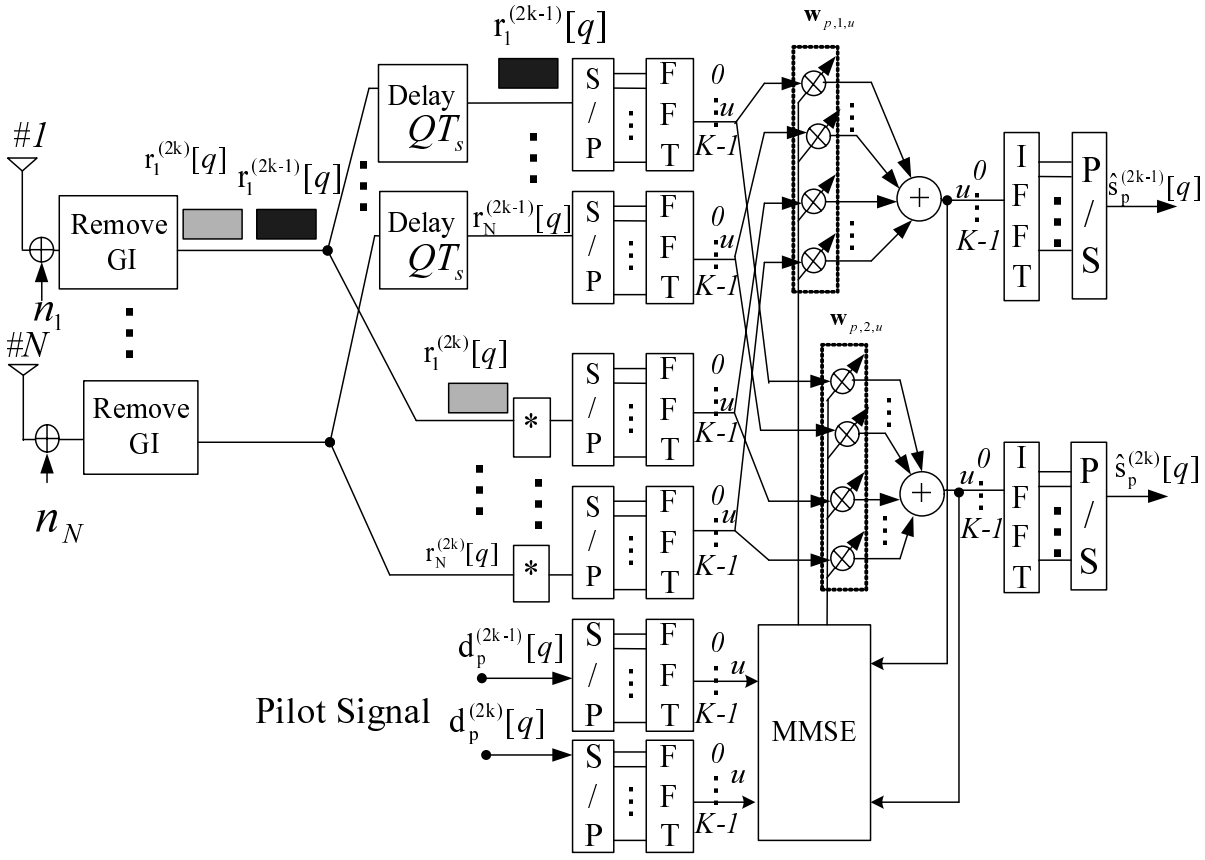

(b) Receiver

Figure 4.3: The configuration of transceiver of STBC-SBAA.

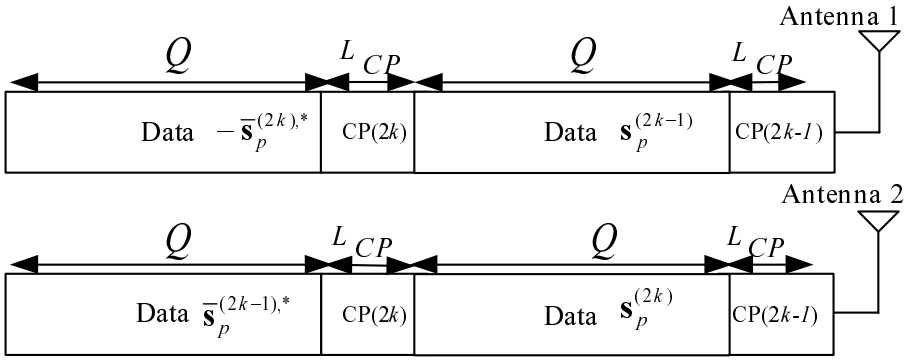

Figure 4.4: Block transmission scheme for STBC-SBAA.

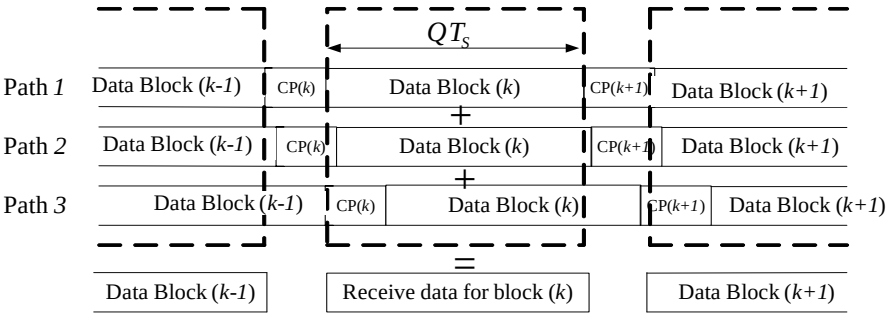

Figure 4.5: Illustration of block data by removing GI.

(4.28) into the vector form. First we define the transmit signal, receive signal and noise as follows.

$$\grave{\boldsymbol{s}}_p^{(k)}[q] = \left[\begin{array}{cc} (\boldsymbol{s}_p^{(2k-1)}[q])^T & (\boldsymbol{s}_p^{(2k)}[q])^T \end{array} \right]^T \tag{4.29}$$

$$\boldsymbol{n}^{(\nu)}[q] = \left[\begin{array}{cccc} (\boldsymbol{n}_1^{(\nu)}[q])^T & (\boldsymbol{n}_2^{(\nu)}[q])^T & \dots & (\boldsymbol{n}_N^{(\nu)}[q])^T \end{array} \right]^T \tag{4.30}$$

$$\boldsymbol{r}^{(\nu)}[q] = \left[\begin{array}{cccc} (\boldsymbol{r}_1^{(\nu)}[q])^T & (\boldsymbol{r}_2^{(\nu)}[q])^T & \dots & (\boldsymbol{r}_N^{(\nu)}[q])^T \end{array} \right]^T \tag{4.31}$$

where $\nu \in \{2k-1, 2k\}$. The above expression can be summarized as

$$\grave{\boldsymbol{n}}^{(k)}[q] = \left[\begin{array}{cc} (\boldsymbol{n}^{(2k-1)}[q])^T & (\boldsymbol{n}^{(2k)}[q])^H \end{array} \right]^T \tag{4.32}$$

$$\grave{\boldsymbol{r}}^{(k)}[q] = \left[\begin{array}{cc} (\boldsymbol{r}^{(2k-1)}[q])^T & (\boldsymbol{r}^{(2k)}[q])^H \end{array} \right]^T \tag{4.33}$$

By using the notation from (4.9) and (4.29) to (4.33), we can rewrite the receive signal (4.27) and (4.28) to be

$$\grave{\boldsymbol{r}}^{(k)}[q] = \sum_{p=1}^{P} \sum_{l=0}^{L-1} \tilde{\boldsymbol{H}}_p^l \grave{\boldsymbol{s}}_p^{(k)}[q-l] + \grave{\boldsymbol{n}}^{(k)}[q] \tag{4.34}$$

Define $\mathcal{F}_{u,q} = \exp(-j\frac{2\pi}{Q}uq)$ as the Fourier transform operator. After taking the FFT, we obtained the Eq. (4.34) at each uth subbands as

$$\breve{\boldsymbol{r}}_u^{(k)}[q] = \sum_{q=0}^{Q-1} \mathcal{F}_{u,q}\hat{\boldsymbol{r}}^{(k)}[q] \tag{4.35}$$

$$= \sum_{q=0}^{Q-1}\sum_{p=1}^{P}\sum_{l=0}^{L-1} \mathcal{F}_{u,q}\tilde{\boldsymbol{H}}_p^{\,l}\hat{\boldsymbol{s}}_p^{(k)}[q] + \sum_{q=0}^{Q-1} \mathcal{F}_{u,q}\hat{\boldsymbol{n}}^{(k)}[q] \tag{4.36}$$

where $u = \{0, 1, \ldots, K-1\}$. Note that for critical sampling, $K = Q$. From equation (4.36), both channels coefficients after FFT operation are *Alamouti-like orthogonal matrices*. Therefore, decoding process in our proposed scheme can be done using linear processing and the full rate and full diversity gain are guaranteed. At the same time, the reference signal $\boldsymbol{d}_p[q] = [\boldsymbol{d}_p^{(2k-1)}[q]), \boldsymbol{d}_p^{(2k)}[q]]^T$ are also converted into subband signals in the same manner to be $\boldsymbol{d}_{p,u}[q] = [\boldsymbol{d}_{p,u}^{(2k-1)}[q], \boldsymbol{d}_{p,u}^{(2k)}[q]]^T$ [44, 46]. In the training process, the complex weights in subband are updated by the error signal. Using the MMSE as the criterion, the $2N \times 1$ optimal weight vector at each subband for estimating $\hat{\boldsymbol{s}}_p^{(2k-1)}[q]$ and $\hat{\boldsymbol{s}}_p^{(2k)}[q]$ is derived as following equations.

$$\boldsymbol{w}_{p,1,u} = \arg\min E\{|\boldsymbol{d}_{p,u}^{(2k-1)}[q] - (\boldsymbol{w}_{p,1,u})^H\breve{\boldsymbol{r}}_u^{(k)}[q]|^2\} \tag{4.37}$$

$$\boldsymbol{w}_{p,2,u} = \arg\min E\{|\boldsymbol{d}_{p,u}^{(2k)}[q] - (\boldsymbol{w}_{p,2,u})^H\breve{\boldsymbol{r}}_u^{(k)}[q]|^2\} \tag{4.38}$$

Here, $\boldsymbol{w}_{p,1,u}$ and $\boldsymbol{w}_{p,2,u}$ are the optimal weights of odd and even block at each subbands. Note that, we use the same covariance matrix to calculate the optimal weight. Satisfying (4.37) and (4.38) gives us the optimal weight vectors for uth subband as given by following equations.

$$\boldsymbol{w}_{p,1,u} = (\boldsymbol{R}_{rr}^u)^{-1}\boldsymbol{X}_{p,u}^{(2k-1)} \tag{4.39}$$

$$\boldsymbol{w}_{p,2,u} = (\boldsymbol{R}_{rr}^u)^{-1}\boldsymbol{X}_{p,u}^{(2k)} \tag{4.40}$$

where

$$\boldsymbol{R}_{rr}^u = E[\breve{\boldsymbol{r}}_u^{(k)}[q](\breve{\boldsymbol{r}}_u^{(k)}[q])^H] \tag{4.41}$$

is the covariance matrix, and

$$\boldsymbol{X}_{p,u}^{(2k-1)} = E[\breve{\boldsymbol{r}}_u^{(k)}[q](\boldsymbol{d}_{p,u}^{(2k-1)}[q])^*] \tag{4.42}$$

$$\boldsymbol{X}_{p,u}^{(2k)} = E[\breve{\boldsymbol{r}}_u^{(k)}[q](\boldsymbol{d}_{p,u}^{(2k)}[q])^*] \tag{4.43}$$

are the correlation vectors of receive signal and reference signal of desired user.

The subbands signal after weighted by the optimal weight are synthesized through the inverse fast Fourier transform (IFFT) to get the output signal as below as

$$\hat{\boldsymbol{s}}_p^{(2k-1)}[q] = \frac{1}{Q}\sum_{u=0}^{Q-1} \mathcal{F}_{u,q}^{-1}\{(\boldsymbol{w}_{p,1,u})^H\breve{\boldsymbol{r}}_u^{(k)}[q]\} \tag{4.44}$$

$$\hat{\boldsymbol{s}}_p^{(2k)}[q] = \frac{1}{Q}\sum_{u=0}^{Q-1} \mathcal{F}_{u,q}^{-1}\{(\boldsymbol{w}_{p,2,u})^H\breve{\boldsymbol{r}}_u^{(k)}[q]\}. \tag{4.45}$$

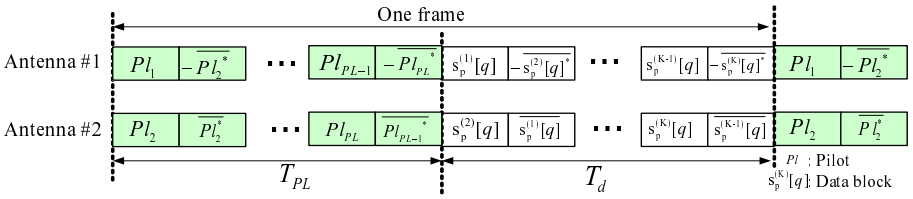

Figure 4.6: Frame format of STBC-SBAA transmission (T_{Pl}:pilot block duration, T_d: data blocks duration, PL: total number of pilot blocks).

Table 4.1: Simulation parameters

Simulation Parameter	Value
STBC type	Alamouti-STBC ($M = 2$)
Data length of each block	$Q = 8$
Number of data blocks	100000
Number of trials	100 times
Number of subbands	$K = Q = 8$
Number of taps (TDLAA)	$L_r = 8$
Adaptive algorithm	Sample matrix inversion (SMI)

Effect of Cyclic prefix in STBC-SBAA

Next, we consider the length of CP which affects the performance of the adaptive receivers. A judicious selection of the length is needed to achieve best performance. In this chapter, we use CP length of L_{CP} symbols out of the Q symbols, which will give a CP power penalty of $Q/(L_{CP} + Q)$. For example, even if $Q = 8$, $L_{CP} = 2$, the degradation in the efficiency is 1 dB. If the larger gain than the above degradation is obtained, we can say that the proposed scheme is effective. The use of longer CP could mitigate the multipath signal and improve the Output SINR and BER performance. But, the use of longer CP will bring a reduction of transmission rate. Therefore, choosing of the CP length and data block length is important in order to mitigate the multipath signal and improve the performance of the proposed scheme.

4.5 Computer Simulation

4.5.1 Simulation Condition

We investigate the performance of the proposed scheme through computer simulations. The simulation parameters are shown in Table 4.1. Here, we consider the case of BPSK (Binary Phase Shift Keying) modulation transmission. Moreover, for a higher order modulation scheme, it can be applied in the proposed scheme without any modifications. In

our simulation the transmitter is equipped with $M = 2$ transmit antennas and uses the Alamouti's STBC to encode the BPSK data symbols. The receiver is equipped with $N = \{2, 4\}$ antennas. The transmit power from each transmit antenna is set equal to $1/2$ to normalize the total power to 1. The channel is assumed to be Rayleigh frequency selective fading channel with the maximum delay of $L-1$, and with uniform power delay profile. The delay profile adopted here may not be realistic in actual environment, but it is suitable to investigate the ability of the proposed scheme in suppressing the interferences. The channel between each transmit antenna ith and receive antenna jth is assumed to be i.i.d and quasi-static Rayleigh fading channel with path coefficient $|h^l_{p,ji}|$ being generated using a complex Gaussian random generation function with zero mean and variance σ_n^2 per complex dimension. Beside that, in order to apply the MMSE method, the channel is set to be constant over the whole block length, i.e., is *quasi-static* over each data block. Noise in each receive antenna is assumed spatially and temporally uncorrelated, and is generated using the same process as channel coefficients. We also assume that the pilot signal is available in the receiver and sample matrix inversion (SMI) is used as the adaptive algorithm. The pilot is sent periodically with data block as shown in Fig. 4.6. Since the data block is sent using STBC, the pilot blocks also sent using the same method. Detailed investigation into convergence behavior of SMI may reduce the length of pilot signal. However, in this chapter we are interested in the system performance rather than the behavior of the employed adaptive algorithm, detailed discussion on the method to reduce the length of pilot signal will be omitted. In the following simulations, we always assume a perfect symbol synchronization. Furthermore, in order to show the effect of frequency selective fading channel, we put $Q = 8$. The longer length of Q would be used to have a better convergence in its output in the case of $L_{CP} = 0$, however as shown in Fig. 4.7, it is enough to assume $Q = 8$ for examining the efficiency of the proposed scheme with $L_{CP} = 2$.

Here, P_S and P_n represent the signal power and noise power, and SNR which denotes the power ratio of the signal and noise. These values are given by

$$E[|\boldsymbol{s}_p|^2] = P_S \tag{4.46}$$

$$E[|\boldsymbol{n}_1|^2] = E[|\boldsymbol{n}_2|^2] = \ldots E[|\boldsymbol{n}_N|^2] = P_n \tag{4.47}$$

$$\text{SNR} = P_S/P_n. \tag{4.48}$$

In order to demonstrate and show the ability of the proposed scheme in frequency selective fading channel, the output signal to interference plus noise ratio (Output SINR) [33, 43] and bit error rate (BER) have been used to evaluate the performance. Output SINR is used in this chapter to represent the interference cancellation capability given by updated weight of the proposed scheme. Define the cross-correlation coefficient given as follows:

$$\rho = \frac{E[\hat{s}_p[t]d_p[t]^*]}{\sqrt{E[|\hat{s}_p[t]|^2]E[|d_p[t]|^2]}} \tag{4.49}$$

where $\hat{s}_p[t]$, $d_p[t]$ are the received signal and the reference signal of pth user, respectively.

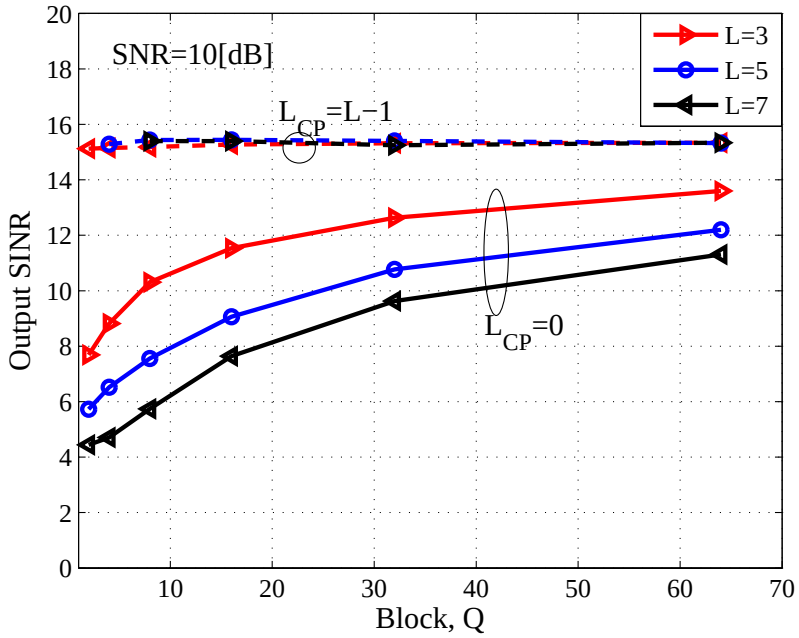

Figure 4.7: Analysis of block length(Q) of STBC-SBAA with $L_{CP} = \{0, L-1\}$ for $L = \{3,\ 5,\ 7\}$

The output SINR [65] is expressed using ρ by the equation:

$$\text{SINR} = \frac{|\rho|^2}{1-|\rho|^2} \tag{4.50}$$

4.5.2 Results

First, we perform the simulation to compare the capability of STBC-SBAA with the conventional STBC, SBAA+CP [49] and STBC-TDLAA [61] in the single user environment. Here we consider a 2×2 MIMO system for STBC[3], STBC-TDLAA, STBC-SBAA and 1×2, 1×4 SIMO (Single Input Multiple Output) for SBAA+CP. The input SNR is changed from 0 dB up to 16 dB, and $L_{CP} = \{0, 2\}$ symbol. Here, the channel model for each $h^l_{p,ji}$ is a typical $L = 3$ path equal power, whereas the preceding path signal is arrived without delay and the third path signal with the delay of two symbols. To maintain the validity of the channel, we assume that the amplitude of the second path is equal to zero. The results are shown in Fig. 4.8 and Fig. 4.9. First, we observe the efficiency of transmission using STBC with SBAA+CP. From Fig. 4.8 and 4.9, it is seen that Output SINR and BER performance of STBC-SBAA increases compare to conventional SBAA+CP due to increasing diversity gain, respectively. For example, focusing at

[3]Conventional STBC refers to the STBC proposed by Alamouti et al. [17] with MLD.

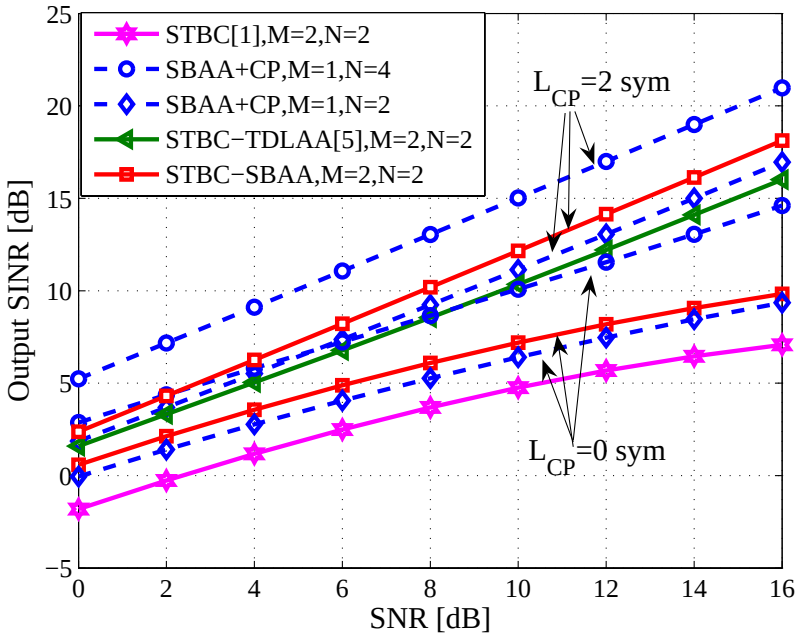

Figure 4.8: Output SINR performance of STBC-SBAA ($M = 2,\ N = 2$), SBAA+CP ($M = 1, N = \{2, 4\}$) for $L_{CP} = \{0, 2\}$ symbols in 2 path equal power frequency selective fading channel model.

BER=10^{-4} and 10^{-6} at Fig. 4.9, it is observed that STBC-SBAA have about 2 dB and 3 dB gain improvement compare to conventional SBAA+CP when $N = 2$ with $L_{CP} = 2$, respectively. These results show that by applying STBC with SBAA+CP jointly would increase the diversity gain. Furthermore, in Fig. 4.9 the curve of STBC-SBAA ($N = 2$) is also located between SBAA+CP with $N = 2$ and $N = 4$, which mean that STBC-SBAA achieve a higher diversity order compared to SBAA+CP when the receive antennas is the same. Although 2×2 STBC-SBAA with $L_{CP} = 2$ has a 3 dB power penalty compare to 1×4 SBAA+CP, STBC-SBAA still achieve the same diversity order as SBAA+CP. Thus the effectiveness of STBC-SBAA is proved.
From both figures, at $L_{CP} = 0$ symbol, it is observed that under frequency selective fading channel, STBC-SBAA can maintain the high Output SINR, while that of the conventional STBC scheme degrades. We can see that the ability of STBC-SBAA with $L_{CP} = 0$ symbol is positioned between the STBC-TDLAA and the conventional STBC method. However, it is also observed that the proposed scheme cannot reach the performance of STBC-TDLAA since the $L_{CP} = 0$ symbol. In order to overcome this problem, we use the single carrier CP. Here, a $L_{CP} = 2$ symbols length of each block are copied and pasted to the top of each block as a GI. From Fig. 4.8, it is seen that the Output SINR of STBC-SBAA with $L_{CP} = 2$ symbols has $2 \sim 4$ dB better than that of without CP ($L_{CP} = 0$ symbol). Equivalently, the BER performance also shows the effectiveness of STBC-SBAA as shown in Fig. 4.9. This performance enhancement is due to the

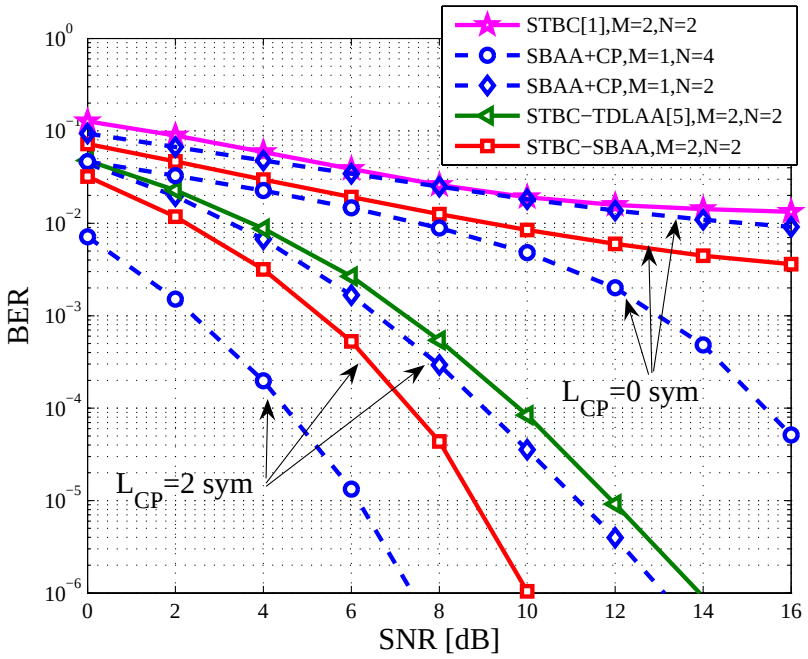

Figure 4.9: BER performance of STBC-SBAA ($M = 2,\ N = 2$), SBAA+CP ($M = 1, N = \{2, 4\}$) for $L_{CP} = \{0, 2\}$ symbols in 2 path equal power frequency selective fading channel model.

path diversity gain thanks to joint function of STBC and SBAA in the proposed scheme. Furthermore, it is also observed that with the help of CP, the proposed scheme (STBC-SBAA) has a better performance compare to STBC-TDLAA about 0.5 dB. In addition, from the point of computational load, STBC-SBAA has an advantage, as described in the Section 4.5.4.

Next, we compare the BER performance for STBC-SBAA ($M = 2,\ N = 4$), SIMO-SBAA ($M = 1, N = 4\}$) for multiuser cases, with $L_{CP} = \{2\}$[4] symbols in two paths equal power delay profile frequency selective fading channel. Here, the users are ranging from single user to five users. The result is illustrated in Fig. 4.10. From the figure, we can see that the BER degraded as number of users increase. However, when $P = 5$ users, the performance degraded very much due to CCIs which cannot be canceled by the receiver, either the STBC-SBAA nor the SIMO-SBAA. Generally, STBC-SBAA shows a better performance compare to SIMO-SBAA in the multiuser environment.

In Fig. 4.11 and Fig. 4.12, we show how the delay length affect the Output SINR and BER of STBC-SBAA for three different SNR, -10 dB, 0 dB and 10 dB. Here, we use the same 2 path equal power channel model as before, but the delayed signal are kept changing from 0 to 5 symbols. The simulation is done for two cases of $L_{CP} = 0$ symbol and $L_{CP} = 2$ symbols. From both figures, when there is no delay signal, i.e *delay symbol* $= 0$ symbol, both Output SINR and BER have the same performance output for the proposed scheme

[4]All delayed signal is completely combined at the receiver.

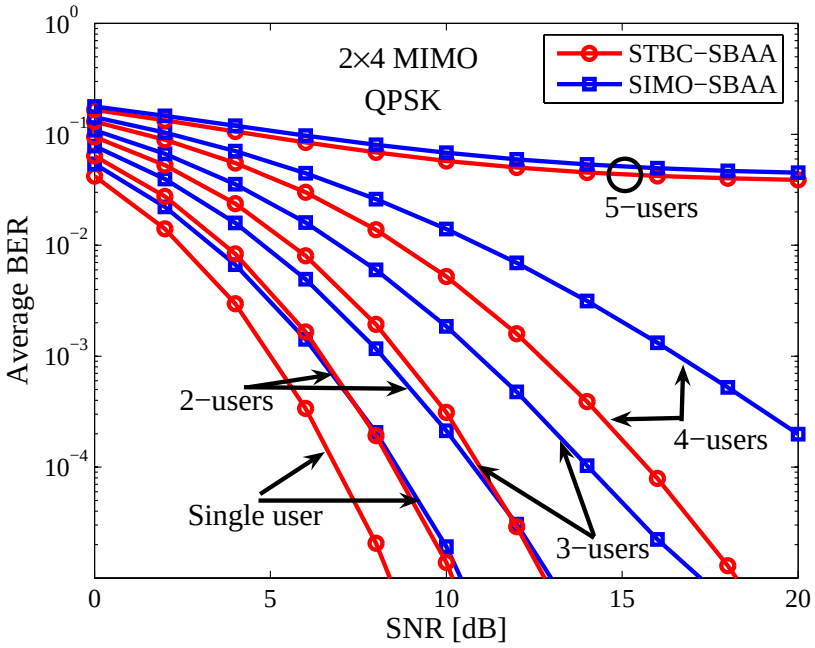

Figure 4.10: BER performance of STBC-SBAA ($M = 2,\ N = 4$), SIMO-SBAA ($M = 1, N = 4\}$) for $L_{CP} = \{2\}$ symbols in 2 path equal power frequency selective fading channel model.

with $L_{CP} = 0$ symbol and $L_{CP} = 2$ symbols. When the *delay symbol* $= 2$ symbols, the proposed scheme with $L_{CP} = 2$ symbols maintain its Output SINR and BER, but performance degradation is observed when the scheme not applying CP, i.e. ($L_{CP} = 0$ symbol). When the *delay symbol* > 2 symbols, for the entire input power signal, the proposed scheme (with and without CP) shows a degradation in its Output SINR and BER performances, respectively. It is seen that, at *delay symbol* $= 3$, the Output SINR of STBC-SBAA reduced about 3, 1, 0.5 dB at 10, 0, -10 dB, respectively. From the experiments, we can conclude that the Output SINR and BER are improved when the delay is shorter than CP length, but degraded when the delayed symbol exceeded the CP length.

Moreover, in Fig. 4.11 and Fig. 4.12, it is observed that at a low input power, the effect of CP application is smaller compared to the case of large input power. The result shows that at lower SNR, the absorption of the delay signal is not significant, but at the case of higher SNR, the receiver removes nearly all the interference since the total energy during the combination of multipath is increased. This result shows that the usage of CP works better at a higher transmit power compare to lower transmit power.

Lastly, to examine the efficiency of the proposed method in the real radio environment, we simulate the proposed scheme applied in frequency selective fading channel with the normalized exponential delay profile distribution. The delay spread is changed $\sigma_\tau = 0 \sim 5T_s$ of multipath waves over one symbol period. The power delay profile is given as

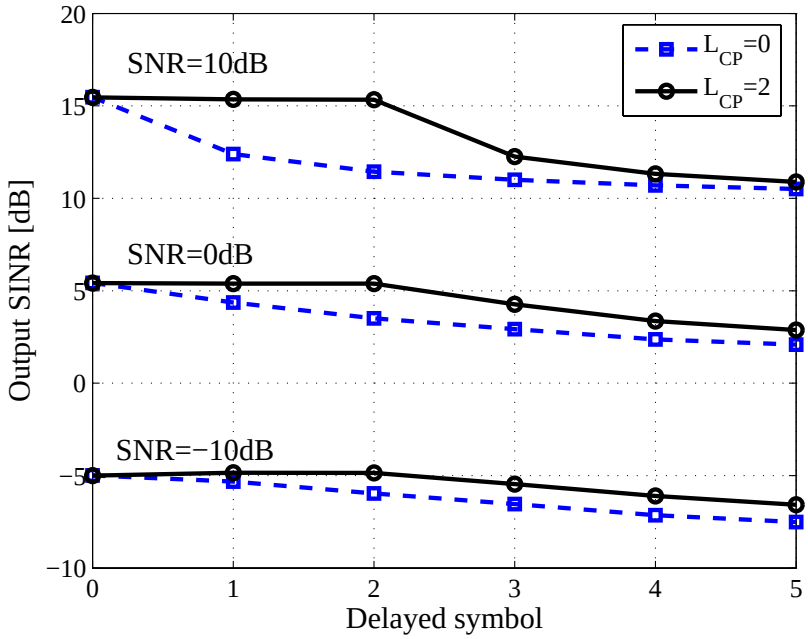

Figure 4.11: Effect of CP length in STBC-SBAA for three different input power signal for $M = 2,\ N = 2$ MIMO system in 2-path equal power frequency selective fading channel model.

Table 4.2: Number of multipath L, versus σ_τ

σ_τ	0	T_s	$2T_s$	$3T_s$	$4T_s$	$5T_s$
L	1	10	19	27	33	40

below [63]:

$$P_l(\tau) = \frac{1}{\sigma_\tau}\sum_{l=0}^{L-1}\exp(-\frac{\tau}{\sigma_\tau})\delta(\tau - lT_s) \tag{4.51}$$

Here, the actual length of delay profiles is infinite, but L path of them are used to make the influence of duration clear. The relationship between σ_τ and L is given in Table 4.2. We performed a simulation for the cases of 2×2 and 2×4 MIMO system. The SNR is set to 10 dB. The simulation result is shown in Fig. 4.13. From this figure, it is shown that BER performance is gradually degraded when delay spread increased. However, a better performance is achieved when a CP is used in the proposed scheme, especially when the number of receiver is increased. For example, at $\sigma_\tau = 2$, $L = 19$, STBC-SBAA shows an acceptable performance eventhough in the multipath rich environment. This improvement is more significant when $N = 4$, which gives more degree of freedom (DOF) to the receiver for combining the desired signal. This result shows that the *antenna gain*

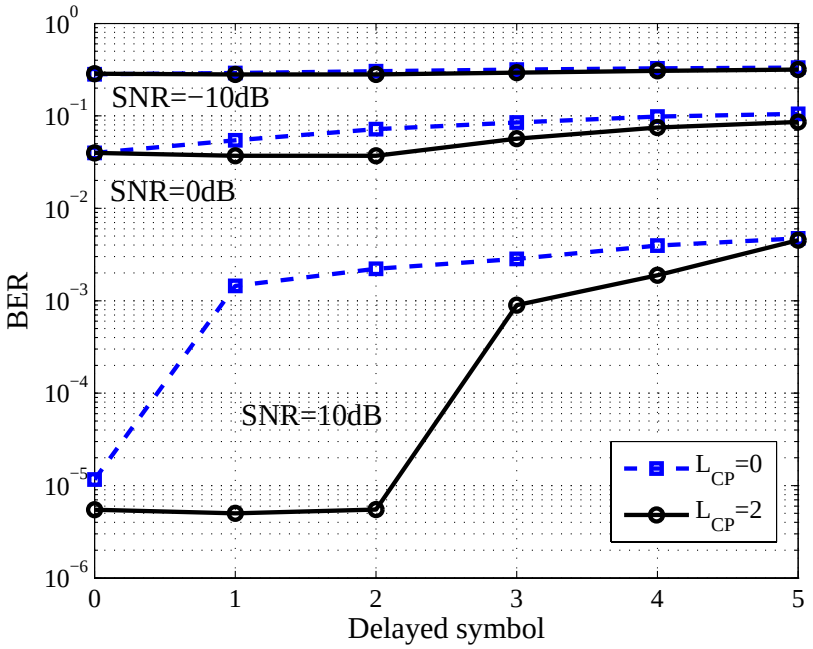

Figure 4.12: BER of STBC-SBAA when the delayed symbol changed for $M = 2,\ N = 2$ MIMO system for the 2 path frequency selective fading channel with uniform power delay profile.

diversity helped to improve the overall performance of the proposed scheme.

4.5.3 Comparison with OFDM Transmission

Next, we present the performance comparison between conventional SIMO-SBAA, proposed STBC-SBAA with SIMO-OFDM, and STBC-OFDM. Here, we assume the antenna configuration as 1×1, 1×2, 1×4 for SIMO-SBAA and SIMO-OFDM, 2×1, 2×2, 2×4 for STBC-SBAA and STBC-OFDM, respectively, while $L = 2$ path equal power delay profile are considered. The length of CP is kept to $L_{CP} = 2$ symbol. The result is shown in Fig. 4.14. From the figure, the performance of STBC-SBAA has a best BER performance among the entire method. It is shown that STBC-SBAA (single carrier) is superior compare to multicarrier system as OFDM transmission for all the antennas configuration. This is because, due to the considered channel, the STBC-SBAA which works in time domain exploit the spatial diversity while OFDM which exploit the frequency diversity, cannot exploit the diversity unless the channel is time varying. These trend imply that the exploitation of frequency diversity can potentially provide better performance gains for OFDM transmission than the utilization of spatial diversity alone. Furthermore, STBC-SBAA systems employing linear MMSE equalization perform relatively well in rich scattering environment.

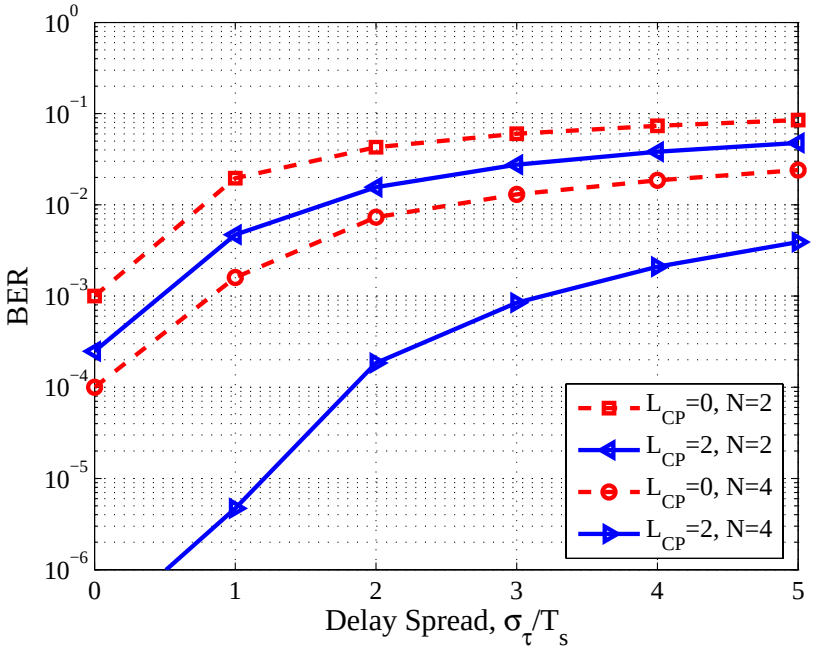

Figure 4.13: BER of STBC-SBAA when the delay spread changed from $\sigma_\tau = 0 \sim 5T_s$ with $M = 2$ for the frequency selective fading channel with the exponential power delay profile.

4.5.4 Computational Load

Since the adaptive processing in MIMO system tends to have high complexity, it is important to investigate the computational load for our proposed scheme. We approximate the complexity by counting the number of multiplications.

STBC-TDLAA scheme uses sample by sample processing to update the weight, while the proposed scheme uses block by block processing. We can show the number of the multiplication B in each step of weight update using the equation below. While STBC-TDLAA with L_r tap requires $2(L_rN)^3$ multiplication for each weight update, while STBC-SBAA with K subbands, needs only $2KN^3$ multiplication, and as FFT/IFFT are used, it is requires $4K\log_2 K$ more multiplications. Hence, the total multiplication number is given by next equations [43].

$$B_{STBC-TDLAA} = 2(L_rN)^3 \tag{4.52}$$

$$B_{STBC-SBAA} = 2K(N^3 + 2\log_2 K) \tag{4.53}$$

From the above equations, at $K = L_r$ we can see that $B_{STBC-TDLAA}$ work on the third order $\mathcal{O}(K^3)$ processing, compare to $B_{STBC-SBAA}$ which on the first order $\mathcal{O}(K)$ processing. For example, when $K = 8$, and $L_r = 8$, STBC-TDLAA need about 4096 multiplications compare to STBC-SBAA which only need about 79 multiplications.

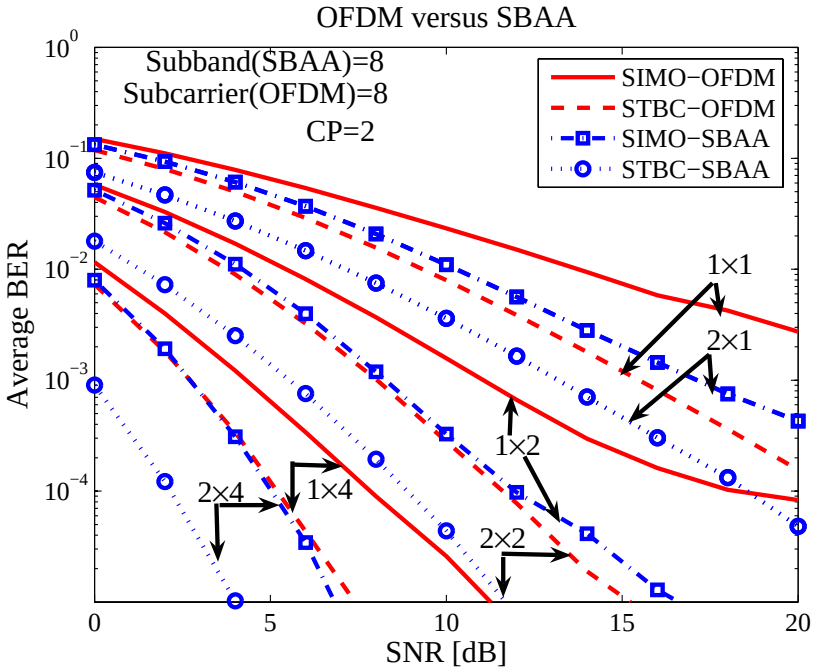

Figure 4.14: Performance comparison between SIMO-SBAA, STBC-SBAA, SIMO-OFDM, and STBC-OFDM transmission in the frequency selective fading channel with $L = 2$, $L_{CP} = 2$ symbol.

4.5.5 Effect of STBC-SBAA in Time Varying Fading Channel

In the previous section, we discussed the STBC-SBAA so far assuming that the channel remains aproximately constant over two frames. However, in practice, there may be situations when the channel is changing so fast that even the assumptions are not adequate. This assumption is still relevance even though in the time varying fading channel if the pilot is adequately tracked. In this case, the parameter which describes the time varying fading channel are the maximum Doppler frequency f_D and frame interval, $T_f = T_d + T_{PL}$. In order to make this assumption to be relevant in time varying fading channel, the frame length which contains pilot and data blocks must be within $\Delta << f_D T_f$. The performance of STBC-SBAA would be affected by time varying fading channel if the frame length more than Δ.

For example, consider a 2 GHz wireless system where the user terminal is moving with 30 m/s, namely $f_D = 200$ Hz. Assuming that $T_s = 0.1\mu$s, $Q = 8$, $PL = 8$(block), $K = 50$(block), then $T_{PL} = 2PL \times Q \times T_s = 12.8\mu$s and $T_d = 2 \times K \times Q \times T_s = 80\mu$s, which leads $f_D T_f = 0.018$. In this case the effect due to time varying fading channel can be treated as quasi-static in general. STBC-SBAA would be affected by time varying fading channel if we use the frame length longer than described above or using a higher frequency.

4.6 Conclusion

In this chapter, we propose a combined CSI estimation and signal detection scheme for MIMO transmission scheme using STBC adopting SBAA (STBC-SBAA) processing under frequency selective fading channel. In the receiver, the received signal is divided into two independent group of signal and adaptive processing is carried out in frequency-domain to equalize the frequency selective fading channel and estimate the desired signal. A novel construction of SBAA is introduced to process the received signal. Through computer simulations, it has been verified that the proposed scheme shows a better performance than STBC of conventional type. Its ability is positioned between conventional STBC and the STBC-TDLAA scheme. Furthermore, to enhance the performance of the proposed scheme, we evaluate the idea of single carrier CP into STBC-SBAA. It is also demonstrated that the proposed scheme with CP achieves a better performance compare to STBC-TDLAA scheme, with less computational load. We shall extend the proposed scheme to the application with CDMA in the next chapter.

Chapter 5

Subband Adaptive Array for STBC CDMA System

This chapter presents interference suppression using a STBC-SBAA for uplink CDMA system over frequency selective fading channel. The proposed scheme utilizes CDMA system with STBC and a receive array antenna with SBAA processing at the receiver. The received signal is converted into the frequency domain before despreading and adaptive processing is performed for each subband. A novel SBAA construction is introduced to process CDMA signals based on STBC. To improve the performance of the proposed scheme, we evaluate STBC-SBAA using spreading codes CP. Simulation results demonstrate an improved performance of the proposed system for single and multiuser environments compared to competing related techniques.

5.1 Introduction

There is an ever-increasing need for next generation wireless systems to provide higher data transmission rates to meet the emerging demand for new multimedia applications. This presents a major challenge for wireless technology, namely to increase system capacity and quality within the limited available frequency spectrum. It is well known that CDMA system is a promising means to meet the high data rate demands of next generation wireless systems [3, 64, 65].

In radio communication systems, the quality of high-speed data transmission is severely degraded by multipath fading channel resulting from multiple propagation paths with different time delays. To achieve high-speed data transmission, high-quality communication or high-capacity communication, countermeasures should be employed to combat these impairments. Many studies have been made on the use of multiple antennas (multiple input multiple output (MIMO)) to counter multipath fading channel and provide spatial diversity. Of these methods, space time spreading (STS) [66] and STBC [17] are the most efficient due to their provision of full spatial diversity and a simple linear decoder. For multiuser communication systems, STBC can be used in conjunction with receive

adaptive beamforming to suppress co-channel interference (CCI) [67]. Furthermore, it has been proposed that STBC can be used with direct sequence (DS) CDMA system to counter the impairment of multiuser channels [68, 69].

However, in the frequency selective fading channel, transmission using STBC suffers from inter-chip interference (ICI) and increased multiple access interference (MAI), which dramatically deteriorates the performance. A CDMA system which utilizes a transmit array antenna at the transmitter and a receive array antenna with tap delay line (TDL) filters at both side [70] shows significant performance and capacity improvement in frequency selective fading channel environments. However, when the delay spread is longer and the number of users increases, both the transmitter and receiver TDL memories will be longer and the complexity increased exponentially. The SBAA [65, 71], which can reduce the computational complexity through block processing, is a solution to the limitations of the TDL adaptive array (TDLAA), even though its performance is slightly degraded, especially in the long delay spread frequency selective fading channel in comparison. Recently, SBAA for STBC (STBC-SBAA) [72] has been proposed, which can reduce the computational complexity through block processing and exploiting the multipath gain through STBC, thus improving the performance of the system with the help of cyclic prefix (CP) in the single user frequency selective fading channel environment. On the other hand, single-carrier block transmission (SCBT) DS-CDMA system, recently proposed as chip-interleaved block spread (CIBS) in [73] can effectively deals with frequency selective fading channel through zero-padding (ZP) of the chip blocks. Moreover, SCBT DS-CDMA system preserves the orthogonality between users regardless of the underlying multipath channel, which enables deterministic maximum likelihood (ML) user separation through low complexity code-matched filtering. However, this method only considers the single input single output (SISO), and no results for MIMO environment have been produced. In Ref. [74], a combination of time reversal STBC (TR-STBC) and SCBT for downlink frequency selective fading channels was proposed. However, it was assumed that the CSI was known for the equalization process at the receiver. In [79], a receiver with multistage interference cancellation and equalization method using the parallel interference cancellation (PIC) and successive interference cancellation (SIC) after the STBC decoding for CDMA system has been proposed. Remarkably, the computational complexity of the method in [79] increases with increasing the number of users. In [80], a non-CDMA frequency domain equalization and interference cancellation for multiuser STBC has been proposed. Here, the number of users and receive antennas have to be equal in order to separate the user's signal. This would lower the degree of flexibility of the system.

In this chapter, we propose a novel CDMA system using SBAA, designed for STBC transmission over frequency selective fading channel, assuming CSI at the transceivers is unknown, while a pilot signal is available during the training period. The proposed scheme utilizes STBC for the transmit diversity and a receive antenna with an SBAA. At the receiver, a novel SBAA construction to process CDMA signals based on STBC is introduced. The receive block signal is divided into two groups and adaptive processing is performed at the chip-level to equalize and estimate the desired signal. Here, the

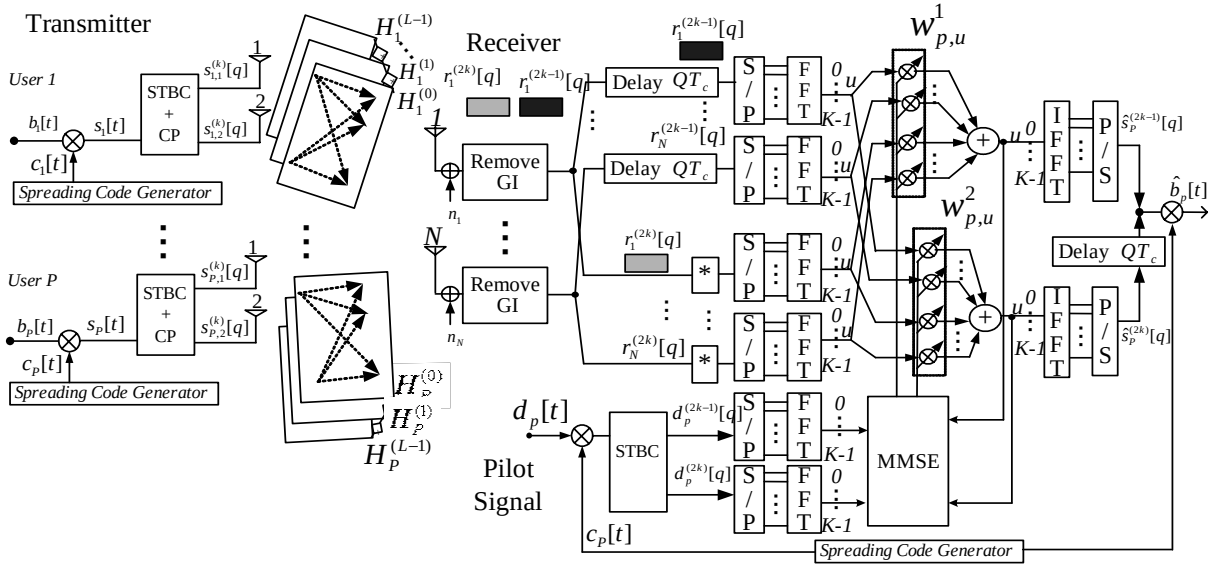

Figure 5.1: Configuration of wideband STBC-SBAA for uplink CDMA system.

equalization of received signal and MAI suppression is done simultaneously, which lowers the complexity of the receiver's configuration. In addition, to improve the performance of STBC-SBAA, we apply the spreading code CP [71]. Simulation results demonstrate that the performance of the proposed transceiver is outstanding compared to competing alternatives.

The rest of the chapter is organized as follows: In Section 5.2, the proposed system of STBC-SBAA for CDMA system is introduced. The simulation and results are presented in Section 5.3. Finally, Section 5.4 summarizes the chapter.

5.2 Configuration of STBC-SBAA for Uplink CDMA System

5.2.1 STBC-SBAA

In this chapter, we consider an asynchronous multiuser CDMA system employing STBC at each transmitter. On the base-station (BS), we propose a SBAA based on STBC (STBC-SBAA) to estimate the desired user's signal. Each mobile station (MS) utilizes M transmit antennas and the BS utilizes N receive antennas. The configuration of the proposed STBC-SBAA for CDMA system is illustrated in Fig. 5.1. The SBAA was first introduced by Compton [37] and has been studied further in [44, 72, 77]. In this chapter, we restricted our system to Alamouti's STBC [17] with $M = 2$. An extension to more general types of STBC, namely with $M > 2$ is quite straight forward.

In this chapter, we assume an frequency selective fading channel with a total of mul-

tipath L with time spacing of chip duration T_c, as given by the next equation.

$$\boldsymbol{H}_p(\tau) = \sum_{l=0}^{L-1} \boldsymbol{H}_p^{(l)} \delta[\tau - lT_c] \tag{5.1}$$

$$\boldsymbol{H}_p^{(l)} = \begin{bmatrix} h_{p,11}^l & h_{p,12}^l \\ \vdots & \vdots \\ h_{p,N1}^l & h_{p,N2}^l \end{bmatrix}, \tag{5.2}$$

where, δ is the Dirac delta function and $h_{p,ji}^l$ is the channel coefficient with l-th delay between i-th ($i = 1, 2$) transmit and j-th ($j = 1, \ldots, N$) receive antenna elements for p-th user. In contrast to conventional STBC [17], in the proposed method STBC-SBAA transmission is carried out in block sequence as the method to decrease the effect of ICI, as shown in Fig. 4.4. In frequency selective fading channel, the sequentially transmitted symbols interfere with each other at the receiver, and therefore we need to consider a sequence, or block of symbols instead of single symbol at one time. This operation is to keep the full spatial diversity in STBC.

Consider the uplink multiuser communication system where P mobile users exist. The data signal of each user is given by $b_p[t]$, where $p = \{1, 2, \ldots, P\}$. Suppose that each user employs M-sequences (maximal length code)[1] $c_p[t]$, which is generated by different polynomials but their period are identical. The pth code is periodic and period equal to the spreading factor Q, and it is denoted as follows:

$$\boldsymbol{c}_p = \begin{bmatrix} c_p(0) & c_p(1), & c_p(1), & \ldots & c_p(Q-1). \end{bmatrix} \tag{5.3}$$

Let us define $s_p(n)$ as the chip sequence corresponding to data sequence $b_p[t]$ of pth user as

$$s_p[n] \triangleq b_p[t] c_p(\lfloor n \rfloor_Q),\ n = 1, 2, \ldots,\ t = \lfloor \frac{n}{Q} \rfloor, \tag{5.4}$$

where we have used operator $\lfloor i \rfloor_L \triangleq i \mod L$ and $\lfloor x \rfloor_L$, which select the largest integer that equals or does not exceed x (floor function). The spread signal of each user $s_p[n]$ is then divided into chip blocks of length Q. The kth ($k \in \mathbb{Z}$) chip-block with each element is represented as

$$s_p^{(k)}[q] = s_p[kQ + q], \tag{5.5}$$

where $q \in \{0, 1, \ldots, Q-1\}$.

The kth chip blocks $\boldsymbol{s}_p^{(k)}[q] = [s_p^{(k)}[0], \ldots, s_p^{(k)}[Q-1]]$ contains Q chips. The input chip block signal is encoded by STBC [17], where at odd time slot of $2k-1$, $(= \{1, 3, 5, 7, \ldots\})$, a pair of chip blocks $\boldsymbol{s}_p^{(2k-1)}[q]$ and $\boldsymbol{s}_p^{(2k)}[q]$ are transmitted from first and second antenna, respectively. Similarly, at the even time slot of $2k$, $(= \{2, 4, 6, \ldots\})$, a pair of chip blocks

[1]Here we use Gold Sequence

$-\bar{\boldsymbol{s}}_p^{(2k)*}[q]$ and $\bar{\boldsymbol{s}}_p^{(2k-1)*}[q]$ are transmitted from first and second antenna, respectively. Note that the superscript * denotes complex conjugate, and $\bar{s}_p^{(2k-1)*}[q] = s_p^{(2k-1)*}[Q-q-1]$ and $\bar{s}_p^{(2k)*}[q] = s_p^{(2k)*}[Q-q-1]$ are time-reversed and element-by-element complex-conjugated (TRCC) version of $s_p^{(2k-1)}[q]$ and $s_p^{(2k)}[q]$, respectively. The operation of time-reversion is for handling the frequency domain processing in the receiver [59]. The transmit signal $s_{p,i}^{(k)}[q]$ at antenna $i \in \{1,2\}$ of pth user can be shown as below.

$$s_{p,1}^{(2k-1)}[q] = s_p^{(2k-1)}[q], \quad s_{p,1}^{(2k)}[q] = -\bar{s}_p^{(2k)*}[q] \tag{5.6}$$

$$s_{p,2}^{(2k-1)}[q] = s_p^{(2k)}[q], \quad s_{p,2}^{(2k)}[q] = \bar{s}_p^{(2k-1)*}[q] \tag{5.7}$$

Then, CP is applied, i.e., the last L_{CP} chip of each block is copied and pasted at the top of each block as a guard interval (GI), making the total length of $Q + L_{CP}$ as shown in Fig. 4.4[2]. This operation minimizes the effect of ICI and produces multipath gain [71,72]. The block configuration at first and second antennas after the addition of CP can be shown below for $v \in \{2k-1, 2k\}$.

$$\grave{\boldsymbol{s}}_{p,1}^{(v)} = [s_{p,1}^{(v)}[Q-1-(L_{CP}-1)], \ldots, s_{p,1}^{(v)}[Q-1], s_{p,1}^{(v)}[0], \ldots, \ldots, s_{p,1}^{(v)}[Q-1]]^T \tag{5.8}$$

$$\grave{\boldsymbol{s}}_{p,2}^{(v)} = [s_{p,2}^{(v)}[Q-1-(L_{CP}-1)], \ldots, s_{p,2}^{(v)}[Q-1], s_{p,2}^{(v)}[0], \ldots, \ldots, s_{p,2}^{(v)}[Q-1]]^T \tag{5.9}$$

After the transmission over the frequency selective fading channel, assuming that CP is chosen to satisfy $Q + L_{CP} \geq L - 1$. Then, after discarding the CP, the received signals at antenna jth for block of $v \in \{2k-1, 2k\}$ are given as follows:

$$r_j^{(v)}[q] \;=\; \sum_{p=1}^{P} \sum_{l=0}^{L-1} \{h_{p,j1}^l s_{p,1}^{(v)}[q-l] + h_{p,j2}^l s_{p,2}^{(v)}[q-l]\} + n_j^{(v)}[q], \tag{5.10}$$

where $n_j^{(v)}[q]$ is the additive white Gaussian noise (AWGN) at jth antenna, which is assumed to be independent and identically distributed (i.i.d.) with zero mean and variance of σ_n^2 at each real dimension. Note that when the delay spread length is larger than the block length $(Q + L_{CP})$, the receive block signal is shifted to the previous block, .i.e. for $l > q$, $s_{p,i}^{(v)}[q-l] = s_{p,i}^{(v-1)}[Q+L_{CP}+q-l]$. Here, the transmission power from each antenna is half of the value in the single-transmit antenna case, so that the total transmit power is kept constant irrespective of the number of transmit antennas.

At the receiver, as shown in Fig. 5.1, the chip synchronization is done before the part of *Remove GI*, then the first L_{CP} symbols corresponding to the GI are removed from each block. Then, $r_j^{(2k-1)}[q]$ is delayed about QT_c to synchronize with the even block data. At the same time, the even blocks are complex-conjugated to become $r_j^{(2k)*}[q]$ to extract the component of $\boldsymbol{s}_p^{(2k-1)}[q]$ and $\boldsymbol{s}_p^{(2k)}[q]$ without conjugation.

[2]The block configuration of STBC-SBAA for CDMA system is similar to the Fig. 4.4, however the each data block consist of chips block, not symbol blocks as STBC-SBAA in Chapter 4.

5.2.2 MMSE Detection

We now present the theoretical model of minimum mean square error (MMSE) multiuser detector for STBC-SBAA. We describe the configuration by rewriting (5.10) in the vector form as follows:

$$\breve{\boldsymbol{r}}^{(k)}[q] = \sum_{p=1}^{P}\sum_{l=0}^{L-1} \tilde{\boldsymbol{H}}_p^l \breve{\boldsymbol{s}}_p^{(k)}[q-l] + \breve{\boldsymbol{n}}^{(k)}[q] \tag{5.11}$$

where,

$$\breve{\boldsymbol{s}}_p^{(k)}[q] = \begin{bmatrix} s_p^{(2k-1)}[q] & s_p^{(2k)}[q] \end{bmatrix}^T \tag{5.12}$$

$$\breve{\boldsymbol{n}}^{(k)}[q] = \begin{bmatrix} (\boldsymbol{n}^{(2k-1)}[q])^T & (\boldsymbol{n}^{(2k)}[q])^H \end{bmatrix}^T \tag{5.13}$$

$$\breve{\boldsymbol{r}}^{(k)}[q] = \begin{bmatrix} (\boldsymbol{r}^{(2k-1)}[q])^T & (\boldsymbol{r}^{(2k)}[q])^H \end{bmatrix}^T \tag{5.14}$$

and, $\boldsymbol{n}^{(v)}[q],\ \boldsymbol{r}^{v}[q]$ for $v \in \{2k-1, 2k\}$ as

$$\boldsymbol{n}^{(v)}[q] = \begin{bmatrix} n_1^{(v)}[q] & n_2^{(v)}[q] & \dots & n_N^{(v)}[q] \end{bmatrix}^T \tag{5.15}$$

$$\boldsymbol{r}^{(v)}[q] = \begin{bmatrix} r_1^{(v)}[q] & r_2^{(v)}[q] & \dots & r_N^{(v)}[q] \end{bmatrix}^T \tag{5.16}$$

Note that the superscript $(\cdot)^T$ and $(\cdot)^H$ denotes the transpose and Hermitian transpose operation, respectively. We redefine the frequency selective fading channel of (5.2), as follows

$$\tilde{\boldsymbol{H}}_p^l = \begin{bmatrix} \boldsymbol{h}_{p,1}^l & -\boldsymbol{h}_{p,2}^{l*} \\ \boldsymbol{h}_{p,2} & \boldsymbol{h}_{p,1}^{l*} \end{bmatrix}. \tag{5.17}$$

where,

$$\boldsymbol{h}_{p,1}^l = [h_{p,11}^l\ h_{p,21}^l\ h_{p,31}^l\ \dots\ h_{p,N1}^l]^T \tag{5.18}$$

$$\boldsymbol{h}_{p,2}^l = [h_{p,12}^l\ h_{p,22}^l\ h_{32,p}^l\ \dots\ h_{p,N2}^l]^T \tag{5.19}$$

In this chapter, subband adaptive processing with the most popular linear multiuser method, namely, MMSE is used to detect transmitted signals from the P users. To perform adaptive signal processing in subbands, the receive signal $\breve{\boldsymbol{r}}^{(k)}[q]$ is decomposed into subbands using an analysis filter. The analysis filter employed in the proposed configuration utilizes *critical sampling*, i.e. the received signal at each array element is decimated with maximum rate Q. This operation will result in block processing mode and thus helps to save a great amount of computational load compare with sliding window processing [37, 44, 72]. As shown in Fig. 5.1, in order to work with STBC, the subband processing is performed by referencing two consecutive blocks as input. Therefore there are two groups of optimal weight vector exist to maximize the output power of detected

signal. This is different from a conventional SBAA which references one input block signal, thus producing only one optimal weight vector.

Let us define the Fast Fourier Transform (FFT) operation by $\mathcal{F}_{u,q} = e^{-j\frac{2\pi}{Q}uq}$. After taking FFT, we obtain the frequency samples at the u-th subband as follows:

$$\tilde{\boldsymbol{r}}_u^{(k)}[q] = \sum_{q=0}^{Q-1} \mathcal{F}_{u,q}(\breve{\boldsymbol{r}}^{(k)}[q]) \tag{5.20}$$

$$= \sum_{q=0}^{Q-1} \mathcal{F}_{u,q}(\sum_{p=1}^{P}\sum_{l=0}^{L-1} \tilde{\boldsymbol{H}}_p^l \breve{\boldsymbol{s}}_p^{(k)}[q]) + \sum_{q=0}^{Q-1} \mathcal{F}_{u,q}(\breve{\boldsymbol{n}}^{(k)}[q]), \tag{5.21}$$

where $u = \{0, 1, \ldots, K-1\}$, and K is the total number of subbands. Since critical sampling is used in STBC-SBAA, we assume that $K = Q$.

In order to generate the receive antenna weights, one may use either a blind (reference signal is created from the received signal) or pilot training (reference signal is created from a known training sequence). In this chapter, for simplicity we utilize the pilot training method. Assume that the pth user is taken to be the desired user while the remaining P users are uninterested (undesired) users. Define the pilot signal of pth user as $d_p[t]$, and after being spread and encoded by STBC, the pilot signal for odd and even blocks are given as $d_p^{(2k-1)}[q]$ and $d_p^{(2k)}[q]$. These pilot signals are also converted into subband signals in the same manner to become $\tilde{d}_{p,u}^{(2k-1)}[q]$ and $\tilde{d}_{p,u}^{(2k)}[q]$. By using MMSE criterion, the $2KN \times 1$ optimal weight vectors for estimating $\hat{s}_p^{(2k-1)}[q]$ and $\hat{s}_p^{(2k)}[q]$ are derived as follows.

$$\boldsymbol{w}_{p,u}^1 = \arg\min \; E\{|\tilde{d}_{p,u}^{(2k-1)}[q] - (\boldsymbol{w}_{p,u}^1)^H \tilde{\boldsymbol{r}}_u^{(k)}[q]|^2\} \tag{5.22}$$

$$\boldsymbol{w}_{p,u}^2 = \arg\min \; E\{|\tilde{d}_{p,u}^{(2k)}[q] - (\boldsymbol{w}_{p,u}^2)^H \tilde{\boldsymbol{r}}_u^{(k)}[q]|^2\}. \tag{5.23}$$

Note that $E[\cdot]$ denotes the ensemble average operator. Here, $\boldsymbol{w}_{p,u}^1$ and $\boldsymbol{w}_{p,u}^2$ are the optimal weight vector for the odd and even block at each subband of pth user and updated on a block-by-block basis. Satisfaction of equation (5.22) and (5.23) gives us the optimal weight vector in uth subband as follows:

$$\boldsymbol{w}_{p,u}^1 = (\boldsymbol{R}_{rr}^u)^{-1} \boldsymbol{X}_{p,u}^{(2k-1)} \tag{5.24}$$

$$\boldsymbol{w}_{p,u}^2 = (\boldsymbol{R}_{rr}^u)^{-1} \boldsymbol{X}_{p,u}^{(2k)}, \tag{5.25}$$

where,

$$\boldsymbol{R}_{rr}^u = E[\tilde{\boldsymbol{r}}_u^{(k)}[q](\tilde{\boldsymbol{r}}_u^{(k)}[q])^H], \tag{5.26}$$

is the covariance matrix and

$$\boldsymbol{X}_{p,u}^{(2k-1)} = \mathrm{E}[\tilde{\boldsymbol{r}}_u^{(k)}[q](\tilde{d}_{p,u}^{(2k-1)}[q])^*] \tag{5.27}$$

$$\boldsymbol{X}_{p,u}^{(2k)} = \mathrm{E}[\tilde{\boldsymbol{r}}_u^{(k)}[q](\tilde{d}_{p,u}^{(2k)}[q])^*], \tag{5.28}$$

are the correlation vectors of receive signal and reference signal in the uth subband. In other words, STBC-SBAA multiuser detection can be implemented as a set of "single user" interference suppression filters. From (5.24) and (5.25), the optimal weight vector of odd and even blocks are calculated using the same correlation matrix for maximizing the power of desired signal at each block.

The subband signals after weighted by the optimal weight synthesized through the inverse FFT (IFFT) can be expressed as below.

$$\hat{s}_p^{(2k-1)}[q] = \sum_{u=0}^{K-1} \mathcal{F}_{u,q}^*((\boldsymbol{w}_{p,u}^1)^H \tilde{\boldsymbol{r}}_u^{(k)}[q]) \tag{5.29}$$

$$\hat{s}_p^{(2k)}[q] = \sum_{u=0}^{K-1} \mathcal{F}_{u,q}^*((\boldsymbol{w}_{p,u}^2)^H \tilde{\boldsymbol{r}}_u^{(k)}[q]) \tag{5.30}$$

Note that $\mathcal{F}_{u,q}^* = e^{j\frac{2\pi}{Q}uq}$. After the rearrangement and combination of the IFFT output tap as $\hat{s}_p[Qk+q] = \hat{s}_p^{(k)}[q]$, the desired signal is retrieved by de-spreading with pth user's spreading codes.

$$\hat{b}_p[t] = \frac{1}{Q}\hat{s}_p[n] * c_p^*(\lfloor n \rfloor_Q),\ n = 1, 2, \ldots,\ t = \lfloor \frac{n}{Q} \rfloor, \tag{5.31}$$

5.3 Simulation and Results

5.3.1 Simulation Conditions

The simulation parameters are shown in Table 5.1. In this chapter, we consider the case of BPSK (Binary Phase Shift Keying) modulation transmission with each user utilizing $M = 2$ transmit antennas and the BS utilizing $N = 2$ receive antennas. Each block contains $Q = 31$ chips and we have chosen the Gold spreading codes of length=31 chips as the spreading sequence. In subband processing, $K = 31$ subbands is assumed. In the following simulations, we always assume perfect synchronization and transmission power control in the system. Here a perfect power control assumption means that the signals from all users in the same cell site arrive at the BS with the same average power.

To examine the efficiency of proposed method in a real radio environment, we applied the frequency selective fading channel with a discrete exponential power delay profile with normalized delay spread σ of $T_c \sim 5T_c$. The power delay profile is given by Eq. (4.51), and to be summarized as Tab. 4.2. The received signal is corrupted by a complex AWGN process. We also assume that the pilot signal is available in the receiver and sample matrix inversion (SMI) is used as the adaptive algorithm. A detailed investigation into convergence behavior of SMI may reduce the length of the pilot signal. However, in this chapter since we are interested in system performance rather than the behavior of the employed adaptive algorithm, detailed discussion on the method to reduce the length of pilot signal is omitted. To evaluate the efficiency of the proposed system, we

Table 5.1: Simulation Parameters

Simulation Parameter	Value
STBC type	Alamouti-STBC ($M = 2$)
Receive antenna	$N = 2$, ($N = 1,\ 2,\ 4,\ 8$ for Fig. 5.7)
Modulation Scheme	BPSK
Data length of each block	$Q = 31$ chips
Number of data blocks	8000
Number of trials	100 times
Number of subbands	$K = 31$
Number of taps	$L_r = 31$
Adaptive algorithm	Sample Matrix Inversion (SMI)
Channel	frequency selective fading channel with exponential power profile, σ as Table 4.2

compare the STBC-SBAA with STBC tapped delay line adaptive array (STBC-TDLAA) and STBC-Adaptive Beamforming (STBC-ABF) [68] for a CDMA system. For a fair comparison, the tap number of STBC-TDLAA is put at $L_r = 31$. We plot the result of the output signal to interference plus noise ratio (SINR) [65, 72] versus the average SNR, measured in decibels (dB). Output SINR is used in this chapter to represent the interference cancellation capability given by updated weight of the proposed scheme.

Define, the cross-correlation coefficient is given as follows:

$$\rho_p = \frac{E[\hat{b}_p[t]d_p[t]^*]}{\sqrt{E[|\hat{b}_p[t]|^2]E[|d_p[t]|^2]}} \tag{5.32}$$

where $\hat{b}_p[t]$, $d_p[t]$ are the received signal and the reference signal, respectively. The output SINR [65] is expressed using ρ_p by the equation:

$$\text{SINR}_p = \frac{|\rho_p|^2}{1 - |\rho_p|^2} \tag{5.33}$$

5.3.2 Results

First, in order to examine the interference cancellation capability of the proposed scheme, we considered the cumulative distribution function (CDF) of the Output SINR. Here, we set the input SNR=10 dB and 8000 blocks are generated for a 100 times trial of changing the propagation conditions. We consider an environments occupied by a single user (ICI only) and five users (ICI+MAI) for the cases of $\sigma = T_c$ and $\sigma = 5T_c$. Here, we plot the Output SINR value for dedicated channel propagation. Figure 5.2(a) and 5.2(b) shows the CDF of cases $\sigma = T_c$ and $\sigma = 5T_c$, respectively. From Fig. 5.2(a), at $\sigma = T_c$ the

proposed scheme shows a better cancellation capability compared to STBC-ABF when a single user exist. We can see that the Output SINR distribution of STBC-SBAA with $L_{CP} = 10T_c$ is almost equivalent to that of STBC-TDLAA in the case of single user. However, STBC-SBAA has a lower complexity compared to STBC-TDLAA as presented in Section 5.3.5. Taking the median of CDF(= 0.5), it is shown that STBC-SBAA without CP has a gain about 2.5 dB compared to STBC-ABF, and of about 3 dB when CP is applied. However, the Output SINR of STBC-SBAA, STBC-TDLAA and STBC-ABF all degrade for the case of five users.

Furthermore, in Fig. 5.2(b) when the delay spread becomes large ($\sigma = 5T_c$), it is observed that the proposed scheme exhibits a better interference cancellation capability for both a single user and five users. It is observed that at the median CDF, for the case of single user, STBC-SBAA has a gain of 6 dB compared to STBC-ABF, and a gain of 9 dB when CP is applied. Moreover, for the case of five users, STBC-SBAA has a gain of 4.5 dB compared to STBC-ABF, and a gain of 6.5 dB when CP is applied. This is due to multipath diversity gain. Therefore, the cancellation capability of STBC-SBAA is clearly seen in the propagation channel with a longer delay spread. Furthermore, from both figures, it is also observed that STBC-SBAA adopting CP of $L_{CP} = 10T_c$ achieved a higher Output SINR, thanks to the help of CP which absorbs the multipath delay signal arriving within the GI. It is clear that when the users have the same number of subbands and taps, the performance of the proposed method is almost equivalent to STBC-TDLAA. From both figures, it is seen that STBC-SBAA has a higher diversity order compared to STBC-ABF, and almost the same diversity order with STBC-TDLAA, especially in the frequency selective fading channel with longer delay spread ($5T_c$). This clearly shows that the efficiency of the proposed scheme is achieved by joint working of STBC and SBAA. It seems that the effect of STBC itself is small in long delay spread environments, and the SBAA works to equalize and suppress the ICI and MAI. However, the adoption of STBC is inevitable for realizing transmission diversity without CSI at the transmitter side. Thus the cooperative work of STBC and SBAA will enhance the performance of CDMA system. The use of STBC with SBAA becomes necessary in order to maximize the multipath diversity. We conclude that STBC-SBAA simultaneously eliminates ICI and MAI, thus maintain a higher Output SINR.

The efficiency of the STBC-SBAA is clearly observed when we simulate the proposed scheme for the case of single and five active users in the frequency selective fading channel with $\sigma = T_c$ and $\sigma = 5T_c$. The input SNR is changing at $0 \sim 12$ dB. The output SINR and BER are taken after considering the propagation channel 1000 times for each input SNR. This value is equal to the average Output SINR output for the whole channel. The results of Output SINR and average BER[3] are depicted in Fig. 5.3 and 5.4, for $\sigma = T_c$ and $\sigma = 5T_c$, respectively. From these figures, in the case of single user, the Output SINR and BER of STBC-SBAA shows a significant performance improvement compared to STBC-ABF, especially when σ becomes larger. When the system has occupied with five users, the Output SINR and BER performance of STBC-SBAA and STBC-ABF are

[3]Note that, for this simulation the processing gain is normalized to unity.

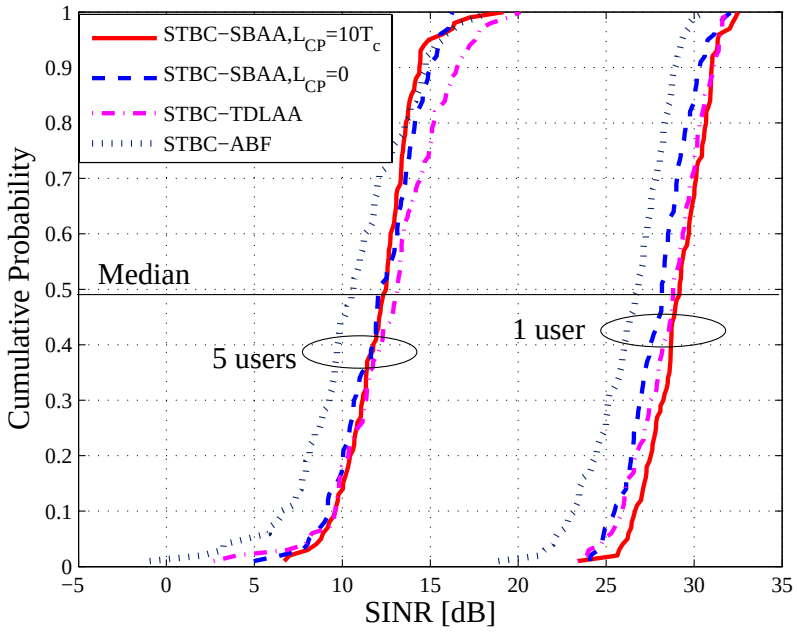

(a) $\sigma = T_c$, SNR =10 dB

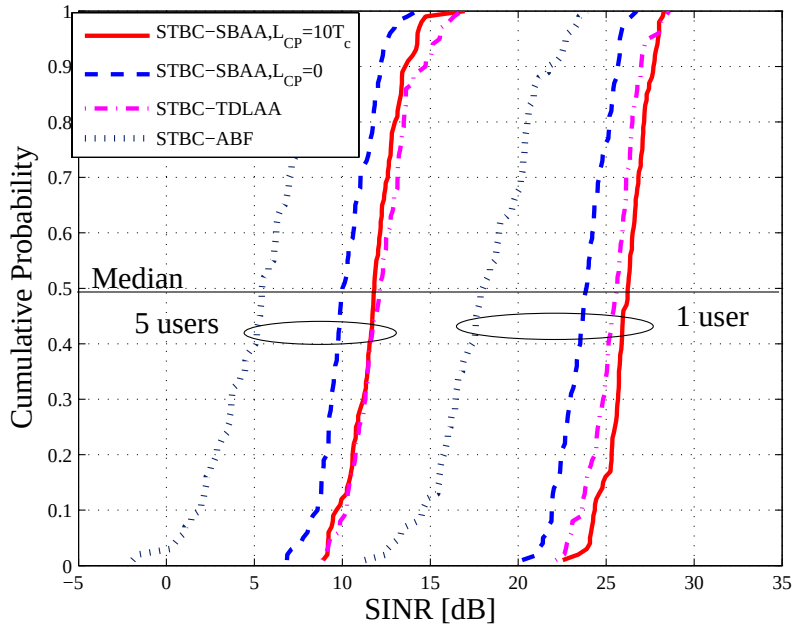

(b) $\sigma = 5T_c$, SNR =10 dB

Figure 5.2: CDF of Output SINR for 2×2 STBC-SBAA CDMA system in frequency selective fading channel with (a) $\sigma = T_c$ and (b) $\sigma = 5T_c$ (Spreading gain is not normalized).

degraded and saturated, respectively compare to the case of single active user as the SNR increased. This scenario is due to the increase of MAI in the receiver, which corrupts the desired signal. However, Output SINR and BER of STBC-SBAA (with and without CP) shows only a small degradation. We also observe that for both single and multiuser, the performance of STBC-SBAA is almost equivalent to STBC-TDLAA at both $\sigma = T_c$ and $\sigma = 5T_c$.

From this figure, it is clear that the STBC-SBAA interferences cancellation technique can separate the interferes with less performance degradation. Moreover, as shown in Fig. 5.3, the use of a long CP in the frequency selective fading channel with a smaller delay spread does not bring additional benefits to STBC-SBAA since almost the entire delayed multipath signal arrived within the GI to be accumulated into the preceding wave only[4]. In a smaller delay spread frequency selective fading channel environment, by putting $L_{CP} = 10T_c$, STBC-SBAA has to sacrifice the transmission rate without the significant improvement in the SINR. On the other hand, the use of CP in the frequency selective fading channel with a bigger delay spread would bring additional improvement to STBC-SBAA since the CP which can absorb the multipath delay signal, arrived within the GI. Therefore, the use of CP would be chosen properly regarding the propagation channel. Here, we suggest that $L_{CP} = 0$ should be chosen for the transmission of STBC-SBAA in the frequency selective fading channel with a small delay spread, thus enhancing the transmission rate.

Next, we elaborate the performance comparison of the proposed scheme in the frequency selective fading channel with different delay spreads. Here, we consider two cases of $\sigma = T_c$ and $5T_c$ for five users. As depicted in Fig. 5.3 and 5.4, for both $\sigma = T_c$ and $\sigma = 5T_c$, Output SINR and BER of STBC-SBAA shows the performance improvement compared to STBC-ABF. However, the improvement level is smaller as SNR increased. We can see that the Output SINR is saturated as SNR become higher. However, at both $\sigma = T_c$ and $\sigma = 5T_c$, STBC-SBAA can still achieve a better performance compare to STBC-ABF. It is also clearly observed that the Output SINR of STBC-SBAA improved very much in multipath rich frequency selective fading channels, thus the effectiveness of the proposed scheme is verified. For a single user, it is noticed that when the CP is employed and working well in single input multiple output (SIMO), the output SINR is maximized to the upper bound of theoretical limit given by [65], and extended to CDMA system as follows:

$$\text{SINR dB} = 10\log_{10}(N) + 10\log_{10}(K) + \text{SNR}. \tag{5.34}$$

Focusing on the MAI cancellation capability, we simulate the proposed system for three types of input SNR=$\{-10,\ 0,\ 10[\text{dB}]\}$ for different delay spreads which varies from $\sigma = T_c$ to $\sigma = 5T_c$. The number of user is set to five users. The result is depicted in Fig. 5.5 which shows that the performance of STBC-SBAA and STBC-ABF degrade when σ increases, due to the existence of ICI and MAI. However, STBC-SBAA shows a

[4]The orthogonality of spreading codes is protected, therefore the effects of inter-block interference can be avoided.

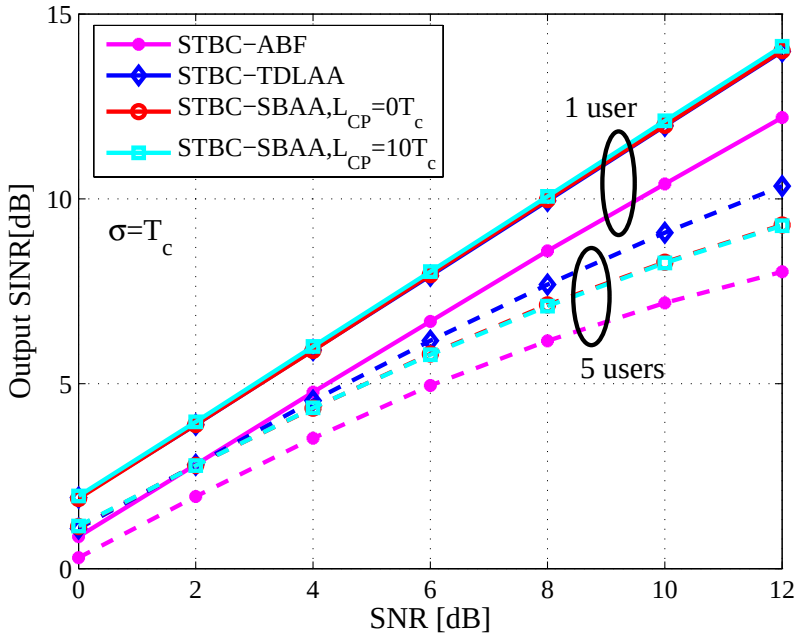

(a) Output SINR

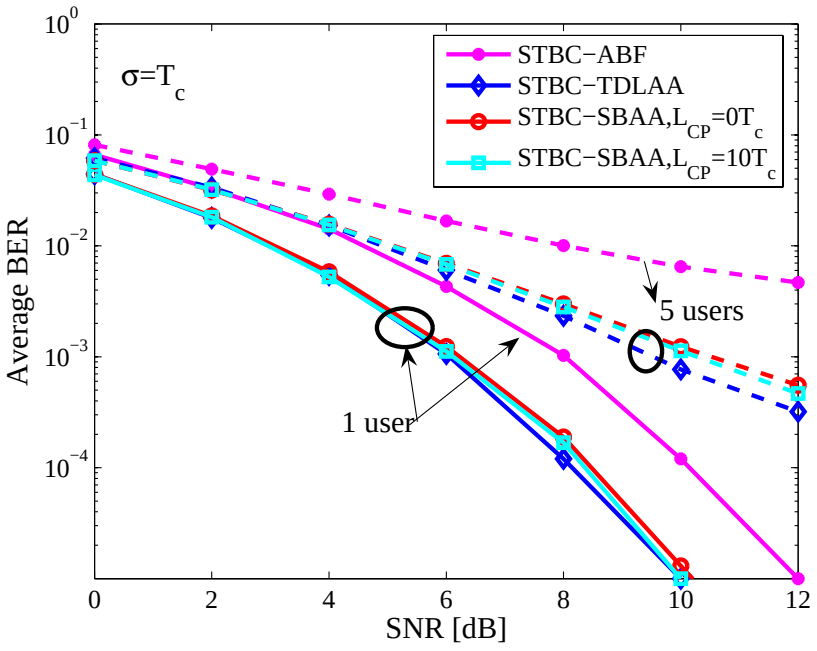

(b) BER

Figure 5.3: Performance comparison for 2×2 STBC-SBAA CDMA system with single and five active users in frequency selective fading channel with $\sigma = T_c$ and normalized spreading gain.

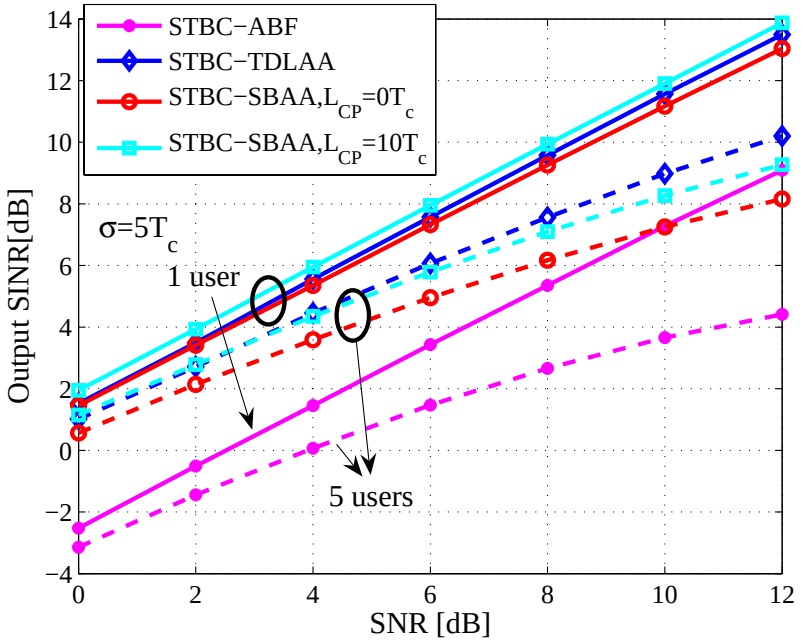

(a) Output SINR

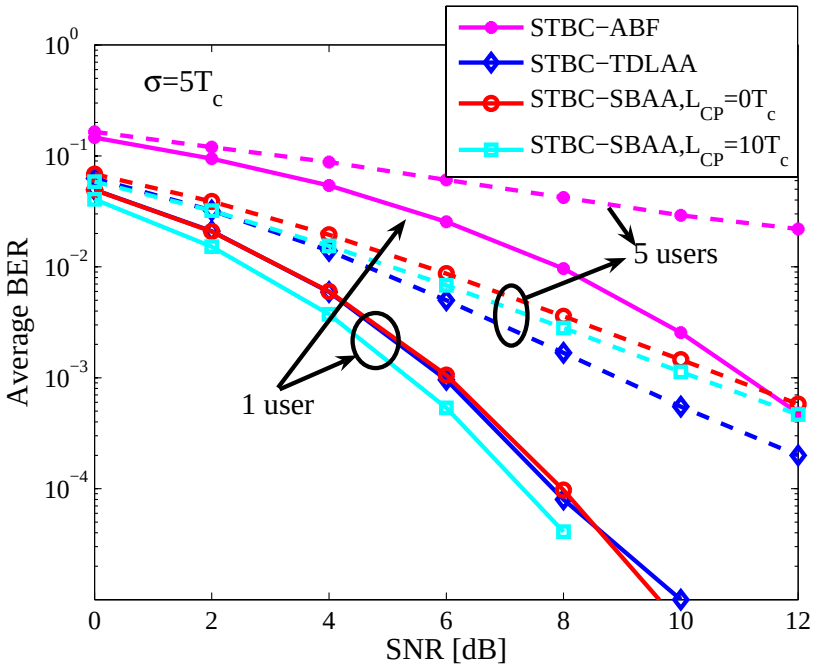

(b) BER

Figure 5.4: Performance comparison for 2×2 STBC-SBAA CDMA system with single and five active users in frequency selective fading channel with $\sigma = 5T_c$ and normalized spreading gain.

better performance compared to STBC-ABF for the entire input SNR. A close observation of Fig. 5.5 shows that STBC-SBAA improves very much at the higher SNR, since the average power of combined multipath signal is bigger than MAI, therefore the ability of STBC-SBAA to mitigate MAI is higher.

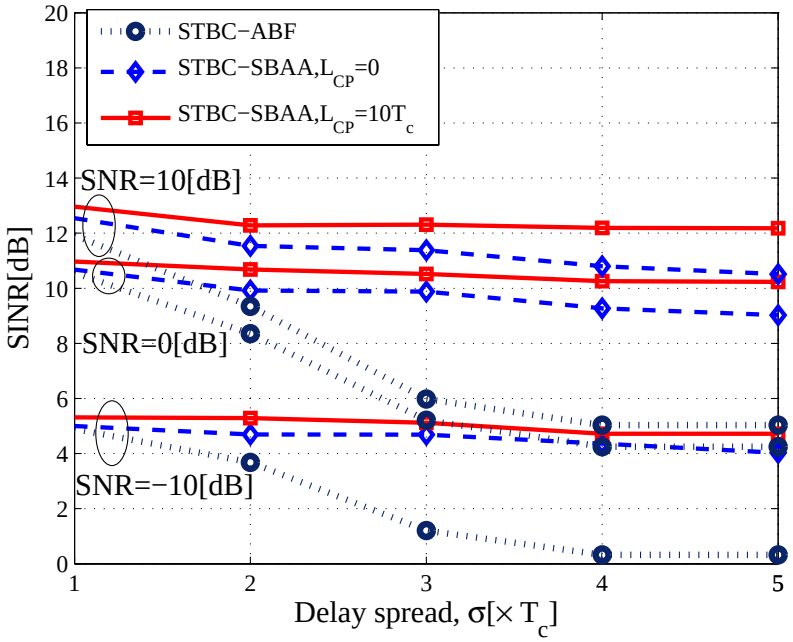

Figure 5.5: Average SINR for five users 2×2 STBC-SBAA CDMA system as a function of delay spread, σ.

Figure 5.6 presents the SINR of STBC-SBAA versus the number of active users in the system with SNR=10 dB. It is shown that the SINR decreases as the number of users increases, especially when the number of users is greater than 9. By taking the minimum SINR as 7 dB, it is shown that the number of active users can occupy in the system is 8 users. This represents only 26% of the total user capacity of 31 users, and exceeds the number of users accommodated by the matched filter receiver [78][5], which is limited to about 10% only. The maximum number of users can be increased by using advanced forward error correction or power control.

5.3.3 Effect of Antenna Diversity Combining

The simulated Output SINR performance using STBC-SBAA and antenna (receive) diversity is plotted in Fig. 5.7 with the number of receive antenna, N. The number of users is set to five users and for the case of $\sigma = T_c$ and $\sigma = 5T_c$. From the figure, the Output

[5]This comparison might be unfair, however it shows us the user occupancy and availability from the viewpoint of SISO system [78] to MIMO system (as shown in this dissertation).

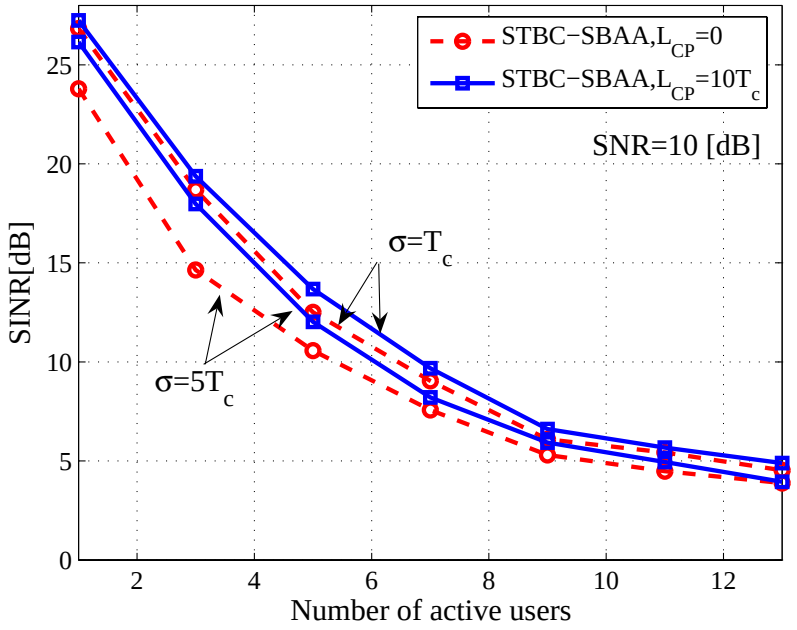

Figure 5.6: Average Output SINR performance versus the number of active users in 2×2 STBC-SBAA CDMA system.

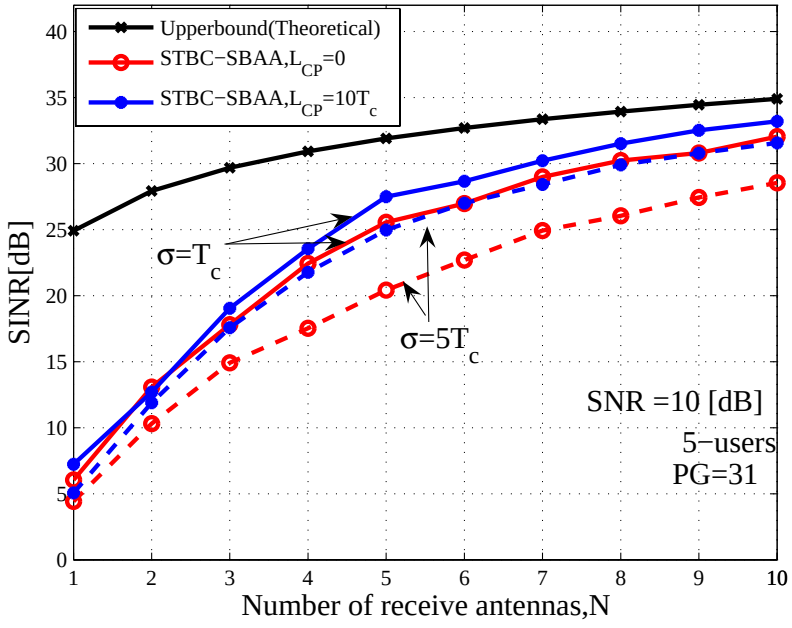

Figure 5.7: Average Output SINR performance of 5 users STBC-SBAA CDMA system versus the number of receive antennas, N.

SINR of STBC-SBAA for $\sigma = T_c$ and $\sigma = 5T_c$ increased close to the upper bound value given in (5.34) when N is increased. Note that, in the previous simulation, by setting $N = 2$ which produce the degree of freedom (DOF) $= N - 1 = 1$ to cancel the interference. It is clearly observed that the more receive antennas are used, the larger the spatial diversity gain achieved and thus a better output SINR is obtained. Moreover, the use of more receive antennas also increases the ability of receiver to cancel the interference since its DOF increases.

5.3.4 Effect of L_{CP} in STBC-SBAA CDMA System

A judicious selection of the CP length is needed to achieve the best performance. In this chapter, we use a CP length of L_{CP} chips out of the Q chips, which gives a CP power penalty of $Q/(L_{CP} + Q)$. For example, even if $Q = 31$, $L_{CP} = 10$, the degradation in the efficiency is 1.2 dB. If a larger gain than the above degradation is obtained, we can say that the proposed scheme is effective. The use of longer CP could mitigate the multipath signal and improve the Output SINR. But, the use of longer CP will bring a reduction of transmission rate.

Furthermore, in Fig. 5.2 to Fig. 5.5, the effect of CP is small in the case of 2×2 MIMO system due to insufficient of DOF. However, the influence of CP increases when $N \geq 4$, as shown in Fig. 5.7 since the ability of canceling the interference become bigger, especially when $\sigma = 5T_c$. Therefore, it is confirmed that the joint operation of CP and STBC increases the Output SINR of the CDMA system, especially in the frequency selective fading channel.

5.3.5 Complexity of the System

The complexity of STBC-SBAA and STBC-TDLAA in CDMA system can be compared using the computational complexity. The main difference between STBC-SBAA and STBC-TDLAA is in their processing modes. STBC-TDLAA processes the input signal on a sample-by-sample basis, while STBC-SBAA processes on a block-by-block basis. As a result, STBC-SBAA requires less computational operations than STBC-TDLAA. In our proposed STBC-SBAA, K subbands require $2KN^3$ multiplications, as FFT/IFFT is used, requiring $4KN \log_2 K$ further multiplications. On the other hand, STBC-TDLAA with L_r-tap requires $2(L_rN)^3$ multiplications. Taking $K = L_r$, we can see that STBC-TDLAA works on third order $\mathcal{O}(K^3)$ processing, whereas STBC-SBAA works on first order $\mathcal{O}(K)$ processing. For example, when $K = L_r = 31$, STBC-TDLAA needs about $476,656$ multiplications, while STBC-SBAA only needs about $1,353$ multiplications.

5.4 Conclusion

In this chapter, for high reliability multiuser transmission over frequency selective fading channel, we have proposed a novel CDMA system utilizing SBAA in the receiver. A novel construction of SBAA is introduced to process CDMA signals based on STBC before

despreading. In addition, spreading code CP is introduced to improve the performance of STBC-SBAA. Through computer simulations, it is verified that STBC-SBAA achieves good Output SINR compared to STBC-TDLAA and STBC-ABF, with less complexity in both single and multiuser environments. We proved that the proposed scheme can achieve significant performance by exploiting the effects of transmit diversity and SBAA.

In the next chapter, we shall consider STBC-SBAA with multirate multicode CDMA systems for high data rate transmission in frequency selective fading channel.

Chapter 6

STBC-SBAA for Multirate Multicode CDMA System

This chapter present an interference suppression using subband adaptive array (SBAA) for space-time block coding (STBC) with multirate multicode code division multiple access (CDMA) system over the frequency selective fading channel. The proposed scheme has a flexible configuration which allows base station (BS) to dynamically adapt to multirate transmission requests from mobile stations (MS). At the receiver, the received signal undergoes STBC based subband adaptive array processing at each subband to suppress the inter-chip interference (ICI), multicode interference (MCI) and multiple access interference (MAI) simultaneously. The proposed system is simulated under different channel conditions and is compared against conventional SBAA.

6.1 Introduction

Future wireless systems such as fourth generation (4G) cellular will need flexibility to provide subscribers with a variety of services such as voice, data, images, and video. Because these services have widely different data rates and traffic profiles, future generation systems will have to accommodate a wide variety of data rates [7]. This has motivated research on multi-code CDMA systems which allow variable data rates [65, 81] by allocating multiple codes, and hence varying degrees of capacity to different users. Recently, variable spreading and multicode are two methods which have been adopted in multirate implementation in high data rate (HDR) and flexible data rate communications over wireless channels [82, 83]. The basic concept of multicode CDMA system is to split the user data into a number of streams and use parallel orthogonal channel codes to modulate. The introduction of multicode transmission causes several problems, namely multicode interference (MCI) [82]. One is the high envelope variation, which results from a linear sum of signal over multicode streams. Beside that, the multicode transmission introduces the inter-chip interference (ICI) caused by different delays of users signal in a multipath environment.

On the other hand, in radio communication systems, the quality of HDR transmission is severely degraded due to multipath fading channel resulting from the presence of many propagation paths with different time delay. In order to achieve a HDR transmission, high quality communications or high capacity communications, countermeasures should be employed to combat these impairments. As a solution, there have been a large number of works on use of multiple antenna (multiple input multiple output (MIMO)) system to combat multipath fading channel and provide spatial diversity. Among them, space time block coding (STBC) [17] is the most efficient method due to its provision of full spatial diversity and simple linear decoder. For multiuser communication systems, STBC can be used in conjunction with receive adaptive beamforming to suppress the co-channel interferences (CCIs) [67]. Besides, STBC have been also proposed to use with DS-CDMA system to combat the impairments of multiuser channels [70].

However, in the frequency selective fading channel, the transmission using STBC suffers from inter-chip interferences (ICI) and increased multiple access interference (MAI), which dramatically deteriorates the performance. A CDMA system which utilizes a transmit antenna array at the transmitter and a receive antenna array at the receiver side with tap delay line (TDL)s filters at both side [70] shows a significant performance and capacity improvement in frequency selective fading channel environments. However, when the delay spread is higher and number of user increased, both transmitter and receiver's TDL memory will be longer and the complexity is increased exponentially. Recently, subband adaptive array (SBAA) for STBC (STBC-SBAA) [72, 88] has been proposed, which can reduce the computational complexity through block processing and improve the performance of the system with the helps of cyclic prefix (CP) would be one of the solution to TDL Adaptive Array (TDLAA).

In this chapter, as the continuous work described in the previous chapter [72, 88], we present a novel multirate multicode CDMA system using SBAA designed for STBC transmission over frequency selective fading channel, which allows the flexible data rate transmission with affordable complexity. Here, we propose a joint equalization scheme which utilizes a STBC as transmit diversity and receive antenna with SBAA. At the receiver, a novel construction of SBAA to process multirate multicode CDMA signal based on STBC is introduced. The receive block signal is divided into two groups and adaptive processing is done in chip-level to equalize and estimate the desired signal. Simulation results demonstrate the effectiveness of STBC-SBAA for multicode multirate CDMA system in the uplink frequency selective fading channel.

This chapter is organized as follows: In Section 6.2, the proposed system of STBC-SBAA for CDMA system is introduced. The simulation and results are presented in Section 6.3. Finally, Section 6.4 summarizes the chapter.

6.2 Configuration of the Proposed Method

6.2.1 Multirate Multicode CDMA System

Fig. 6.1 shows the configuration of transmitter of pth user (MS (mobile station)) which supports $v, (:= \{1, \ldots, V\})$ different data rates correspond to each class of services. Those with the LDR (basic rate) R_1 are called Class 1 users, and the users of class v has its data rate $R_v = vR_1$, where v is an integer. The signal of of HDR user's $\boldsymbol{b}_p[t]$ is decomposed into v streams of $b_{p,v}[t]$. Therefore, vth code stream of pth user is considered transmission data from *effective user* $b_{p,v}[t]$. Thus a *physical user* (p) is said to contain v *effective users*. In order to spread these code stream signals, the subcode concatenation process should be done to create v subcodes from the primary code assigned to pth user $(p = \{1, \ldots, P\})$. Since the primary codes assigned to users in CDMA systems are pseudo-random (PN) codes and in effect not orthogonal. The use of this PN codes directly for effective users may cause MCI for a physical user comprised of several effective users, extremely for HDR users. The purpose of the subcode concatenation process is to create v orthogonal subcodes for user (p, v) in which, $c_{p,i}[t] \perp c_{p,l}[t]$ for $i \neq l$. The function of the subcode concatenation block is thus similar to Walsh-Hadamard function. Here, all streams are spread by different codes of the same length, thus it can be done in the similar way as in a single code CDMA system.

Let us define $s_p(n)$ as the chip sequence corresponding to data sequence $b_p[t]$ of pth user as

$$s_p[n] \triangleq \sum_{v=1}^{V} b_{p,v}[t] c_{p,v}(\lfloor n \rfloor_Q),\ n = 1, 2, \ldots,\ t = \lfloor \frac{n}{Q} \rfloor, \tag{6.1}$$

where we have used operator $\lfloor i \rfloor_L \triangleq i \mod L$ and $\lfloor x \rfloor_L$, which select the largest integer that equals or does not exceed x (floor function). The spread signal of each user $s_p[n]$ is then divided into chip blocks of length Q.

6.2.2 STBC-SBAA for Multirate Multicode CDMA System

Transmitter Configuration

In this chapter, we shall consider the asynchronous multiuser CDMA system employing STBC at each MS. On the BS, we propose a SBAA based on STBC (STBC-SBAA) to estimate the desired user's signal. Each MS utilizes M transmit antennas and the BS utilizes N receive antennas. The configuration of the proposed transmitter and receiver of STBC-SBAA for CDMA system are illustrated in Fig. 6.1 and Fig. 6.2, respectively. In this chapter we restricted our system for Alamouti's STBC [17] with $M = 2$. Extension to more general type of STBC [19], namely with $M > 2$ is quite straight forward.

Consider that the spread multirate multicode CDMA signal of each MS is given by (6.1). The spread signal of each user $s_p[t]$ is then be divided into chip blocks of length Q.

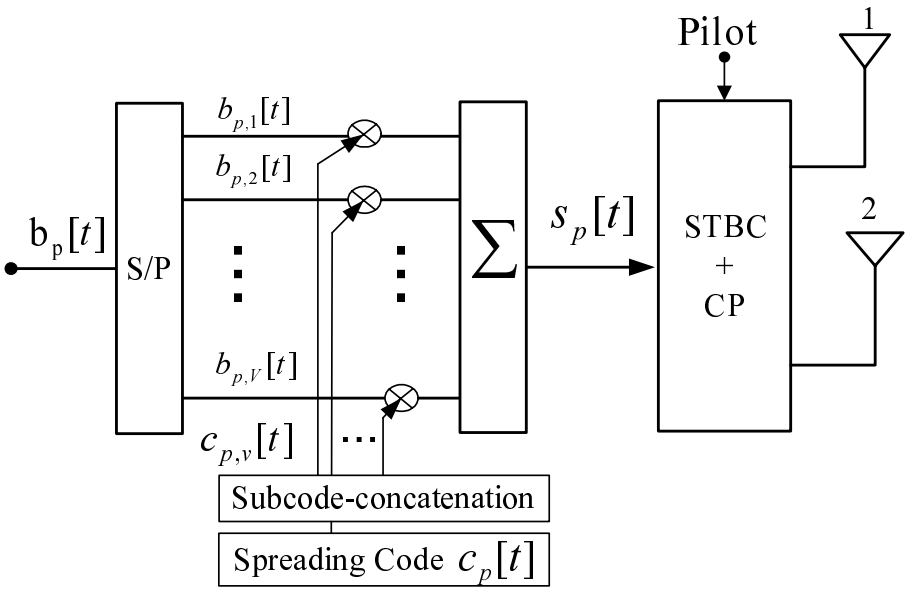

Figure 6.1: The transmitter of multirate multicode CDMA system.

The kth chip-block with each element is represented as

$$s_p^{(k)}[q] \;=\; s_p[kQ+q] \tag{6.2}$$

where $q \in \{0,1,\ldots,Q-1\}$. The kth chip block $\boldsymbol{s}_p^{(k)} = [s_p^{(k)}[0],\ldots,s_p^{(k)}[Q-1]]$ contain Q chips. The input chip block signal is encoded by STBC [17], where at odd slot of $2k-1, (=1,3,5,7,\ldots)$, a pair of chip blocks $\boldsymbol{s}_p^{(2k-1)}[q]$ and $\boldsymbol{s}_p^{(2k)}[q]$ are transmitted from antenna 1 and 2, respectively. Similarly, at the even time slot of $2k, (=2,4,6,\ldots)$, a pairs of chip block $\bar{\boldsymbol{s}}_p^{(2k)}[q]$ and $-\bar{\boldsymbol{s}}_p^{(2k-1),*}[q]$ are transmitted from antenna 1 and 2, respectively. Note that $\bar{s}_p^{(2k-1),*}[q] = s_p^{(2k-1),*}[Q-q-1]$ and $\bar{s}_p^{(2k),*}[q] = s_p^{(2k),*}[Q-q-1]$ are time-reversed and element by element complex-conjugated version of $s_p^{(2k-1)}[q]$ and $s_p^{(2k)}[q]$, respectively. The operation of time-reversed is for handling the frequency domain processing in the receiver [59]. The transmit signal $s_{p,i}^{(k)}[q]$ at antenna $i \in \{1,2\}$ of pth user can be shown as below.

$$s_{p,1}^{(2k-1)}[q] = s_p^{(2k-1)}[q], \quad s_{p,1}^{(2k)}[q] = -\bar{s}_p^{(2k),*}[q] \tag{6.3}$$

$$s_{p,2}^{(2k-1)}[q] = s_p^{(2k)}[q], \quad s_{p,2}^{(2k)}[q] = \bar{s}_p^{(2k-1),*}[q] \tag{6.4}$$

Then, the CP is applied, i.e., the last L_{CP} chip of each block is copied and pasted at the top of each block as guard interval (GI), to make the total length of $Q+L_{CP}$ as shown in Fig. 4.4[1]. This operation is for minimizing the effect of ICI and producing multipath

[1]The block configuration of STBC-SBAA for multicode multirate CDMA system is similar to the Fig. 4.4, however the each data block consist of chips block, not symbol blocks as STBC-SBAA in Chapter 4.

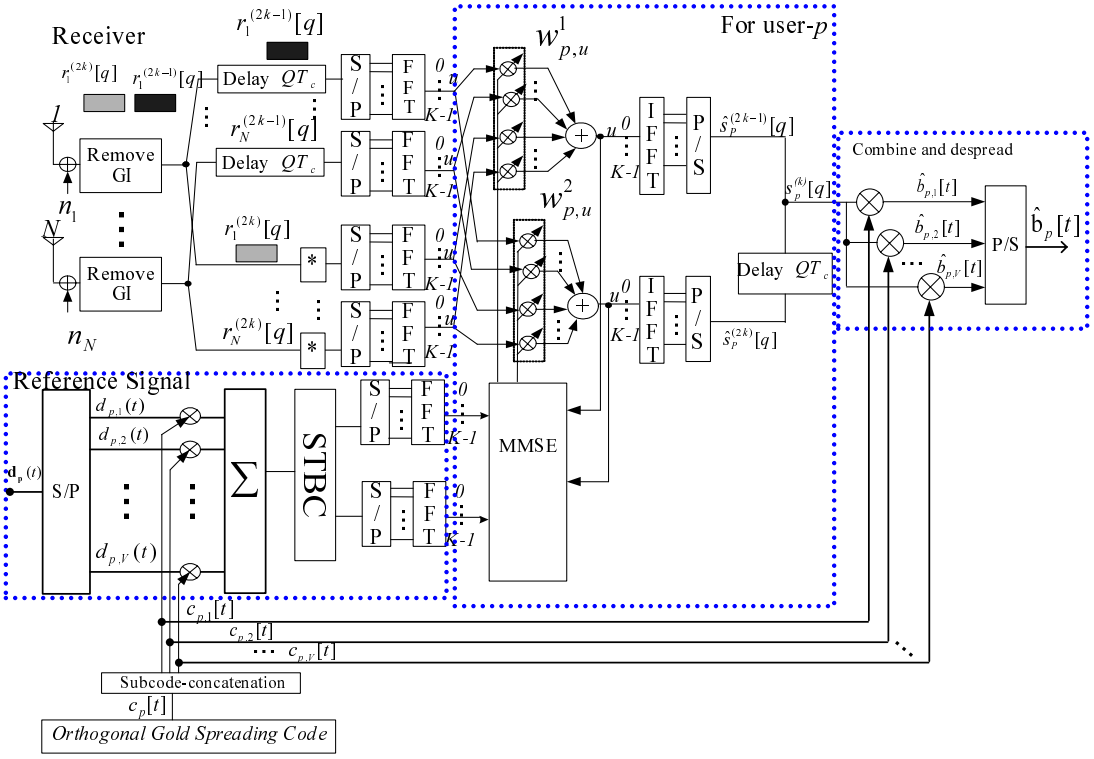

Figure 6.2: The receiver of STBC-SBAA for multirate multicode CDMA system

gain [72]. It is shown as below for $v \in \{2k-1, 2k\}$ at ith antennas as,

$$\grave{\boldsymbol{s}}_{p,i}^{(v)}[q] \;=\; [s_{p,i}^{(v)}[Q-1-L_{CP}], \ldots, s_{p,i}^{(v)}[Q-1], \ldots, s_{p,i}^{(v)}[0], \ldots, s_{p,i}^{(v)}[(Q-1)]]^T. \quad (6.5)$$

Channel Model

We assume a frequency selective fading channel with the total of multipath L with time spacing of chip duration T_c, is given by (5.2) in Chapter 5.

Receiver Configuration

After the transmission through the frequency selective fading channel and assuming that CP is chosen to satisfy $L_{CP} \geq L-1$ and after discarding the CP, the receive signals at antenna j for block $v \in \{2k-1, 2k\}$ is given as follows:

$$r_j^{(v)}[q] \;=\; \sum_{p=1}^{P}\sum_{l=0}^{L-1}\{h_{p,j1}^{l}s_{p,1}^{(v)}[q-lT_c] + h_{p,j2}^{l}s_{p,2}^{(v)}[q-lT_c]\} + n_j^{(v)}[q] \quad (6.6)$$

where $n_j^{(v)}[q]$ is the additive white gaussian noise (AWGN) at antenna j, which are assumed to be independent and identically distributed (i.i.d) with mean 0 and variance σ_n^2 at each

real dimension. Here, the transmitted power from each antenna is half of its value in the single antenna case, so that the total transmission power is fixed.

At the receiver, as shown in Fig. 6.2, the chip synchronization is done before the part of *Remove GI*, then the first L_{CP} symbols corresponding to GI are removed from each block. Then, $r_j^{(2k-1)}[q]$ is delayed about QT_c to synchronize with even block data. At the same time, the even blocks are complex-conjugated to be $r_j^{(2k),*}[q]$ to extract the component of $\boldsymbol{s}_p^{(2k-1)}[q]$ and $\boldsymbol{s}_p^{(2k)}[q]$ without conjugation.

6.2.3 Adaptive MMSE Detection

In this chapter, the subband adaptive processing with the most popular linear multiuser method, namely MMSE, is used for detecting transmitted signals from P users. To perform adaptive signal processing in subband, the receive signal is decomposed into subbands using fast Fourier transform (FFT). As shown in Fig. 6.2, in order to work with STBC, the subband processing is done by referring two consecutive blocks as its input; therefore two groups of optimal weight exist for maximizing the output power of detected signal.

Since the operation at the receiver is similar to the non-multicode CDMA system as Section 5, we can consider the operation from (5.11) to (5.29).

After rearrange and combined the IFFT output tap as $\hat{\boldsymbol{s}}_p[kQ+q] = \hat{s}_p^{(k)}[q]$, the desired signal is retrieved by despreading with pth user's subcode concatenation spreading codes to form the V parallel LDR streams. Then, all this streams are to be parallel-to-serial (P/S) to make the estimated HDR streams as,

$$\hat{b}_{p,v}[t] = \frac{1}{Q}\hat{s}_p[n] * c_{p,v}^*(\lfloor n \rfloor_Q),\ n = 1, 2, \ldots,\ t = \lfloor \frac{n}{Q} \rfloor, \tag{6.7}$$

$$\hat{\boldsymbol{b}}_p[t] = [\hat{b}_{p,1}[t] \ldots \hat{b}_{p,v}[t] \ldots\ \hat{b}_{p,V}[t]]^T. \tag{6.8}$$

6.2.4 Weight determination for Generalized STBC-SBAA

In the previous subsection, we consider the Alamouti's STBC with $M = 2$, and the optimal weight are given as (5.24) and (5.25). Here, we show the weight determination for the generalized STBC-SBAA multirate multicode CDMA system with arbitrary number of transmit and receive antennas [19]. Given that each $\boldsymbol{s}_p^{(k)}$[2] block is encoded with STBC according to design rules in Ref. [19]. This operation will generate M parallel block sequence of length D which can represent by a transmission matrix $\mathcal{G}_m$ of size $M \times D$ with entries of $\boldsymbol{s}_p^{(1)},\ \boldsymbol{s}_p^{(2)}, \ldots, \boldsymbol{s}_p^{(C)}$ such that $\mathcal{G}_m^T \mathcal{G}_m = \mathcal{D}$, where $\mathcal{D}$ is a diagonal $\mathcal{D}_{ii}, i = 1, 2, \ldots, D$. Note that $\mathcal{D} = (|\boldsymbol{s}_p^1|^2 + |\boldsymbol{s}_p^2|^2 + \ldots + |\boldsymbol{s}_p^C|^2)\boldsymbol{I}_C$. The coding rate of $\mathcal{G}_m$ is $R = C/D$. These sequences are transmitted through M antennas simultaneously in D time period. Therefore, the weight vector for $\boldsymbol{s}_p^{(1)},\ \boldsymbol{s}_p^{(2)}, \ldots, \boldsymbol{s}_p^{(C)}$ can be calculated by

[2]For simplicity, we omit the q.

Table 6.1: Simulation Parameters

Simulation Parameter	Value
STBC type	Alamouti-STBC ($M = 2$)
Modulation scheme	QPSK
Spreading code	Orthogonal Gold sequence (32 chip)
Subcode concatenation	Walsh-Hadamard Codes (32 chip)
Data length of each block	$Q = 32$ samples
Number of data blocks	5000
Number of trials	100 times
Number of subbands	$K = 32$
Adaptive algorithm	Sample Matrix Inversion (SMI)
Channel	frequency selective fading channel with exponential power profile, (delay profile σ is given in Table 4.2)

extending the equation (5.22) and (5.23) for multiple C. The general optimum weight will comprise the weight vector for each code can be represented as below.

$$\boldsymbol{w}_{p,u} = [\boldsymbol{w}_{p,u}^{1,T}, \ldots, \boldsymbol{w}_{p,u}^{c,T}, \ldots, \boldsymbol{w}_{p,u}^{C,T}]^T \tag{6.9}$$

6.3 Simulation and Results

6.3.1 Simulation Parameters

The simulation parameters are shown in Table 6.1. We consider the QPSK (Quadrature Phase Shift Keying) data modulation with $M = N = 2$ and 3 classes of user with each user per class. The spreading code is normalized such that $c_p^2[t] = 1$, for all t. We always assume the perfect synchronization and transmission power control in the simulation. To examine the efficiency of proposed method in the real radio environment, the frequency selective fading channel with discrete exponential power delay profile with normalized delay spread σ of T_c is applied. The power delay profile is given by Eq. (4.51), and to be summarized as Tab. 4.2.

To evaluate the efficiency of the proposed system, we compare the STBC-SBAA with 1×2 conventional multirate multicode CDMA system with SBAA [65] by plotting the result of the output signal to interference plus noise ratio (SINR) [65,72], average bit error rate (BER) versus the average energy per bit to noise ratio (E_b/N_0), measured in decibels (dB).

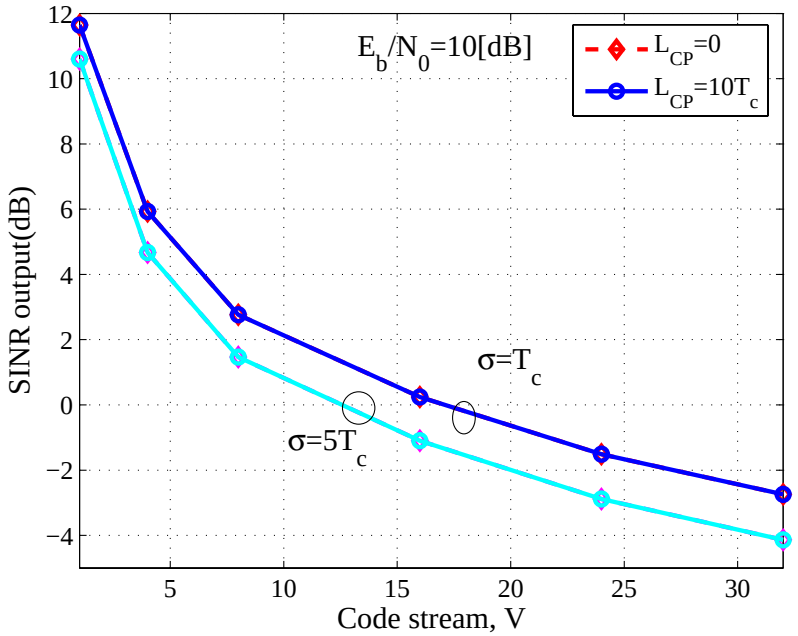

Figure 6.3: Output SINR of single user with different class of data rates at $E_b/N_0 = 10$ dB for $\sigma = \{T_c, 5T_c\}$.

6.3.2 Results

Firstly, we consider the performance of single user with different class V. Here, $E_b/N_0 = 10$ dB and code stream is given as $V = \{1, 4, 8, 16, 24, 32\}$. In Fig. 6.3, it is shown that, the performance of STBC-SBAA is degraded as V is increased. It is noted that the LDR class users have better Output SINR than HDR. However, this performance is not due to MCI, which can been seen that degraded value is equal to number of different code streams, e.g.$10(\log_{10} 4 - \log_{10} 1) = 6$ dB which equal to power normalization of each cases as the transmit power of each user as unity. It is proved that our proposed scheme which using the subband adaptive array for STBC can totally suppress the MCI with used of the subcode concatenation.

Next, in order to examine the interferences cancellation capability of the proposed scheme, we consider the cumulative probability distribution of Output SINR. Here, we set the input E_b/N_0=10 dB and 3 users are occupied in the system where each user is holding different data rates (class) of Class 1, Class 2, and Class 3, respectively. Note that, data rate for Class 1 < Class 2 < Class 3. From Fig. 6.3.1, for $\sigma = T_c$, the STBC-SBAA shows a better cancellation capability compared to conventional SBAA both at Class 1 and Class 3, respectively. Taking the median of cumulative probability(= 0.5), it is shown that STBC-SBAA without CP has about 1 dB gain against SBAA, and about 3 dB when CP is applied. However, the SINR of both STBC-SBAA and SBAA degraded for Class 3 users, due to the average power of each bit allocated is smaller compared Class

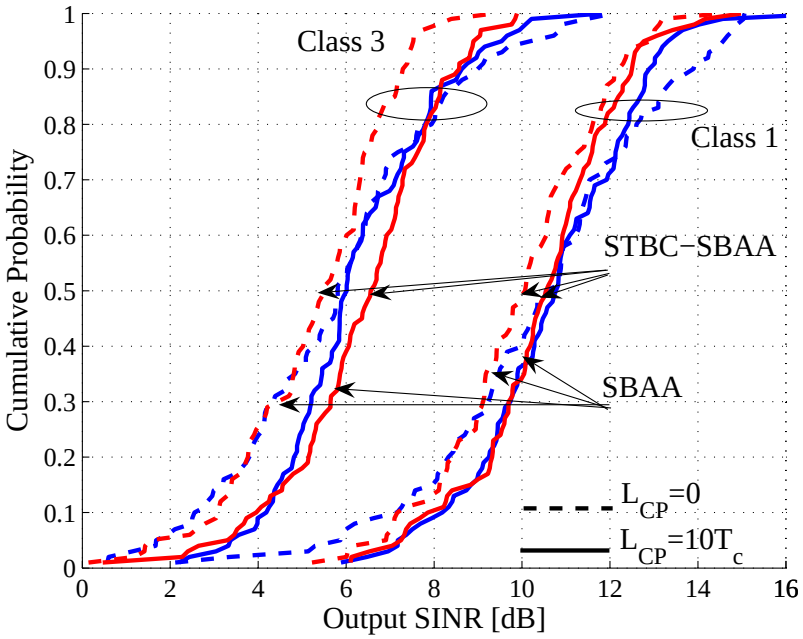

]

(a) $\sigma = T_c$, $E_b/N_0 =$ 10 [dB

]

(b) $\sigma = 5T_c$, $E_b/N_0 =$ 10 [dB

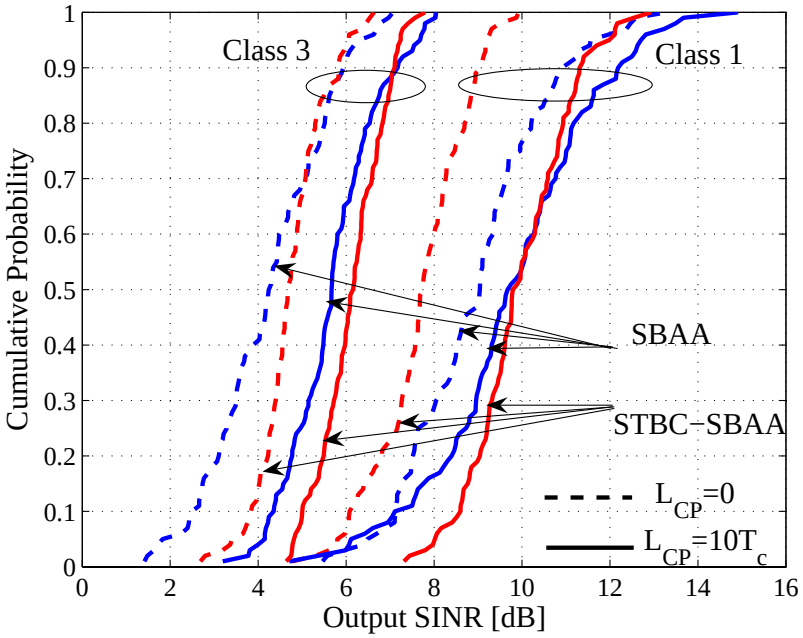

Figure 6.4: The CDF of output SINR for 2×2 multicode multirate CDMA system with STBC-SBAA in frequency selective fading channel with $\sigma = T_c$ and $\sigma = 5T_c$.

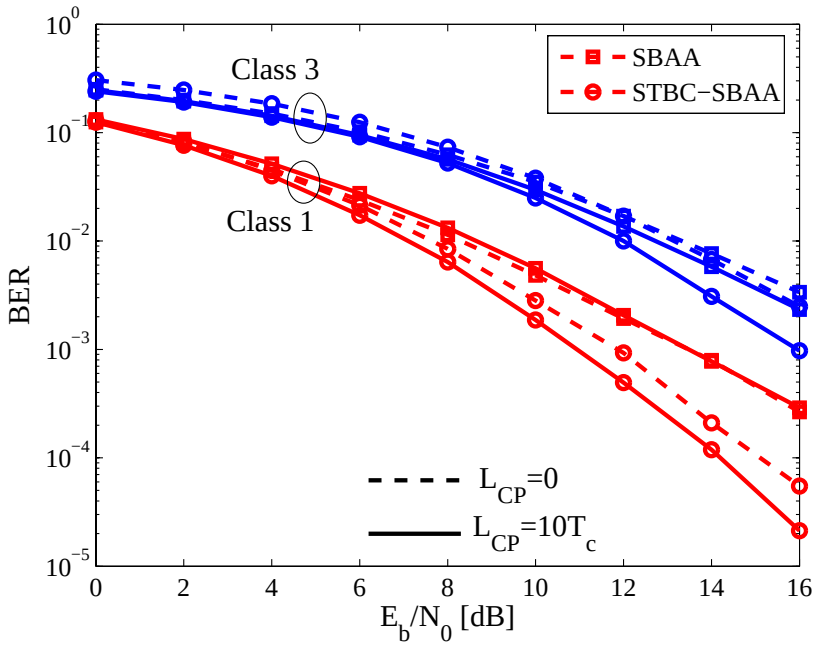

(a) BER

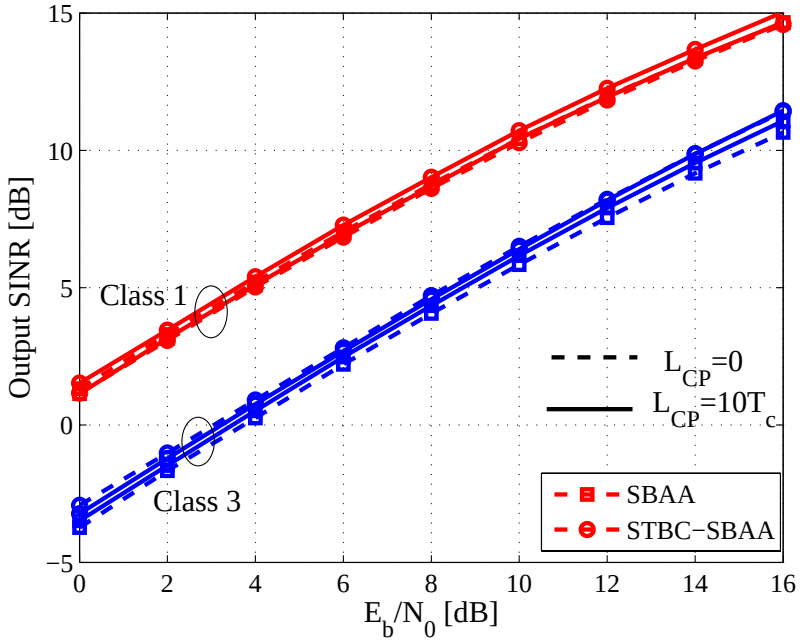

(b) Output SINR

Figure 6.5: BER and Output SINR performance of multirate multicode CDMA system with STBC-SBAA in frequency selective fading channel with $\sigma = T_c$.

1.

On the other hand, from Fig. 6.3.1 at $\sigma = 5T_c$, it is also observed that the proposed scheme shows a better interference cancellation capability both at Class 1 and Class 3 users. At the median value, Output SINR of STBC-SBAA has 2 dB gain compared to SBAA, and 4 dB gain when CP is applied for the both Class 1 and Class 3 users. Therefore, the cancellation capability of STBC-SBAA becomes clearer in the propagation channel with the bigger delay spread. We can conclude that, the STBC-SBAA simultaneously eliminates ICI and MAI, thus maintain a higher Output SINR.

Next, we simulate the proposed scheme for the case of the 3 classes (3 users) in the frequency selective fading channel with $\sigma = T_c$ and $\sigma = 5T_c$. The input E_b/N_0 is changing at $0 \sim 16$ dB. The results of BER and Output SINR are depicted in Fig. 6.5 and 6.6 for $\sigma = T_c$ and $\sigma = 5T_c$, respectively. From these figures, it is shown that the performance degradation of STBC-SBAA and conventional SBAA, due to increasing number of data stream V, is obvious. Here, in the case of Class 1 user which has only one code stream, both BER and Output SINR of STBC-SBAA shows a significant performance compared to SBAA. On the other hand, for Class 3 user which have a three code streams are assume to have 3 different users in the same channel resulting both performance of STBC-SBAA and SBAA are degraded and saturated compare to the case of Class 1 user as the E_b/N_0 increased. However, STBC-SBAA shows a small degradation. Throughout these figures, it is cleared that STBC-SBAA interference cancellation technique can separate interferer without sacrificing performance.

Moreover, the efficiency of STBC-SBAA for multicode multirate transmission can be emphasized using the diversity order. Traditionally, the diversity order offered by a fading channel is defined as the magnitude of the high-E_b/N_0 slope of average BER as a function of E_b/N_0 (on a log-log scale) [85, 86]. It is seen that from the slope (gradient value) of BER curves in Fig 6.5(a) and Fig 6.6(a), STBC-SBAA has a higher gradient compare to conventional SBAA which mean, our proposed scheme has achieved a higher diversity order compare to conventional SBAA. At the mean time, we show that the LDR user‘s and HDR users have the same slope of BER curves. Therefore, we can conclude that each user has achieved the same diversity order which mean, STBC-SBAA can accommodate LDR and HDR users with the same diversity gain.

Focusing on the MAI cancellation capability, we simulate the proposed system for three type of input $E_b/N_0 = \{-10,\ 0,\ 10[\text{dB}]\}$ in different delay spread which varies from $\sigma = T_c$ to $\sigma = 5T_c$. The result is depicted in Fig. 6.7 for LDR (Class 1) and HDR (Class 3) which shows that the both curve for HDR and LDR users performance of STBC-SBAA degraded when the σ increased due to the existence of ICI and MAI for the entire input E_b/N_0. A close observation of Fig. 6.7 also shows that the STBC-SBAA improves very much at the higher E_b/N_0, since the average power of combined multipath signal is bigger than MAI, therefore the ability of STBC-SBAA to mitigate MAI is higher.

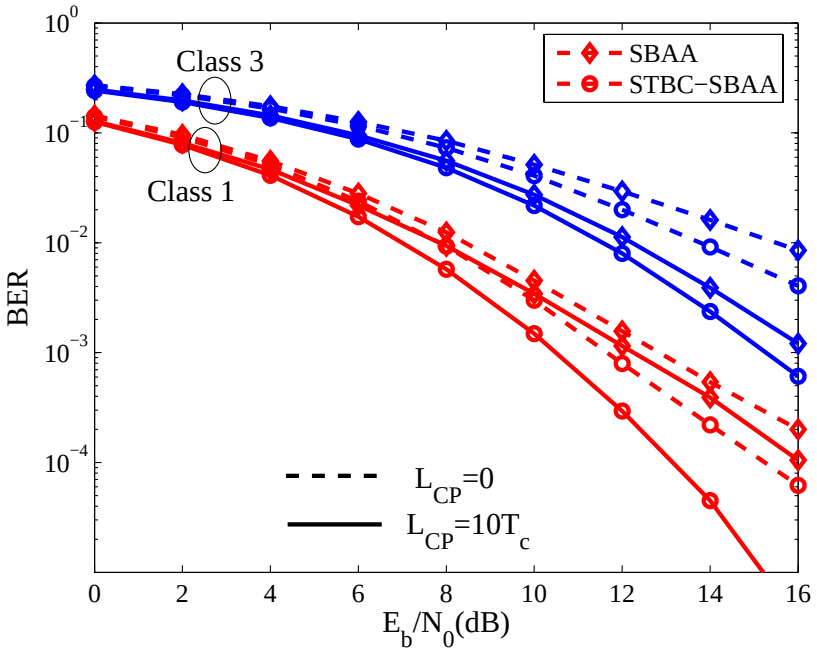

(a) BER

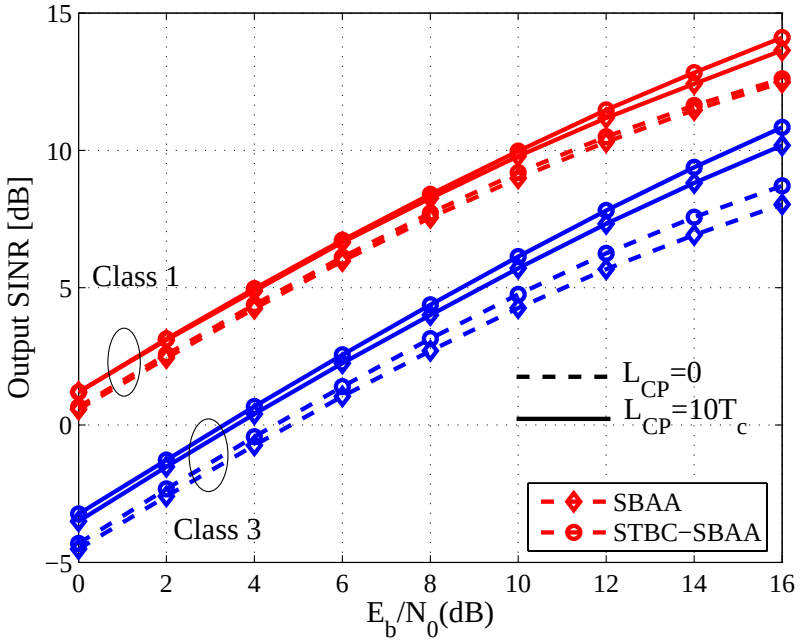

(b) Output SINR

Figure 6.6: BER and Output SINR performance of multirate multicode CDMA system with STBC-SBAA in frequency selective fading channel with $\sigma = 5T_c$.

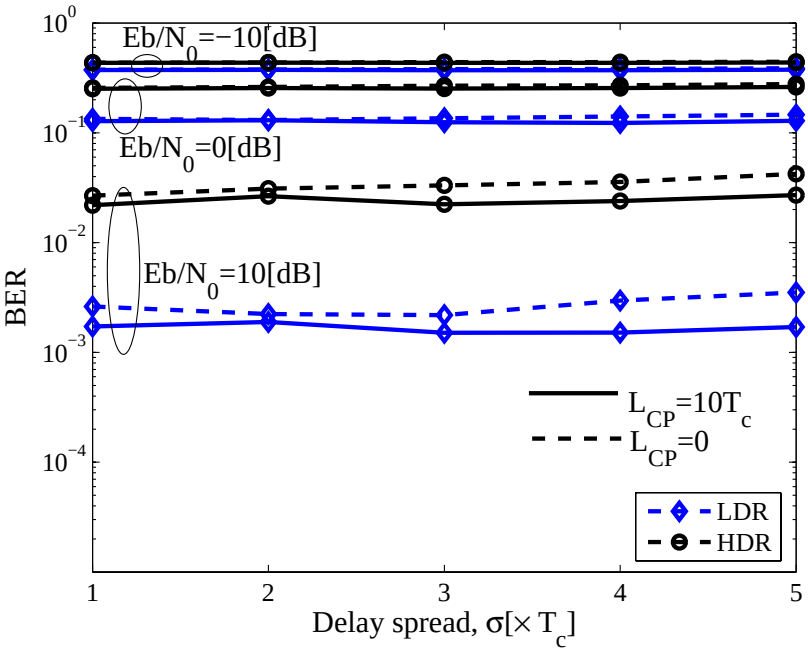

(a) BER

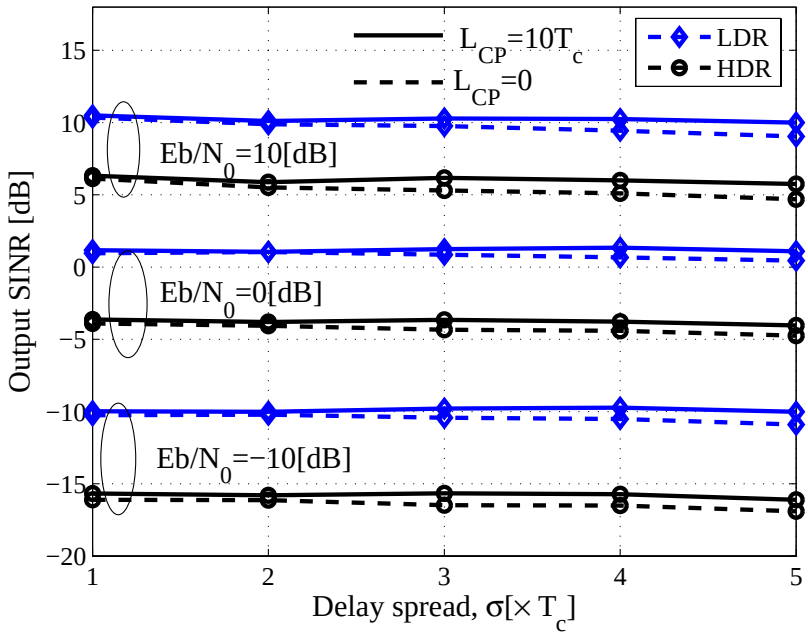

(b) Output SINR

Figure 6.7: Effects of delay spread in multirate multicode CDMA system with STBC-SBAA in frequency selective fading channel ($\sigma = \{T_c, \ldots, 5T_c\}$).

6.4 Conclusion

We have proposed an interference suppression technique for multirate multicode CDMA system using SBAA based on STBC transmission over frequency selective fading channel. The proposed scheme has a flexible configuration which allows BS to dynamically adapt to multirate transmission requests from MS. This scheme utilizes a STBC as transmit diversity and receive antenna with SBAA to process the multirate multicode CDMA signal. At the receiver, a novel construction of SBAA to process CDMA signal based on STBC is introduced. Simulation results demonstrate that the proposed scheme can totally avoid the MCI while suppressing the ICI and MAI. We also show that our proposed scheme achieved a higher diversity order compare to conventional SBAA and maintaining the same diversity order for both LDR and HDR users.

Chapter 7

Wideband Spatio-Temporal Adaptive Array for Multiuser STBC Transmission

In this paper, we present a modified spatio-temporal adaptive array for multiuser space-time block code (STBC) (Modified STBC-STAA) transmission in frequency selective fading channel with the presence of co-channel interferences (CCIs). This method based on the transversal filter adaptive array performing the joint interference suppression and equalization to overcome the problem of *one symbol delay*, namely codes synchronization error. The presented Modified STBC-STAA can maximize the transmission efficiency by incorporating the receive signal component for both non-conjugated and the complex conjugated version of desired signal in the receive signal, which is not only dispersed in space, but also in the time. Furthermore, Modified STBC-STAA overcomes the timing errors by re-aligning the asynchronous multiuser signal to undergo the synchronous joint interference suppression and equalization. Simulation results show that our proposed scheme has a better performance than the conventional STBC-STAA over frequency selective fading channel.

7.1 Introduction

Recent advances in communications are driven by the requirement of next-generation wireless systems to provide high quality, high-data-rate and multi services at anywhere and anytime. This could be achieved by exploiting the spatial diversity with multiple antennas at both the transmit and receive sides, which forms a multiple-input multiple-output (MIMO) system [4, 14]. However, the transmission of high data rate signal in the multipath fading environment experience the signal distortion which classified as intersymbol-interference (ISI) due to signal delay of going through the multipath channel, and co-channel interference (CCI) due to the multiple access. This problematic

environment may degrade the system performance significantly, which need an effective interference mitigation scheme especially for high data rate signal reception.

Diversity transmission using Alamouti's space time block coding (STBC) scheme [17] for MIMO system has been proposed in several wireless standards to combat the fading effects. Unlike flat fading channels, the detection of STBC signals in frequency selective fading channels is complicated because signals from different antennas are dispersed not only in space, but also in time. Therefore, STBC which has been designed for flat Rayleigh fading channel is not working well in the presence of ISI due to frequency selective fading, which corrupts the received signal, and shows a degraded performance. Many works have been proposed to overcome STBC transmission in frequency selective fading channel [62, 72, 73, 80, 91, 92]. In particular, Time-Reversal STBC (TR-STBC) [62] and single-carrier Frequency Domain Equalization (FDE) [72, 73, 80, 91, 92] have received the most attention. The advantages of FDE is that it can easily alleviate the effect of ISI thanks to longer symbol duration and appended guard interval. However, the use of guard interval reduces the efficiency of data transmission, which is proportionally to the delay spread of the channel. When computational complexity is acceptable by high speed signal processors, time domain equalizer can be considered as a possible alternative to FDE.

On the other hand, adaptive array processing is well known as an effective solution for suppressing CCI [37, 50]. The combination of adaptive array and the equalization techniques has been introduced recently to solve CCI together with ISI for multiuser STBC transmission. In [61], synchronous STBC transmission with spatio-temporal adaptive array (STBC-STAA)[1] at the receiver was proposed to overcome the ISI and CCIs. Although the spatio-temporal equalization achieved by the STBC-STAA approach reduces ISI significantly, there always is some residual ISI due to *one-symbol delay*, namely the *codes synchronization error*. This problem was initially addressed in [93] for STBC transmission in cooperative distributed environment. This error would destroy the orthogonality imposed on the transmitted signals by STBC. The impact of residual ISI will be more crucial in higher order constellations required for higher data rate in a band-limited channel. In [94], tapped delay line adaptive array is used to defeat the effect of asynchronous multiuser STBC transmission in narrowband fast fading channel. However, this paper did not consider the effects of multipath signal which without appropriate compensation method, the performance would be degraded due to increased ISI.

In this paper, in order to enhance the transmission efficiency of STBC in frequency-selective fading channel, we present a Modified spatio-temporal adaptive array for multiuser STBC transmission (Modified STBC-STAA). The Modified STBC-STAA estimates both the conjugated and non-conjugated desired signal from the receive signal in order to restore the orthogonality structure of STBC, thus reduces the effect of residual ISI. A discussion on the asynchronous STBC reception is also given. With computer simulation, it is shown that Modified STBC-STAA can overcome the code synchronization error and achieve a higher performance improvement for both of synchronous and asynchronous STBC transmission in frequency selective fading channel.

[1]It is known as STBC-TDLAA in the previous chapter.

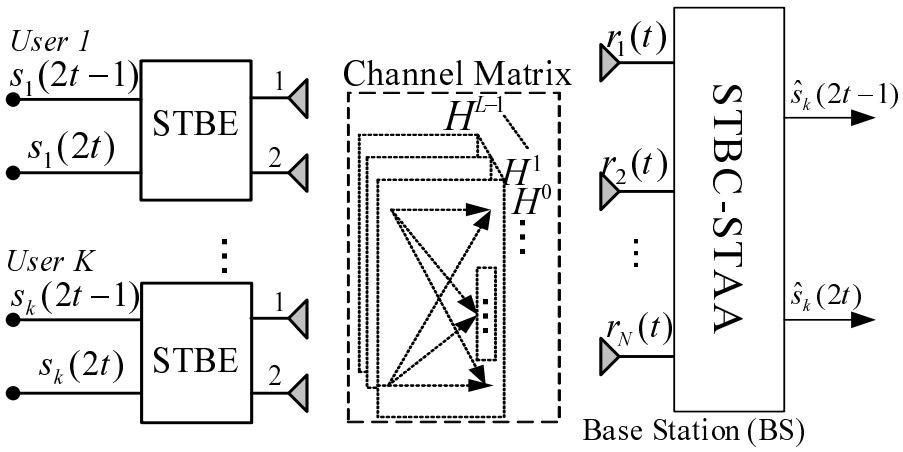

Figure 7.1: System overview of multiuser STBC transmission.

This paper is organized as follows: We describe the proposed method namely as Modified STBC-STAA, to overcome the frequency selective fading channel in 7.2. Simulations and discussions are given in Sec. 7.3, and conclusions are provided in Section 7.4.

7.2 Configuration and Signal Model of the Proposed Scheme: Modified STBC-STAA

In this chapter, we consider an uplink system as illustrated in Fig. 7.1, in which multiple users access the base station (BS). Each users employ the Alamouti's STBC with $M = 2$ transmit antennas, and there are N receive antennas at the BS. Extension to more general type of STBC [19] is quite straight forward.

In frequency selective fading channel, although the spatio-temporal equalization achieved by the STBC-STAA [61] approach reduces intersymbol-interference (ISI) significantly, there always is some residual ISI due to *one-symbol delay*, namely the *codes synchronization error*. The desired signal in the received signals, namely $s_k(2t-1)$ and $s_k(2t)$ are not only dispersed in space, but also in time. Note that at the receiver, the conventional method of STBC-STAA as shown in Fig. 4.1, only detect and combine the non-conjugated desired signal, and the conjugated version of complex signal was not considered during the adaptive processing. This method would work under the transmission of BPSK modulation technique, where all the transmitted signal is in the form of real part only. However, for a higher order of modulation techniques which has the real and imaginary part of complex signal, the perfect code synchronization is required for maximized the detected power of desired signal. Without an appropriate compensation method, the multipath signal would destroys the required orthogonal structure of STBC and thus makes the decoding of STBC-STAA become fail. Therefore, in order to reduce the effect of residual ISI, the receive signal $r_j(t)$ is divided into $\hat{\boldsymbol{r}}(t) = [r_j(2t-1)\ r_j^*(2t)\ r_j(2t)\ r_j^*(2t-1)]^T$.

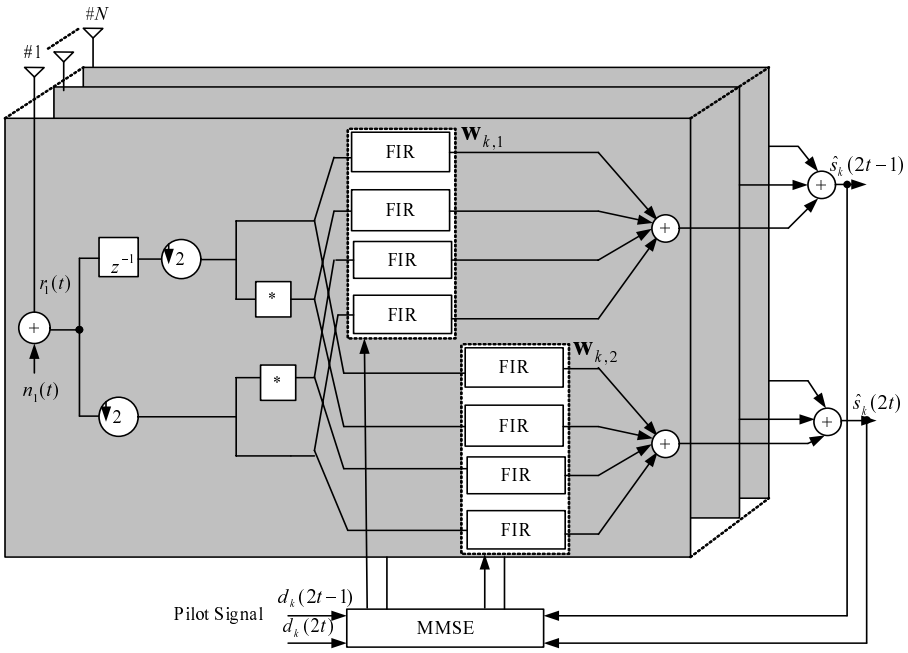

Figure 7.2: Configuration of receiver for Modified STBC-STAA.

The configuration of Modified STBC-STAA is shown in Fig. 7.2. All the sample signals are then put through FIR filters for temporal equalization and estimating $\tilde{s}_k(2t-1)$ and $\tilde{s}_k(2t)$, respectively.

Recall (4.15), the input for FIR will be expressed as

$$\tilde{\boldsymbol{r}}(t) = [\hat{\boldsymbol{r}}(t)^T \ \hat{\boldsymbol{r}}(t)^H \quad \hat{\boldsymbol{r}}(t-T_s)^T \ \hat{\boldsymbol{r}}(t-T_s)^H \quad \ldots \\ \ldots \hat{\boldsymbol{r}}(t-L_rT_s+T_s)^T \ \hat{\boldsymbol{r}}(t-L_rT_s+T_s)^H]^T \quad (7.1)$$

where $\tilde{\boldsymbol{r}} \in \mathbb{C}^{4NL_r \times 1}$.

Assume the coefficients of FIR filter as

$$\boldsymbol{w}_{k,u,j} = [w_{k,u,j}(1) \ \ldots \ w_{k,u,j}(l_r) \ \ldots \ w_{k,u,j}(L_r)]^T \quad (7.2)$$

where $w_{k,u,j}(l_r)$ and $\boldsymbol{w}_{k,u,j}$ are the weight coefficient at l_rth's tap and vector represents the weight coefficient of FIR filters at jth antenna, respectively ($u \in \{1,2\}$). Note that, $l_r = 1, 2, \ldots, L_r$ is the filter tap number. By considering all the receive antennas, the optimal weight $\tilde{\boldsymbol{w}}_{p,u}$ can be shown as follows:

$$\tilde{\boldsymbol{w}}_{p,u} \ = \ \left[\ \boldsymbol{w}_{p,u,1}^T \quad \boldsymbol{w}_{p,u,2}^T \quad \ldots, \boldsymbol{w}_{p,u,j}^T, \ldots, \boldsymbol{w}_{p,u,N}^T \ \right]^T \quad (7.3)$$

The output signal is extracted by multiplying receiver weights $\boldsymbol{w}_{p,1}$ for odd signal $(2t-1)$, and $\boldsymbol{w}_{p,2}$ for even signal $(2t-1)$, with the dimension of $4NL_r \times 1$, for all the receive

Table 7.1: Simulation Parameters

Parameter	Value
STBC Type	Alamouti-STBC ($M = 2$)
Receive antenna	$N = 2, 3, 4$
Number of taps	$L_r = 1, 2, 3, 4$
Adaptive algorithm	Sample Matrix Inversion (SMI)
Channel Model	L path uniform power delay profile frequency selective fading channel as Fig. 7.3.

antennas. Using the minimum mean square error (MMSE) criterion, the optimal weights are decided for u as follows:

$$\tilde{\boldsymbol{w}}_{p,1} = \arg\min E[|d_p(2t-1) - \tilde{\boldsymbol{w}}_{p,1}^H \tilde{\boldsymbol{r}}(t)|^2] \quad (7.4)$$

$$\tilde{\boldsymbol{w}}_{p,2} = \arg\min E[|d_p(2t) - \tilde{\boldsymbol{w}}_{p,2}^H \tilde{\boldsymbol{r}}(t)|^2] \quad (7.5)$$

Solving (7.4) and (7.5), the optimal weight can be represented as below:

$$\tilde{\boldsymbol{w}}_{p,1} = \boldsymbol{R}_{\tilde{r}\tilde{r}}^{-1} \boldsymbol{X}_{rd,(2t-1)} \quad (7.6)$$

$$\tilde{\boldsymbol{w}}_{p,2} = \boldsymbol{R}_{\tilde{r}\tilde{r}}^{-1} \boldsymbol{X}_{rd,(2t)} \quad (7.7)$$

where, $\boldsymbol{R}_{\tilde{r}\tilde{r}} = E[\tilde{\boldsymbol{r}}(t)\tilde{\boldsymbol{r}}(t)^H] \in \mathbb{C}^{2NL_r \times 2NL_r}$ is the covariance matrix of the receive signals, $\boldsymbol{X}_{rd,(2t-1)} = E[\tilde{\boldsymbol{r}}(t)d_p^*(2t-1)] \in \mathbb{C}^{2NL_r \times 1}$ and $\boldsymbol{X}_{rd,(2t)} = E[\tilde{\boldsymbol{r}}(t)d_p^*(2t)] \in \mathbb{C}^{2NL_r \times 1}$, are the correlation vector between receive signal and the reference signal. Here $d_p(2t-1)$ and $d_p(2t)$ are the reference signal at time $2t-1$ and time $2t$, respectively. The output signal is extracted using (7.6) and (7.7) to be resulted as below.

$$\tilde{s}_p(2t-1) = (\tilde{\boldsymbol{w}}_{p,1})^H \tilde{\boldsymbol{r}}(t), \quad (7.8)$$

$$\tilde{s}_p(2t) = (\tilde{\boldsymbol{w}}_{p,2})^H \tilde{\boldsymbol{r}}(t). \quad (7.9)$$

7.3 Simulation and Results

7.3.1 Simulation setup

The simulation parameters are shown in Table 7.1. To examine the efficiency of proposed method, L paths with uniform power delay profile of frequency selective fading channel as shown in Fig. 7.3 is considered. All simulations are conducted using QPSK transmit constellation and the results are averaged over $10,000$ channel realizations for average BER and output signal-to-interference plus noise ratio (SINR) curves.

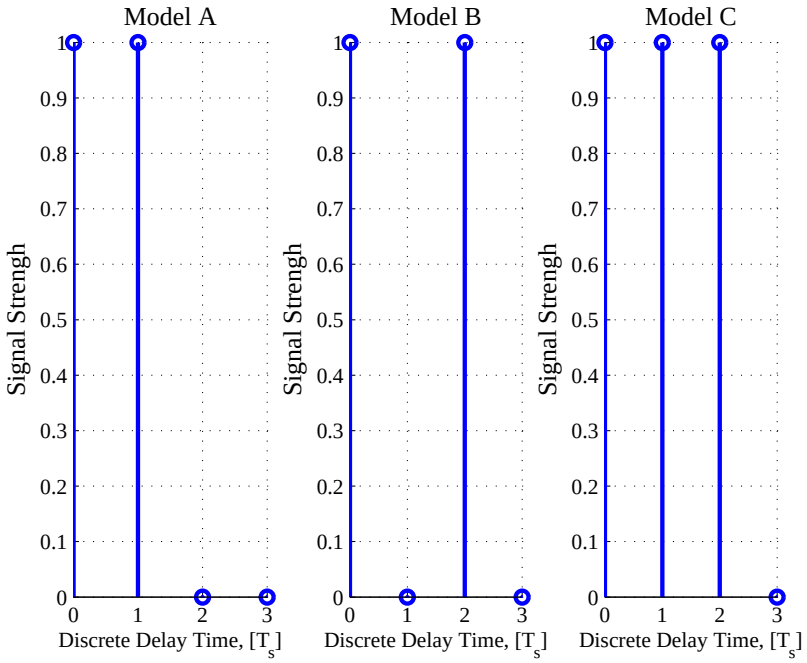

Figure 7.3: Channel model: Model A: Two paths uniform power delay profile with one symbol delay, Model B: Two paths uniform power delay profile with two symbol delay, Model C: Three paths uniform power delay profile.

7.3.2 Effect of Modified STBC-STAA with Synchronous STBC Transmission

We examine the performance between the proposed method and STBC-STAA [61] in presence of ISI only (single user) for $M = 2$, $N = 4$. For the sake of fair comparison, we use the channel model as shown in Fig. 7.3 [61], however the power delay profile is normalized to unity, whereas $L = 2$, with *one-symbol delay* (Model A) and *two-symbol delay* (Model B). Figure 7.4 illustrate the average BER performance of STBC-STAA and Modified STBC-STAA. It is shown that Modified STBC-STAA outperforms the STBC-STAA solutions in both channel models. It is seen that under the frequency selective fading channel with *one-symbol delay*, Modified STBC-STAA improve the average BER very much compare to STBC-STAA. Here, Modified STBC-STAA can mitigate the residual ISI produce by the problem regards to *one-symbol delay* in STBC transmission which destruct the orthogonality of codes. Furthermore, for *two-symbol delay* also, the proposed method can achieve a better average BER compare to conventional STBC-STAA since all the components of desired signal has been perfectly combined.

Next, we consider the performance of Modified STBC-STAA in the presence of ISI and CCIs. The average BER of Modified STBC-STAA is shown in Fig. 7.5 using the similar simulation parameters as above for two users environment. From the figure, in

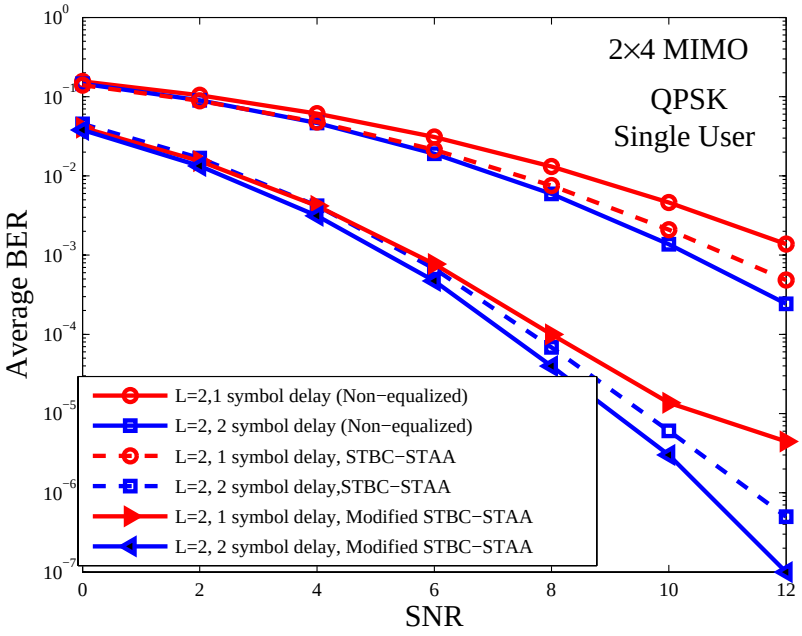

Figure 7.4: Average BERs of the STBC-STAA [61] and Modified STBC-STAA over the frequency selective fading channel without CCIs. with 2×4 MIMO system.

the presence of ISI and CCIs, average BER of the Modified STBC-STAA outperform the conventional STBC-STAA, for the case of *one-symbol delay*. Similarly, in the case of *two-symbol delay*, Modfied STBC-STAA can further improve the average BER, since the orthogonality of STBC codes are preserved.

Effects on the higher order of modulation techniques

We evaluate the proposed method using different order of modulation techniques for single user transmission using 2×4 MIMO system over $L = 2$ paths of Model A channel environment. Here, we assume BPSK, QPSK, and 16PSK modulation techniques with $L_r = 4$ which means that all delayed signals are perfectly combined. As illustrated in Fig. 7.6, it is shown that for BPSK transmission, the performance gaps between STBC-STAA and Modified STBC-SBAA is small, and becomes bigger as the QPSK and 16PSK applied. For BPSK transmission, only the real data signal is transmitted, thus the effects of code synchronization errors is smaller compared to QPSK or 16PSK whereas in this case, both the real and imaginary data of complex signals are transmitted, thus both of the parts contribute to the *codes synchronization error*. It is also shown that the impact of *synchronization errors* becomes crucial for the higher order of modulation techniques, and Modified STBC-STAA has approved to overcome this problem. From the result, we can conclude that our proposed scheme can minimize the impact of code synchronization

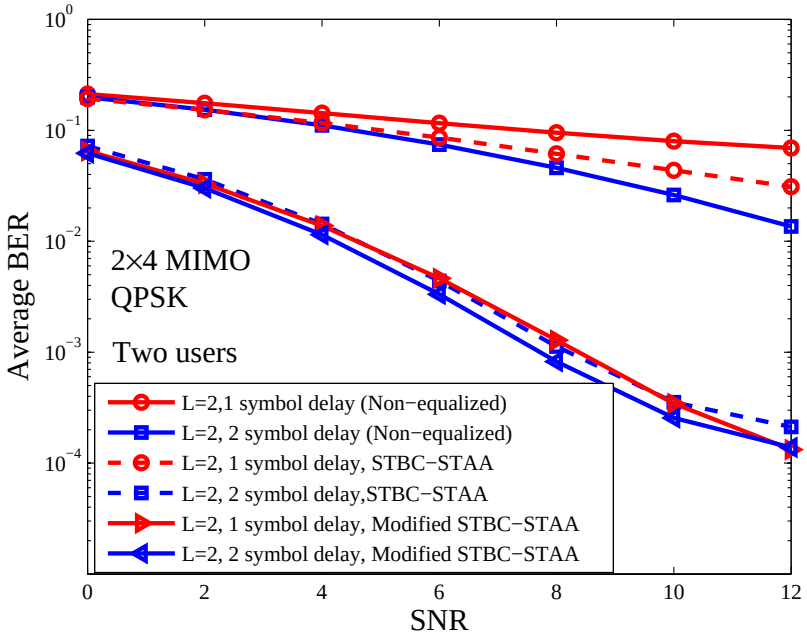

Figure 7.5: Average BERs of the STBC-STAA [61] and Modified STBC-STAA over the frequency selective fading channel with CCIs. with 2×4 MIMO system.

errors in higher order of modulation techniques.

7.3.3 Effect of timing errors due to asynchronous multiuser STBC transmission

So far, we have assumed the ideal transmit power control, and all received signals transmitted from different users are time-synchronous. However, for a practical transmit timing control scheme, the timing error exists in the receive signals due to asynchronous multiuser transmission. Here, we consider the timing error of two users with the errors as shown in Table 7.2. Δ_k denote the timing difference between user $k = k_1$ and $k = k_2$, where $\Delta_k = 0$ is defined as *perfect timing*, $0 < \Delta_k < T_b(= 2T_s)$, ($T_s$:symbol duration, T_b:block duration) is defined as *non-perfect timing* which introduce the *timing error*, and $\Delta_k = \frac{T_b}{2}$ is the the worst case (Case 1). The timing errors would destroy the coding structure of STBC, and make the receiver unable to detect the desired signal. This problem will introduce the ISI even in the flat fading channel, and become serious in the presence of delay spread (in frequency selective fading channel) with the additional ISI and CCIs. In [94], a STBC transmission adopting tapped delay line adaptive array to defeat the effects of asynchronous multiuser transmission in narrowband fast fading channel was proposed. However, this paper did not consider the effects of multipath signal which without appropriate compensation method, the performance would be degraded due to increased

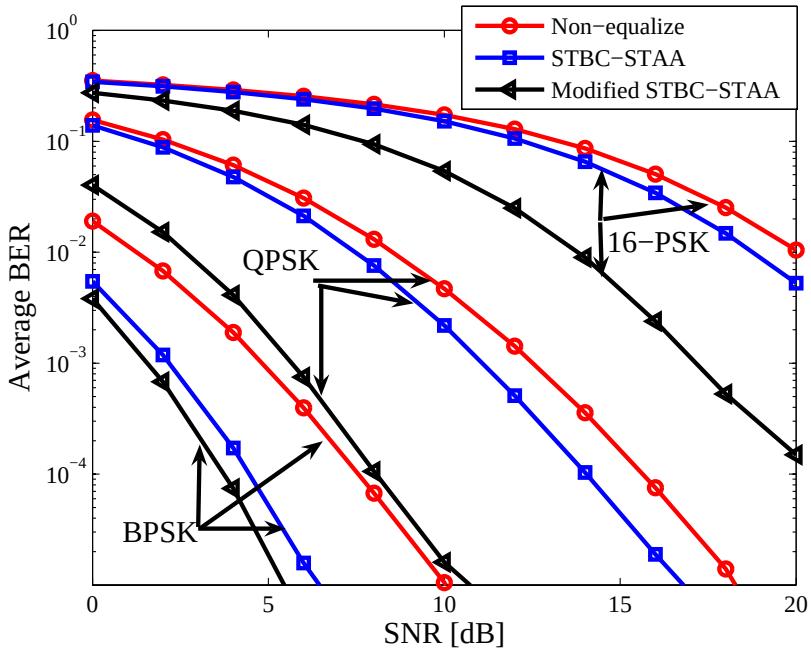

Figure 7.6: Impact of synchronization error for BPSK, QPSK, and 16PSK for single user transmission using 2×4 MIMO system over Model A channel environment.

Table 7.2: Model of asynchronous multiuser STBC transmission applied for simulation.

Case 1	$\Delta_1 = 0$ symbol	$\Delta_2 = 1$ symbol
Case 2	$\Delta_1 = 0$ symbol	$\Delta_2 = 2$ symbol

ISI. Different to [94], our proposed method of Modified STBC-STAA can simultaneously overcome the multiuser timing error and codes synchronization errors in the wideband channel.

The performance of the proposed method is compared in frequency selective fading channel with $L = 3$ (as shown in Fig. 7.3: Model C) for 2×4 MIMO system, and $L_r = \{1 \sim 4\}$. Here, we consider the QPSK modulation and $K = 2$ users. Figure 7.7 shows the average BER of first user for Case 1 and Case 2. From both figures, the performance of Modified STBC-STAA outperform STBC-STAA, both in Case 1 and Case 2, respectively. A possible reason for this is Modified STBC-STAA exploiting all the possible components (real and conjugated version) of desired signal in the received signal, especially when $L_r \geqq L$, compare to STBC-STAA which exploits the real desired signal only. Therefore, it is verified that Modified STBC-STAA is robust to the timing errors due to asynchronous multiuser STBC transmission.

Interference cancellation capability

Next, the interference cancellation capability of both method with *timing errors* are investigated. Here, we plot the results of the average BER and average output signal-to-interference-plus-noise ratio (SINR) versus the average SNR, measured in decibels ([dB]). Average output SINR [61, 72] is used in this paper to represent the interference cancellation capability given by updated weight of the proposed scheme. Simulation conditions as $N = \{2, 3, 4\}$, $L_r = \{1 \sim 4\}$ and Model C channel environment are assumed. As illustrated in Fig. 7.8, average BER and average output SINR performance of Modified STBC-STAA improved as L_r increased. However, Modified STBC-STAA shows a higher average output SINR compare to STBC-STAA, especially when the number of receive antenna N increased. As $L_r = 2$, both method used to realign the asynchronous received signal to perform the synchronous spatial temporal equalization, though the effect of ISI and CCIs are still existed. When $L_r \geq L = 3$, Output SINR of Modified STBC-STAA and STBC-STAA reach each maximum values, respectively. In general, it is shown that Modified STBC-STAA perform a better cancellation capability compare to STBC-STAA.

Effect of Antenna Diversity Combining

The simulated average output SINR performance of proposed method with antenna (receive) diversity is plotted in Fig. 7.9 when the number of receive antenna at BS is increased, namely $N = 1 \sim 10$ at SNR=20 [dB] for two users environment. Here, the synchronous and asynchronous transmission of Case 1 and Case 2 are simulated over the Model C channel environment. From the figure, the average output SINR of Modified STBC-STAA for synchronous and asynchronous transmission of Case 1 and Case 2 are improved when N is increased. Note that, in the previous simulation, for example, by setting $N = 2$ which produce the degree of freedom (DOF) $= N - 1 = 1$ to cancel the CCIs. It is clearly observed that the more receive antennas are used, the larger the spatial diversity gain achieved and thus a better average output SINR is obtained. At the mean time, the use of more receive antennas also increases the ability of receiver to cancel the interference since its DOF increases. Moreover, it is observed that synchronous and asynchronous transmission (Case 1 and Case 2) for Modified STBC-STAA and STBC-STAA, respectively has the similar average output SINR. This mean that the effect of timing error can be neglected for both synchronous and asynchronous transmission using Modified STBC-STAA and STBC-STAA. However, Modified STBC-STAA has a better output SINR compare with STBC-STAA since all the components of desired signal are perfectly combined at the receiver.

7.4 Conclusions

In order to maximize the performance improvement over frequency selective fading channel, we have presented a multiuser STBC transmission scheme by employing a modified

spatio-temporal adaptive array (Modified STBC-STAA) to overcome the problem of *one symbol delay*, namely code synchronization error. Modified STBC-STAA incorporates the target signal component for not only the non-conjugated, but also the complex conjugated version of desired signal, which is dispersed in the received signal due to the multipath fading channel. Furthermore, we examine the effect of timing errors and employ Modified STBC-STAA to re-align the asynchronous multiuser STBC signal to undergo the synchronous joint interference suppression and equalization. Simulation results show that Modified STBC-STAA can achieve a higher performance improvement for both synchronous and asynchronous multiuser STBC transmission in frequency selective fading channel.

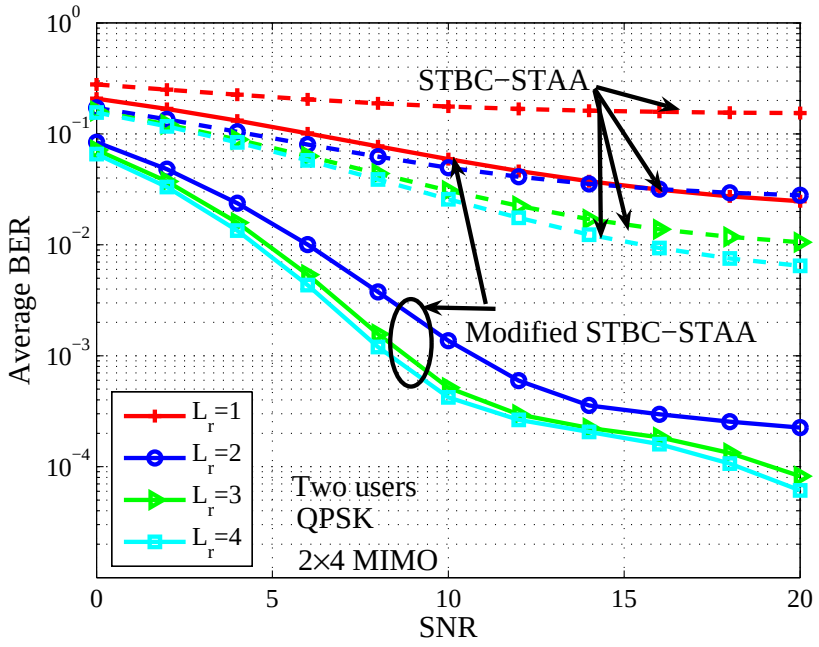

(a) Case 1

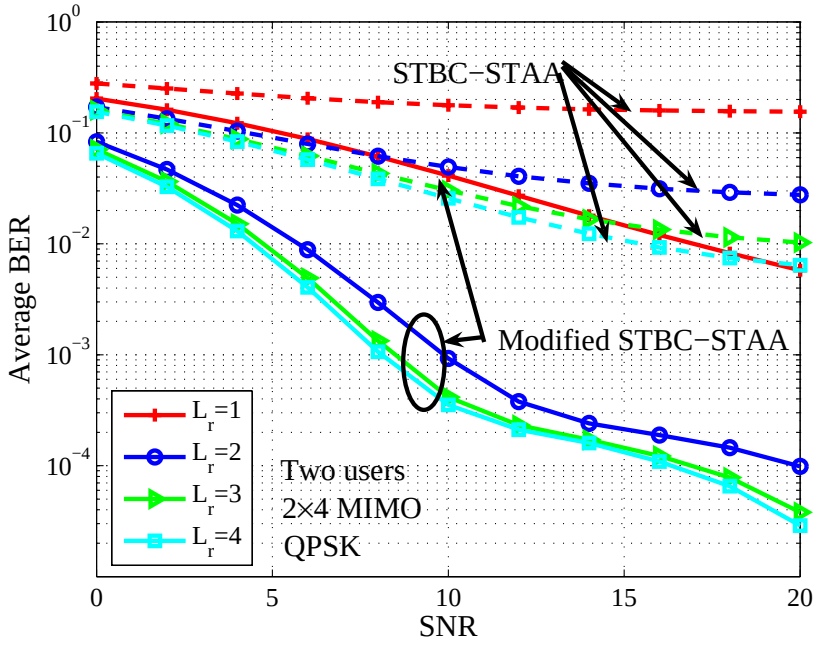

(b) Case 2

Figure 7.7: Performance of asynchronous multiuser STBC transmission with two users in frequency selective fading channel, $L = 3$, 2×4 MIMO system.

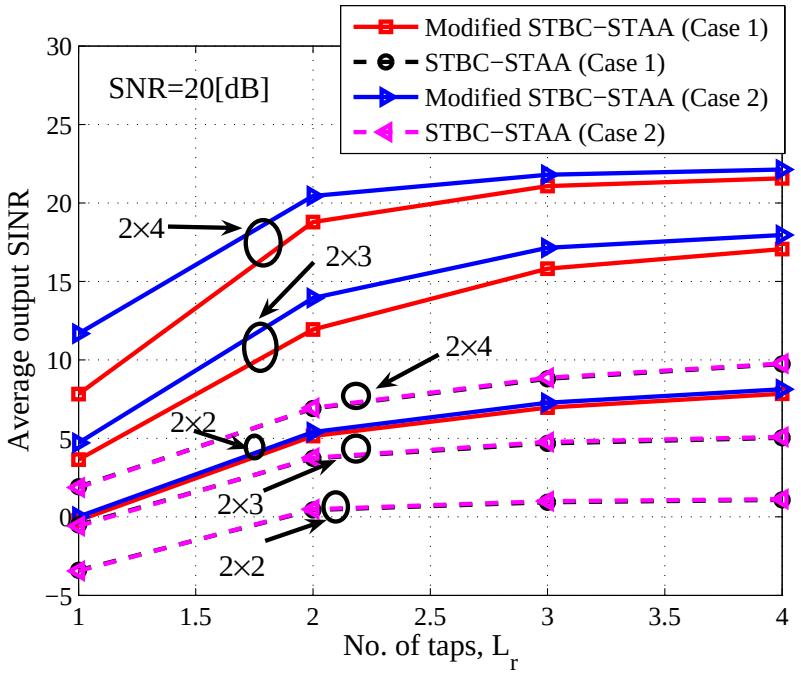

(a) Average output SINR

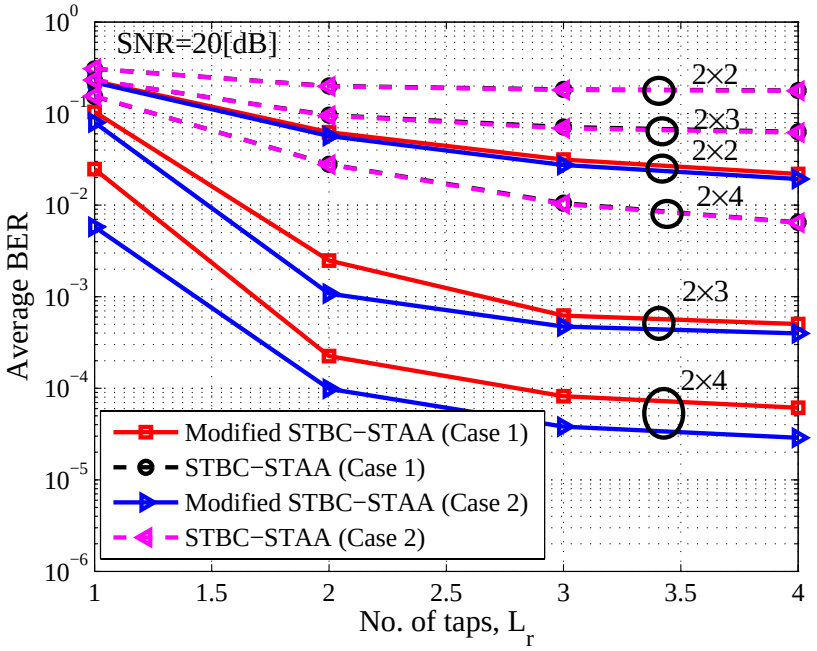

(b) Average BER

Figure 7.8: Average output SINR and average BER performance comparison of STBC-STAA and Modified STBC-STAA at various TDL length L_r for $2 \times 2,\ 2 \times 3,\ 2 \times 4$ MIMO system with Model C channel.

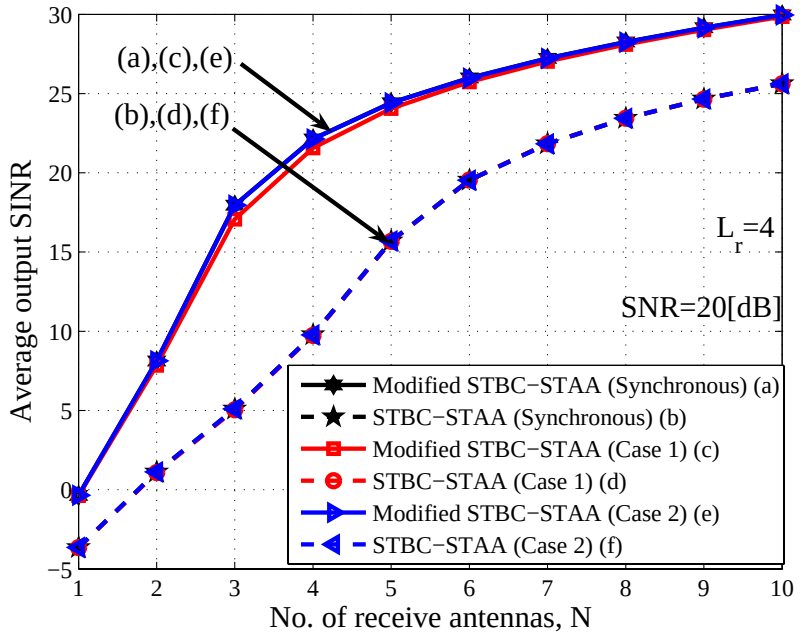

Figure 7.9: Average output SINR of STBC-STAA and Modified STBC-STAA versus the number of receive antenna, N in frequency selective fading channel at SNR=20 [dB], for synchronous transmission and asynchronous transmission (Case 1 and Case 2).

Chapter 8

Conclusions and Future Works

This chapter concludes our work by summarizing the results and future works.

8.1 Dissertation Conclusions

In this dissertation, the overview of MIMO system and STC, and the fundamental of adaptive array was given in Chapter 2 and 3, respectively. In Chapter 4, we present the STBC-SBAA for the transmission in the frequency selective fading channel. We extend the proposed method for the chip-based equalization in CDMA system, as described in Chapter 5. In Chapter 6, for the high data rate transmission, we also present the STBC-SBAA for multirate multicode CDMA system. Finally, a new structure of Modified STBC-STAA was given in the Chapter 7 for maximizing the transmission efficiency in frequency selective fading channel. In order to show the efficiency of the proposed method, the computer simulation was brought, and the following concluding remarks are obtained:

1. **STBC-SBAA**:
   We propose a combined CSI estimation and signal detection scheme for MIMO transmission scheme using STBC adopting subband adaptive array (SBAA) processing under frequency selective fading channel. In the receiver, the received signal is divided into two independent group of signal and adaptive processing is carried out in frequency-domain to equalize the frequency selective fading and estimate the desired signal. A novel construction of SBAA is introduced to process the received signal. Through computer simulations, it has been verified that the proposed scheme shows a better performance than STBC of conventional type. Its ability is positioned between conventional STBC and the STBC-TDLAA scheme. Furthermore, to enhance the performance of the proposed scheme, we evaluate the idea of single carrier CP into STBC-SBAA. It is also demonstrated that the proposed scheme with CP achieves a better performance compare to STBC-TDLAA scheme, with less computational load.

2. **STBC SBAA for CDMA System:**
   A high reliability multiuser transmission under frequency selective fading, we have

proposed a novel MIMO-CDMA system utilizing SBAA in the receiver. A novel construction of SBAA is introduced to process CDMA signals based on STBC before despreading. In addition, spreading code CP is introduced to improve the performance of STBC-SBAA. Through computer simulations, it is verified that STBC-SBAA achieves good SINR compared to STBC-TDLAA and STBC-ABF, with less complexity in both single and multiuser environments. We proved that the proposed scheme can achieve significant performance by exploiting the effects of transmit diversity and SBAA.

3. **Application of STBC-SBAA in Multicode Multirate CDMA System:**
   We have applied the interference suppression technique of STBC-SBAA for multirate multicode MIMO CDMA transmission under frequency selective fading channel. The proposed scheme has a flexible configuration which allows BS to dynamically adapt to multirate transmission requests from MS. This scheme utilizes a STBC as transmit diversity and receive antenna with SBAA to process the multirate multicode CDMA signal. Simulation results demonstrate that the proposed scheme can totally avoid the MCI while suppressing the ISI and MAI. We also show that our proposed scheme achieved a higher diversity order compare to conventional SBAA and maintaining the same diversity order for both LDR and HDR users.

4. **Wideband Spatio-Temporal Adaptive Array for Multiuser STBC Transmission:**
   In order to maximize the performance improvement over frequency selective fading channel, we have presented a multiuser STBC transmission scheme by employing a modified spatio-temporal adaptive array (Modified STBC-STAA) to overcome the problem of *one symbol delay*, namely code synchronization error. Modified STBC-STAA incorporates the target signal component for not only the non-conjugated, but also the complex conjugated version of desired signal, which is dispersed in the received signal due to the multipath fading channel. Furthermore, we examine the effect of timing errors and employ Modified STBC-STAA to re-align the asynchronous multiuser STBC signal to undergo the synchronous joint interference suppression and equalization. Simulation results show that Modified STBC-STAA can achieve a higher performance improvement for both synchronous and asynchronous multiuser STBC transmission in frequency selective fading channel.

8.2 Future Work

Based on this work, there are several areas of this work which could be extended for future research.

1. Throughput the works, we evaluate the proposed method using the computer simulation. The analysis using theoretical method is still open for future research.

2. Almost configurations of the proposed method were introduced for uplink beamforming. Application of STBC for downlink beamforming could be an interesting topic for further study.

3. It is shown that, the use of CP in STBC-SBAA can require up to $15 \sim 20\%$ bandwidth overhead. It is desirable to develop techniques that eliminate or reduce the CP.

4. The investigation on the method to reduce the computational complexity of STBC-TDLAA and Modified STBC-TDLAA would be the future works.

5. Employing error correcting codes such as convolutional coding, or turbo coding would enhance the performance of STBC-SBAA in the longer delay spread would enhance the performance.

6. Through our investigation, it is shown that STBC-SBAA is depending on the length of CP and the length of delays. The performance of STBC-SBAA degraded if the length of channel memory is larger than CP. Therefore, a method is required to cancel or exploit the multipath that exceed the length of CP.

Appendix A

Derivation of $\mathbf{R}_{\tilde{r}\tilde{r}}$

A.1 MMSE Solution for STBC-TDLAA: Derivation of $\mathbf{R}_{\tilde{r}\tilde{r}}$

Problem: Given a STBC-TDLAA system which is described by the (4.15)*. Find two vectors* $\tilde{\mathbf{w}}_1$ *and* $\tilde{\mathbf{w}}_2$ *such that*

$$\tilde{\mathbf{w}}_1 = \arg\min E\{|d(t) - \tilde{\mathbf{w}}_2^H \tilde{\mathbf{r}}(t)|^2\} \tag{A.1}$$

$$\tilde{\mathbf{w}}_2 = \arg\min E\{|d(t+T_s) - \tilde{\mathbf{w}}_2^H \tilde{\mathbf{r}}(t)|^2]\}. \tag{A.2}$$

A.1.1 Solution for $\tilde{\mathbf{w}}_1$

First define that,

$$\begin{aligned} D_1 &= E\{|d(t) - \tilde{\mathbf{w}}_1^H \tilde{\mathbf{r}}(t)|^2\} \\ &= E\{[d(t) - \tilde{\mathbf{w}}_1^H \tilde{\mathbf{r}}(t)][s(t) - \tilde{\mathbf{w}}_1^H \tilde{\mathbf{r}}(t)]^*\} \\ &= E\{d(t)d(t)^*\} - \tilde{\mathbf{w}}_1^H E\{\tilde{\mathbf{r}}(t)d(t)^*\} - E\{d(t)\tilde{\mathbf{r}}(t)^H\}\tilde{\mathbf{w}}_1 + \tilde{\mathbf{w}}_1^H E\{\tilde{\mathbf{r}}(t)\tilde{\mathbf{r}}(t)^H\}\tilde{\mathbf{w}}_1 \end{aligned} \tag{A.3}$$

Since signal is assumed to be uncorrelated with one another, and with the noise, we have

$$\begin{aligned} E\{\tilde{\mathbf{r}}(t)d(t)^*\} &= \sum_{l=0}^{L-1} \tilde{\mathbf{H}}^l E\{\mathbf{s}(t)d(t)\} \\ &= \sum_{l=0}^{L-1} \tilde{\mathbf{H}}^l [\zeta^2 \ 0]^T \end{aligned} \tag{A.4}$$

$$E\{d(t)\tilde{\mathbf{r}}(t)^H\} = [\zeta^2 \ 0](\sum_{l=0}^{L-1} \tilde{\mathbf{H}}^l)^H \tag{A.5}$$

$$\begin{aligned} E\{\tilde{\mathbf{r}}(t)\tilde{\mathbf{r}}(t)^H\} &= E\{\sum_{l_0=0}^{L-1}\tilde{\mathbf{H}}^{l_0}\mathbf{s}(t)\mathbf{s}(t)^{\tilde{H}}(\sum_{l_1=0}^{L-1}\tilde{\mathbf{H}}^{l_1})^H\} + E\{\mathbf{n}(t)\mathbf{n}(t)^H\} \\ &= \sum_{l_0=0}^{L-1}\sum_{l_1=0}^{L-1}\tilde{\mathbf{H}}^{l_0}E\{\mathbf{s}(t)\mathbf{s}(t)^H\}(\tilde{\mathbf{H}}^{l_1})^H + \sigma_n^2\mathbf{I}_{4N} \\ &= \sum_{l_0=0}^{L-1}\sum_{l_1=0}^{L-1}\tilde{\mathbf{H}}^{l_0}\mathbf{\Lambda}(\tilde{\mathbf{H}}^{l_1})^H + \sigma_n^2\mathbf{I}_{4N} \end{aligned} \tag{A.6}$$

where $\mathbf{\Lambda} \in \mathbb{C}^{L_r \times L_r}, l_0, l_1$:path of channel.

$$\mathbf{\Lambda} \triangleq \begin{bmatrix} \mathbf{\Lambda}_1 & 0 & \dots & 0 \\ 0 & \mathbf{\Lambda}_2 & \dots & 0 \\ \vdots & \vdots & & \vdots \\ 0 & 0 & \dots & \mathbf{\Lambda}_{L_r} \end{bmatrix} \tag{A.7}$$

is the diagonal power matrix with element $\mathbf{\Lambda} = \text{diag}(\mathbf{\Lambda}_1, \dots, \mathbf{\Lambda}_{L_r}), \mathbf{\Lambda}_{l_r} = \zeta^2\mathbf{I}_{4N}$, $\zeta \triangleq E\{|s(t)|^2\} = E\{|s(t+T_s)|^2\}$, is the average power of transmitted signal, and $\mathbf{I}_{4N} \in \mathbb{C}^{4N\times 4N}$ is an identity matrix. Note that,

$$\begin{aligned} \sum_{l=0}^{L-1}\tilde{\mathbf{H}}^l[\zeta^2\ 0]^T &= \sum_{l=0}^{L-1}\begin{bmatrix} \mathbf{h}_1^l & \mathbf{h}_2^l \\ \mathbf{h}_2^{l*} & -\mathbf{h}_1^{l*} \end{bmatrix}[\zeta^2\ 0]^T \\ &= \zeta^2\sum_{l=0}^{L-1}[\mathbf{h}_1^{l,T}\ \mathbf{h}_2^{l,H}]^T \\ &\triangleq \hat{\mathbf{h}}_1 \end{aligned} \tag{A.8}$$

$$[\zeta^2\ 0](\sum_{l=0}^{L-1}\tilde{\mathbf{H}}^l)^H = \hat{\mathbf{h}}_1^H \tag{A.9}$$

Then,

$$D_1 = \zeta^2 - \tilde{\mathbf{w}}_1^H\hat{\mathbf{h}}_1 - \hat{\mathbf{h}}_1^H\tilde{\mathbf{w}}_1 + \tilde{\mathbf{w}}_1^H(\sum_{l_0=0}^{L-1}\sum_{l_1=0}^{L-1}\tilde{\mathbf{H}}^{l_0}\mathbf{\Lambda}(\tilde{\mathbf{H}}^{l_1})^H + \sigma_n^2\mathbf{I}_{4N})\tilde{\mathbf{w}}_1 \tag{A.10}$$

Taking the derivative of the D_1 in (A.10), with respect to $\tilde{\mathbf{w}}_1$, we have

$$\frac{\partial D_1}{\partial \tilde{\mathbf{w}}_1} = -\hat{\mathbf{h}}_1^* + (\sum_{l_0=0}^{L-1}\sum_{l_1=0}^{L-1}\tilde{\mathbf{H}}^{l_0}\mathbf{\Lambda}(\tilde{\mathbf{H}}^{l_1})^H + \sigma_n^2\mathbf{I}_{4N})^T\tilde{\mathbf{w}}_1^* \tag{A.11}$$

Put the left side of (A.11) equal to zero, then we obtain

$$\tilde{\mathbf{w}}_1 = (\sum_{l_0=0}^{L-1}\sum_{l_1=0}^{L-1}\mathbf{H}^{l_0}\mathbf{\Lambda}(\mathbf{H}^{l_1})^H + \sigma_n^2\mathbf{I}_{4N})^{-1}\hat{\mathbf{h}}_1 \tag{A.12}$$

.

A.1.2 Solution for $\mathbf{w}_2$

Similarly, using the same procedure above, we obtain

$$\tilde{\mathbf{w}}_2 = (\sum_{l_0=0}^{L-1}\sum_{l_1=0}^{L-1}\tilde{\mathbf{H}}^{l_0}\mathbf{\Lambda}(\tilde{\mathbf{H}}^{l_1})^H + \sigma_n^2\mathbf{I}_{4N})^{-1}\hat{\mathbf{h}}_2. \tag{A.13}$$

Here,

$$\hat{\mathbf{h}}_2 \triangleq \zeta^2\sum_{l=0}^{L-1}[\mathbf{h}_2^{l,T} \ -\mathbf{h}_1^{l,H}]^T. \tag{A.14}$$

Note that the first term on the right side of (A.12) and (A.13) are in fact the inversion of the covariance matrix of the receive signal $\tilde{\mathbf{r}}$, and is expressed as $\mathbf{R}_{\tilde{r}\tilde{r}}^{-1} = [E\{\tilde{\mathbf{r}}\tilde{\mathbf{r}}^H\}]^{-1}$,

$$\mathbf{R}_{\tilde{r}\tilde{r}}^{-1} = (\sum_{l_0=0}^{L-1}\sum_{l_1=0}^{L-1}\tilde{\mathbf{H}}^{l_0}\mathbf{\Lambda}(\tilde{\mathbf{H}}^{l_1})^H + \sigma_n^2\mathbf{I}_{4N})^{-1} \tag{A.15}$$

Therefore the weight vectors $\mathbf{w}_1$ and $\mathbf{w}_2$ can be expressed in the well-known form of the Wiener-Hopf solution as

$$\tilde{\mathbf{w}}_1 = \mathbf{R}_{\tilde{r}\tilde{r}}^{-1}\hat{\mathbf{h}}_1 \tag{A.16}$$

$$\tilde{\mathbf{w}}_2 = \mathbf{R}_{\tilde{r}\tilde{r}}^{-1}\hat{\mathbf{h}}_2 \tag{A.17}$$

where $\hat{\mathbf{h}}_1$ and $\hat{\mathbf{h}}_2$ are the correlation vectors of received signal and reference signal.

Bibliography

[1] J. E. Hudson, *Adaptive Array Principles*, IEE Electromagnetic Wave Series II, 1991.

[2] G. J. Foschini, Jr. and M. J. Gans, "On limits of wireless communication in a fading environment when using multiple antennas," *Wireless Personal Communications*, vol. 6, pp. 311-335, 1998.

[3] A.J Paulraj and C.B Papadius, "Space-time Processing for wireless communications," *IEEE Sig. Processing. Mag.*, vol.14, no.6, pp.49-83, Nov. 1997.

[4] G. J. Foschini, "Layered space-time architecture for wireless communication in a fading environment when using multi-element antennas," *Bell Labs Technical Journal*, Autumn 1996.

[5] T.S. Rappaport, A. Annamalai, R.M. Buehrer, and W.H. Tranter, "Wireless communications: past events and a future perspective," *IEEE Trans. Commun.*, vol. 40, no. 5, pp.148-161, May 2002.

[6] F. Adachi, "Wireless Past and Future - Evolving Mobile Communications Systems," *IEICE Trans. Fund.*, vol. E84-A, no.1,pp.55-60, Jan. 2001.

[7] K. Yungsoo, J.B. Jang, and C. Jaehak, "Beyond 3G: vision, requirements, and enabling technologies," *IEEE Commun. Mag.*, vol.41, no.3, pp.120-124, Mar. 2003.

[8] H. Ekstrom, A. Furuskar, J. Karlsson, M. Meyer, S. Parkvall, J. Torsner, and M. Wahlqvist, "Technical Solutions for the 3G Long-Term Evolution," *IEEE Commun. Mag.*, vol. 44, no. 3, pp. 38-45, Mar. 2006.

[9] R.Attar, D.Ghosh, C.Lott, M.Fan, P.Black, R.Rezaiifar, and P.Agashe, "Evolution of cdma2000 cellular networks: Multicarrier EV-DO", *IEEE Commun. Mag.*, vol.44, no.3, pp.46-53, Mar. 2006.

[10] Broadband Wireless Internet Forum, *http://www.bwif.org.*

[11] TD-SCDMA Forum, *http://www.td-scdma-forum.org.*

[12] UMTS Web site, *http://www.umtsworld.com/technology/hspda.htm.*

[13] M. Schwartz, W.R. Bennett, and S. Stein, *Communication Systems and Techniques*, 1st edition, McGraw-Hill, 1966.

[14] I. E. Telatar, "Capacity of multiantenna Gaussian channels," *European Trans. Telecommunication*, vol. 1, no. 6, pp. 585-595, Nov. 1999.

[15] T.L. Marzetta and B.M. Hochwald, "Capacity of a mobile multiple-antenna communication link in Rayleigh flat fading, " *IEEE Trans. Inform. Theory*, vol. 45, pp. 139-157, Jan. 1999.

[16] A. Narula, M.D. Trott, and G.W. Wornell, "Performance limits of coded diversity methods for transmitter antenna arrays, " *IEEE Trans. Inform. Theory*, vol. 45, pp. 2418-2433, Nov. 1999.

[17] S. M. Alamouti, "A simple transmit diversity technique for wireless communications," *IEEE J. Sel. Areas Commun.*, vol. 16, no. 8, pp. 1451-1458, Oct. 1998.

[18] S. Baro, G. Bauch, A. Pavlic, and A. Semmler, "Improving BLAST performance using space-time block codes and turbo decoding, " in *Proc. IEEE Global Telecommunications Conf. (GLOBECOM)*, vol. 2, pp. 1067-1071, 2000.

[19] V. Tarokh, H. Jafarkhani, and A. R. Calderbank, "Space-time block bodes from orthogonal designs," *IEEE Trans. Inform. Theory*, vol.45, no.5, pp. 1456-1467, July 1999.

[20] V. Tarokh, N. Seshadri, and A.R. Calderbank, "Space-time codes for high data rates wireless communications: Performance analysis and code construction," *IEEE Trans. Inform. Theory*, vol. 44, no. 2, pp. 744-765, Mar. 1998.

[21] V. Tarokh, H. Jafarkhani, and A.R. Calderbank, "Space-time block coding for wireless communications: Performance results," *IEEE J. Sel. Areas Commun.*, vol. 17, no. 3, pp. 451-460, Mar. 1999.

[22] V. Tarokh, A. Naguib, N. Seshadri, and A.R. Calderbank, "Space-time codes for high data rate wireless communication: Performance criteria in the presence of channel estimation errors, mobility, and multiple paths," *IEEE Trans Commun.*, vol. 47, no. 2, pp. 199-207, Feb. 1999.

[23] V. Tarokh, A.F. Naguib, N. Seshadri, and A.R. Calderbank, "Combined array Processing and space-time coding, " *IEEE Trans. Inform. Theory*, vol. 45, no.4, pp.1121-1128, May 1999.

[24] V. Tarokh and H. Jafarkhani, "A differential detection scheme for transmit diversity, " *IEEE J. Sel. Areas Commun.*, vol. 18, no.7, pp. 1169-1174, July 2000.

[25] B. L. Hughes, "Differential space-time modulation," *IEEE Trans. Inform. Theory*, vol. 46, no. 7, pp. 2567-2578, Nov. 2000.

[26] G. Bauch, "Concatenation of space-time block codes and turbo-TCM, " in *Proc. IEEE International Conference on Communications (ICC'99)*, vol. 2, pp. 1202-1206, 1999.

[27] Y. Ogawa, M. Ohmiya, and K. Itoh, "An LMS adaptive array for multipath fading reduction," *IEEE Trans. Aerosp. Electron. Syst.*, vol. AES-23, no. 1, pp. 17-23, Jan. 1987.

[28] S. Anderson, M. Millnert, M. Viberg, and B. Wahlberg, "An adaptive array for mobile communication systems," *IEEE Trans. Veh. Technol.*, vol. VT-40, pp. 230-236, 1991.

[29] Y. Zhang, "Multipath fading equalization by an adaptive array," in *Proc. Int. Symp. Antennas Propagat.*, Sapporo, pp. 149-152, Aug. 1992.

[30] Y. Doi, T. Ohgane, and E. Ogawa, "ISI and CCI canceler combining the adaptive array antennas and the Viterbi equalizer in a digital mobile radio," in *Proc. IEEE VTC*, pp. 81-85, April 1996.

[31] T. A. Thomas and M. D. Zoltowski, "Novel receiver signal processing for interference cancellation and equalization in cellular TDMA communications," in *Proc. ICASSP*, pp. 3881-3884, 1997.

[32] J.-W. Liang and A. Paulraj, "Two stage CCI/ISI reduction with space-time processing in TDMA cellular networks," in *Proc. 30th Annual Asilomar Conf. on Signals, Systems, and Computers*, Pacific Grove, CA, Nov. 1996.

[33] X. N. Tran, T. Taniguchi, and Y. Karasawa, "A novel adaptive beamforming for space-time block codes," in *Proc. IEICE Technical Report*, AP2003-131, pp.89-94, Aug. 2003.

[34] N. Al-Dhahir, "Single-carrier frequency domain equalization for space-time block coded transmission over frequency selective fading channels," *IEEE Commun. Letter*, vol. 5, no. 7, pp. 304-306, July 2001.

[35] A. F. Naguib, "Combined interference suppression and frequency domain equalization for space-time block coded transmission," in *Proc. IEEE Int. Conf. Commun. (ICC'03)*, vol. 26, no. 1, pp. 3261-3266, May 2003.

[36] S. Zhou and G. B. Giannakis, "Single carrier space-time block-coded transmission over frequency selective fading channels," *IEEE Trans. Inform. Theory*, vol.49, no.1, pp.164-179, Jan. 2003.

[37] R. T. Compton, "The relationship between tapped delay line and FFT processing in adaptive arrays," *IEEE Trans. Antennas Propagat.*, vol.36, no.1, pp.15-26, Jan. 1988.

[38] V. Van Veen and K. M. Buckley, "Beamforming: A versatile approach to spatial filtering," *IEEE ASSP Magazine*, vol. 5, no. 2, pp. 4-24. Apr. 1988.

[39] R. A. Monzingo and T. W. Miller, Introduction to Adaptive Arrays, *John Wiley & Sons*, 1980.

[40] L. C. Godara, "Application of Antenna Arrays to Mobile Communications, Part II: Beam-Forming and Direction-of-Arrival Considerations," in *Proc. IEEE*, vol. 85, no. 8, pp. 1195-1245, Aug. 1997.

[41] S. C. Swales, M. A. Beach, and D. J. Edwards "Multi-beam adaptive base station antennas for cellular land mobile radio systems," in *Proc. IEEE Veh. Tech. Conf. (VTC'89)*, vol. 1, pp. 341-348, 1989.

[42] S. C. Swales, M. A. Beach, D. J. Edwards, and J. P. McGeehan, "The performance enhancement of multibeam adaptive base-station antennas for cellular land mobile radio systems," *IEEE Trans. Veh. Tech.*, vol. 29, no. 1, pp. 56-67, Feb. 1990.

[43] X. N. Tran, T. Taniguchi, and Y. Karasawa, "Theoretical analysis of subband adaptive array combining cyclic prefix data transmission scheme," *IEICE Trans. Commun.*, vol. E85-B, no. 12, pp. 2610-2621, Dec. 2002.

[44] Y. Zhang, K. Yang, and G. G. Amin, "Adaptive array processing for multipath fading mitigation via exploitation of filter banks," *IEEE Trans. Antennas Propagat.*, vol. 49, no. 4, pp. 505-516, Apr. 2001.

[45] Y. Karasawa and M. Shinozawa, "Subband signal processing adaptive array with a data transmission scheme inserting a cyclic prefix," *IEICE Trans Commun.*,vol. J85-B, no. 1, pp. 90-96, Jan. 2002 (In Japanese).

[46] P. P. Vaidyanathan, "Multirate digital filters, filter banks, polyphase networks, and application: A tutorial," *Proc. IEEE.*, vol. 78, no. 1, pp. 56-93, Jan. 1990.

[47] P. W. Wolniansky, G.J. Foschini, G. D. Golden, and R. A. Valenzuela, "V-BLAST: An architecture for realizing very. high data rates over the rich-scattering wireless channel, " *URSI Inter. Symp. Signals, Systems, and Electronics*, pp. 295-300, Oct. 1998.

[48] J. B. Anderson, "Array gain and capacity for known random channels with multiple element arrays at both end," *IEEE J. Selec. Areas Commun.*, vol. 18, no. 11, pp. 2172-2178, Nov. 2000.

[49] Y. Karasawa, "On data transmission capability of MIMO channel from wave propagation viewpoint," in *Proc. IEICE Technical Report*, AP2002-101, Oct. 2002.

[50] B. Widrow, P. E. Mantey, L.J. Griffiths, and B. B. Goode, "Adaptive antenna system," *Proc. IEEE*, vol. 55, no. 12, pp. 2143-2159, Dec. 1967.

[51] A. Wittneben, "A new bandwidth efficient transmit antenna modulation diversity scheme for linear digital modulation," in *Proc. IEEE Inter. Conf. Commun. (ICC'93)*, 1993.

[52] N. Seshadri and J. H. Winters, "Two signaling schemes for improving the error performance of frequency-division-duplex (fdd) transmission system," *International Journal of Wireless Information Networks, Springer*, vol. 1, no. 1, pp. 1068-9605, Jan. 1994.

[53] M. Cimini and A. Wittneben, "OFDM with diversity and coding for high bit-rate mobile data applications," in *Proc. Int. Workshop on Mobile Multimedia Communications*, 1996.

[54] V. Weerackody, "Diversity for direct-sequence spread spectrum system using multiple transmit antennas, " in *Proc. IEEE Inter. Conf. Commun. (ICC'93)*, pp. 1775-1779, 1993.

[55] S. Sandhu, R. Heath, and A. Paulraj, "Space-time block codes versus space-time trellis codes," in *Proc. IEEE Inter. Conf. Commun. (ICC'01)*, Helsinki, Finland, vol. 4, pp. 1132-1136, June 2001.

[56] N. Kikuma, *Adaptive Antenna Technology* (in Japanese), Ohmsha, Ltd., Oct. 2003.

[57] G. V. Tsoulos, "Smart antennas for mobile communication systems: benefits and challenges," *Electronic and Communication Engineering Journal*, vol. 11, no. 2, pp. 84-94, Apr. 1999.

[58] D. Agrawal, V. Tarokh, and N. Seshadri, "Space-time coded OFDM for high data-rate wireless communication over wideband channels," in *Proc. IEEE Veh. Tech. Conf. (VTC'88)*, vol. 3, pp. 2232-2236, 1998.

[59] F. W. Vook and T. A. Thomas, "Transmit diversity schemes for broadband mobile communications systems," in *IEEE Veh. Tech. Conf. (VTC'00)*, pp. 2523-2529, 2000.

[60] N. B. Ramli, X. N. Tran, T. Taniguchi, and Y. Karasawa, "Subband adaptive array for space-time block coding," in *Proc. Int. Symp. Antennas & Propagat. (ISAP'04)*, Sendai, Japan, Aug.17-21, 2004, vol. 1, pp. 289-292.

[61] X. N. Tran, T. Taniguchi, and Y. Karasawa, "Spatio-temporal equalization for space-time block coded transmission over frequency selective fading channel with co-channel interference," *IEICE Trans. Fund.*, vol. E88-A, no. 3, Mar. 2005.

[62] E. Lindskog and A. Paulraj, "A transmit diversity scheme for channels with inter-symbol interference," in *Proc. IEEE Int. Conf. Commun. (ICC)*, New Orleans, LA, , pp. 307-311, Jun 2000.

[63] T. S. Rappaport, *Wireless Communications: Principle & Practice*, 2nd Edition, Prentice Hall PTR, 2002.

[64] F. Adachi, M. Sawahashi, and H. Suda, "Wideband DS-CDMA for next generation mobile communications systems," *IEEE Commun. Mag.*, vol. 36, no. 9, pp. 56-69, Sept. 1998.

[65] X. N. Tran, T. Taniguchi, and Y. Karasawa, "Subband adaptive array for multirate multicode DS-CDMA," *IEICE Trans. Fund.*, vol. E86-A, no. 7, pp. 1611-1618, July 2003.

[66] B. Hochwald, T. L.. Marzetta, and C. B. Papadias, "A transmitter diversity scheme for wideband CDMA systems based on space-time spreading," *IEEE J. Sel. Areas Commun*, vol. 191, no. 1, pp. 48-60, Jan. 2001.

[67] M. O. Damen, A. Safavi, and K. Abed-Meriam, "On CDMA with space-time codes over multipath channels," *IEEE Trans. Wirel. Commun.*, vol. 2, no. 1, pp. 11-19, Jan. 2003.

[68] X. N. Tran, A. Rajapakshe, T. Fujino, and Y. Karasawa, "Performance of space-time block coded CDMA systems with adaptive beamforming," in *Proc. 2004 Int. Symp. Antennas & Propagat. (ISAP'04)*, Sendai, Japan, Aug.17-21, 2004, vol. 1, pp. 285-288.

[69] Z. Zhang, G. Li, and J. Zhu, "A novel decoding algorithm of STBC for CDMA receiver in multipath fading environments," in *Proc. IEEE Veh. Tech. Conf.*, vol 4, pp. 1956-1959, 2001.

[70] Ruly Lai-U, Ross D. Murch, and Khaled Ben Letaif, "MIMO CDMA Antenna System for SINR Enhancement," *IEEE Tran. Wirel. Commun.*, vol. 2, no. 2, pp. 240-249, Mar. 2003.

[71] T. Omata and Y. Karasawa, "Implicit 2D-RAKE function of subband signal processing adaptive array for spread spectrum systems with spreading code adding a cyclic prefix," in *Proc. IEICE Technical Report*, AP2001-15, May 2001.

[72] N. B. Ramli, X. N. Tran, T. Taniguchi, and Y. Karasawa, "Subband adaptive array for space-time block coding," *IEICE Trans. Fund.*, vol. E89-A, no. 11, pp. 3103-3113, Nov. 2006.

[73] S. Zhou, G. B. Giannakis, and C. Le Martret, "Chip-interleaved block-spread code division multiple access," *IEEE Trans. Commun.*, vol. 50, no. 2, pp. 235-248, Feb. 2002.

[74] F. Petre, G. Leus, L.. Deneire, M. Engels, M. Moonen, and H. De Man, "Space-time block coding for single-carrier block transmission DS-CDMA downlink," *IEEE J. Sel. Areas Commun.*, vol. 21, no. 3, pp. 350-361, Apr. 2003.

[75] R. T. Compton, Jr., "An adaptive array in a spread spectrum communications system," in *Proc. IEEE*, vol.66, no.6, pp. 289-298, Mar. 1978.

[76] Y. Zhang, K. Yang, M.G. Amin, and Y. Karasawa, "Performance analysis of subband arrays," *IEICE Trans. Commun.*, vol. E84-B, no. 9, pp. 2507-2513, Sept. 2001.

[77] X. N. Tran, T. Taniguchi, and Y. Karasawa, "Performance analysis of subband adaptive array in multipath fading environment," *IEICE Trans. Fund.*, vol. E85-A, no. 8, pp. 1798-1806, Aug. 2002.

[78] K.S. Gilhousen, I.M. Jacobs, R. Padovani, A.J. Viterbi, L.A. Weaver, and C.E Wheatley III,"On the Capacity of a Cellular CDMA System," *IEEE Trans Veh. Tech. (VTC'91)*, vol. 40, no. 2, pp. 303-312, May 1991.

[79] K. Ishihara, K. Takeda and F. Adachi, "Frequency-domain multi-stage MAI cancellation for DS-CDMA uplink with transmit/receive antenna diversity," in *Proc. IEEE Veh. Tech. Conf. (VTC'05)*, Sept. 2005, vol. 1, pp. 78-82.

[80] W.M. Younis, A.H. Sayed, and N. Al-Dahir, "Adaptive frequency-domain joint equalization and interference cancellation for multi-user space-time block-coded systems,"in *Proc 2003 IEEE Int. Conf. Commun. (ICC2003)*, Anchorage, AK., vol. 5, pp. 3230-3235, May 2003.

[81] Y. Yang and T.-S.P. Yum, "Multicode multirate compact assignment of OVSF codes for QoS differentiated terminals," *IEEE Trans. Veh. Tech.*, vol. 54, no. 6, pp. 2114-2124, Nov. 2005.

[82] J. Chen, J. Wang, and M. Sawahashi, "MCI cancellation for multicode wideband CDMA systems," *IEEE J. Sel.. Areas. Commun.*, vol. 20, no. 2, pp. 450-462, Feb. 2002.

[83] C.D. Iskander and P.T. Mathiopoulos, "Performance of multicode DS/CDMA with noncoherent M-ary orthogonal Modulation in multipath fading channels," *IEEE Trans. Wirel. Commun.*, vol. 3, no. 1, pp. 209-223, Jan. 2004.

[84] N. B. Ramli, T. Taniguchi, and Y. Karasawa, "Subband adaptive array for MIMO-CDMA space-time block coded system," *14th European Signal Processing Conference (EUSIPCO)*, Firenze, Italia, Sept. 2006.

[85] J. Ventura-Traveset, G. Caire, E. Biglieri, and G. Taricco, "Impact of diversity reception on fading channels with coded modulation - Part I: Coherent detection," *IEEE Trans. Commun.*, vol. 45, no. 5, pp. 676-686, May 1997.

[86] J. Proakis, *Digital Communications*, 3rd edition, McGraw-Hill, New York, 1995.

[87] W. C. Jakes, *Microwave Mobile Communications*, IEEE Press, 1993.

[88] N.B. Ramli, T. Taniguchi, and Y. Karasawa, "Subband adaptive array for MIMO-STBC CDMA system," *IEICE Trans. Fund.*, vol. E90-A, no. 10, pp. 2309-2317, Oct. 2007.

[89] A.F. Naguib, N. Seshadri, and A.R. Calderbank, "Applications of space-time block codes and interference suppression for high capacity and high data rate wireless systems," in *Proc. 32nd Asilomar Conf. Signals, Systems, and Computers*, vol. 2, pp. 1803-1810, Nov. 1998.

[90] R. Kohno, "Spatial and temporal communications theory using adaptive array," *IEEE Pers. Commun.*, vol. 5, pp.28-35, Feb. 1998

[91] D. Falconer, S. L. Ariyavisitakul, A. Benyamin-Seeyar, and B. Eldson. "Frequency Domain Equalization for Single-Carrier Broadband Wireless Systems", *IEEE Commun. Mag.*, vol. 40, no. 4, pp.58-66, April 2002.

[92] A.F. Naguib, N. Seshadri, and A.R. Calderbank, "Applications of space-time block codes and interference suppression for high capacity and high data rate wireless systems," in *Proc. 32nd Asilomar Conf. Signals, Systems, and Computers*, vol. 2, pp. 1803-1810, Nov. 1998.

[93] X. Li, "Space-time coded multi-transmission among distributed transmitter without perfect synchronization," *IEEE Signal Processing Letters*, vol. 11, no. 12, pp. 948-951, Dec. 2004.

[94] S. Annanab, T. Tobita, T. Taniguchi, and Y. Karasawa, "Asynchronous MIMO STBC Adaptive Array Transmission Scheme for Multiuser over Fast Fading Channel," in *Proc. IEICE Technical Report*, A.P2007-162, pp.231-236, Jan. 2008.

List of Original Publication Related to the Dissertation

Journals

1. N. B. Ramli, N. X. Tran, T. Taniguchi, Y. Karasawa, "Subband Adaptive Array for Space-Time Block Coding," *IEICE Trans. Fund.*, vol. E89-A, no. 11, pp. 3103-3113, Nov. 2006.

2. N. B. Ramli, T. Taniguchi, and Y. Karasawa, "Subband Adaptive Array for MIMO-STBC CDMA System," *IEICE Trans. Fund.* vol. E90-A, no. 10, pp. 2309-2317, Oct. 2007.

3. N. B. Ramli, T. Taniguchi, Y. Karasawa, "Wideband Spatio-Temporal Adaptive Array for Multiuser STBC Transmission," *IEICE Trans. Fund.*, 2008 (submitted for reviewing process).

International Conferences

1. N. B. Ramli, T. Taniguchi, Y. Karasawa, "Spatio-Temporal Adaptive Array for Asynchronous Multiuser MIMO-STBC Transmission", in *Proc. 3rd International Symposium on Communications, Control and Signal Processing (ISCCSP 2008)* (accepted for presentation and publication.)

2. T. Taniguchi, N. B. Ramli, Y. Karasawa, "CORPS - Combined Recursion Processing of Subsets for Adaptive Array Antennas under Frequency Selective Fading", in *Proc. IEEE 65th Veh. Tech. Conf., 2007 (VTC2007)-Spring*, Dublin, pp. 314-318, April 2007.

3. N. B. Ramli, T. Taniguchi, Y. Karasawa, "Subband Adaptive Array for Space-Time Block Coded Multirate Multicode MIMO CDMA System", in *Proc. 2006 Int. Symp. Ant. & Propag. (ISAP'06)*, Singapore, Nov. 1-4, 2006.

4. T. Taniguchi, N. B. Ramli, and Y. Karasawa, "A Design method of Single Carrier Spatio-Temporal MIMO Systems with Reduced Computational Cost," in *Proc. 17th IEEE Int. Symp. on Personal, Indoor and Mobile Commun. (PIMRC2006)*, Helsinki, Finland, Sept. 2006.

5. N. B. Ramli, T. Taniguchi, and Y. Karasawa, "Subband Adaptive Array for MIMO-CDMA Space-Time Block Coded System," in *Proc. 14th European Signal Processing Conference(EUSIPCO)*, Firenze, Italia, Sept. 2006.

6. T. Taniguch, N. B. Ramli, and Y. Karasawa, "Spatio-Temporal MIMO Systems for Multiuser Communications under Frequency Selective Fading," in *Proc. 2006 International Conference on Digital Telecommunications*, Cap Esterel (Agay), France, August 2006.

7. N. B. Ramli, T. Taniguchi, and Y. Karasawa, "Multirate Multicode MIMO-STBC CDMA System with Subband Adaptive Array Processing," in *Proc. Int. Symp. on Advanced ICT(AICT2006)*, UEC, Tokyo, Japan., pp. 145-153, August 2006.

8. N. B. Ramli, X.N. Tran, T. Taniguchi, and Y. Karasawa, "Subband Adaptive Array for Space Time Block Coding," in *Proc. Int. Symp. Antennas & Propagat. (ISAP'04)*, Sendai, Japan, vol. 1, pp. 289-292, August 2004.

Oral Presentations

1. N. B. Ramli, T. Taniguchi and Y. Karasawa, "Efficient Modified Spatio-Temporal Adaptive Array for Multiuser STBC Transmission," in *Proc IEICE General Conference*, B-5-34, March 2008.

2. T. Taniguchi, N. B. Ramli, Y. Karasawa, "Multiuser MIMO Communication System Using Spatio-Temporal Processing," in *Proc IEICE Technical Report* RCS2006-139, pp.37-42, Oct. 2006.

3. T. Taniguchi, N. B. Ramli, Y. Karasawa, "Spatio-Temporal Multiuser MIMO Communication System," in *Proc IEICE Society Conference*, B-1-221, Sept. 2006.

4. T. Taniguchi, N. B. Ramli, Y. Karasawa, "Combined Recursion Processing of Subspace (CORPS) for Communication in Frequency-Selective Fading Environment," in *Proc IEICE Technical Report* RCS (2006.04).

5. N. B. Ramli, T. Taniguchi, and Y. KARASAWA, "Study on Subband Adaptive Array for Space-Time Block Coded CDMA Systems," in *Proc IEICE Technical Report* A.P 2005-139, pp. 41-44, Jan. 2006

6. N. B. Ramli, T. Taniguchi and Y. Karasawa, "Subband Adaptive Array for Space-Time Block Coded CDMA Systems," in *Proc IEICE Society Conference*, B-5-34, Sept. 2005.

7. N. B. Ramli, X. N. Tran, T. Taniguchi and Y. Karasawa, "Subband Adaptive Array for Space-Time Block Coding," in *Proc IEICE Society Conference*, B-1-179, Sept. 2004.

Author Biography

Nordin Bin Ramli was born in Malaysia in 1975. He received his B.Sc(Electrical Engineering) from Keio University, Japan in 1999 and M.Eng(Electronic Engineering) from The University of Electro-Communications, Japan in 2005. He worked with Telekom Malaysia Berhad (TMB) after graduation in 1999 as network engineer. He is currently a Ph.D. student in Advanced Wireless Communications research Center (AWCC), The University of Electro-Communications, Tokyo, Japan. He was listed in the Marquis Who's Who in Science and Engineering as Telecommunication Engineer in 10th Anniversary (2008-2009) Edition. His research interests are in the area of space-time processing, MIMO, and adaptive array antenna.

He is a student member of the Institute of Electronics, Information and Communications Engineer(IEICE), Japan, the Institute of Electrical and Electronics Engineer (IEEE), and the European Association for Signal Processing (EURASIP).